REGULATORY ROLE OF TRIM33 IN MORPHOGENESIS: A PARADIGM FOR COMMON HUMAN CONGENITAL DEFECTS

by

Sudha Rajderkar

A dissertation submitted in partial fulfillment
of the requirements for the degree of
Doctor of Philosophy
(Oral Health Sciences)
in the University of Michigan
2016

Doctoral Committee:

Professor Vesa M Kaartinen, Chair
Assistant Professor Sundeep Kalantry
Professor Yuji Mishina
Professor Charlotte M Mistretta
Assistant Professor Brian A Pierchala

ACKNOWLEDGEMENTS

I thank all mentors, teachers and individuals who contributed to my successful doctoral training:

Vesa Kaartinen, my primary mentor and research advisor, for shaping my scientific thinking and for encouraging bold science ideas where necessary. I deeply appreciate his confidence in my success as a trainee.

My dissertation committee for their valuable contributions through the dissertation process:

Sundeep Kalantry, for insightful, constructive criticism of the project, and mentoring.

Yuji Mishina, for being a kind and strict teacher at the same time and his sense of humor. I took a liking for developmental biology as a rotation student in his lab.

Charlotte Mistretta, for her personal commitment to my career/scientific success. She has also been my academic advisor and in that role, I have benefitted greatly from deep, inspiring conversations with her.

Brian Pierchala, for his unbiased critique and encouragement while pursuing a complex research question.

I thank Jan CC Hu and James Simmer for mentoring me in my very first lab rotation in the OHS Program.

I would like to appreciate all current and past members in the Kaartinen Lab for the lively work environment. In particular, Kenji Yumoto, for early histological data for the Trim33/heart development project and Penelope Thomas, for teaching several techniques, providing knowledgeable comments and sharing fascination for the thought process.

I also acknowledge the funding sources that made my training possible:

University of Michigan School of Dentistry Dean's Fellowship (2010 – 2012)

Rackham School of Graduate Studies, for catalyzing a rewarding graduate school experience and for several financial awards throughout my graduate studies.

Society for Developmental Biology Travel Awards

My mentor's NIH R01DE013085 and NIH R01HL074862 funding supported my training and research through candidacy.

University of Michigan, School of Dentistry and Department of Biologic and Materials Sciences, for excellent research, teaching and training environment.

Elizabeth Rodriguez, for administrative help.

Taocong Jin "Tao", for meticulous help with qRT-PCR experimental set up.

Kimber Converso-Baran at CVC Echocardiography Core Lab, for timely assistance and recording of *ex utero* Doppler data for mouse embryo experiments.

University of Michigan Sequencing Core, for timely execution of RNA Sequencing projects.

Kenneth Weiss at UM Department for Computational Medicine and Bioinformatics, for helping me acquire basic skills for computing RNA Sequencing data.

Kate Karfilis (Stankunas Lab, University of Oregon, Eugene) and Emily Maclary (Kalantry Lab, UM Department of Human Genetics), for peer learning with RNA Sequencing Data.

Unit for Laboratory Animal Medicine staff, for maintaining our mouse colony.

Renee Quinlan: for personally investing in animal welfare.

Oral Health Sciences PhD Program, Jan CC Hu, for her guidance and support as program director

Patricia Schultz, Manette London, Kimberly Smith and Sarah Ellerholz, Charlene Erickson, Misty Gravelin, for readily helping with administrative aspects, program organization in the most cheerful manner.

OHS Buddies, students and alumni in the program, for their friendship and shared experiences.

Yoshihiro Komatsu and Honghao Zhang (Mishina Lab), for scientific discussions and technical help.

My alma mater, Government Dental College and Hospital, Mumbai (India), for a strong foundation in the clinical discipline as part of becoming a clinician-scientist. University Musical Society and University of Michigan Museum of Art: for providing a platform for creative and intellectual upliftment.

My family, friends and well-wishers:

My late grandparents - N.T. and K.N Rajderkar, who continue to be my exemplary role models. Sunita Nasnodkar for believing in me and supporting my bold career decisions. Anuradha Garud, for being a loving teacher and friend; Yashoda Wakankar, for her infectious positive outlook; Madhav and Ramaa Manjrekar - without whom my transition to the US would not have been easy. Kaustubh Kalkundri, my significant other, for his loving support, incredible patience and inspiring companionship.

PREFACE

Following is the description of the contributions to the work presented in this thesis:

I (SR) wrote all chapters with editorial guidance from my mentor, Vesa Kaartinen (VK). VK significantly contributed to the discussion in Chapter 4. Research described in Chapters 4 and 5 is under preparation as manuscripts for publication. VK and I co-designed experiments and all research work presented in this thesis is original. I optimized and conducted all experiments with VK's help to cover time-away; contributions by Kenji Yumoto are kindly acknowledged towards data in Figures 4.10, 4.11 and 4.12 (I – L). I received valuable feedback on experimental procedures from Sundeep Kalantry and Yuji Mishina (YM) through the dissertation process.

VK specifically instructed and trained me in derivation of mouse embryonic stem cell (mESC) lines; I derived the *Trim33*^{FF}*: UbcCre*^{ERT2} mESC lines described in Chapters 4 and 5. I designed and generated *Trim33* RNA *in situ* hybridization (ISH) probes; the *T (Brachyury)* ISH probe is a kind gift from YM. *Sox2-Cre* (Stock # 004783) and *UbcCre-ERT2* (Stock # 007001*)* mice were obtained from Jackson Labs. Mark Lewandoski and Robert Schwartz respectively, kindly provided *T-Cre and Nkx2_5 –Cre* mice. The UM Sequencing Core prepared

cDNA libraries and conducted RNA (Illumina) Sequencing; while computation, bioinformatics and statistical analyses of RNA Sequencing data was done by me.

TABLE OF CONTENTS

LIST OF FIGURES

CHAPTER 1

CHAPTER 2

CHAPTER 4

Chapter 5

LIST OF TABLES

Chapter 1

Chapter 3

Chapter 4

Appendix 1

ABSTRACT

Transforming Growth Factor – beta (TGF-β) signaling plays important, pleiotropic roles in embryonic development as well as tissue homeostasis. TGF-β signaling dose is tightly regulated in a context-specific manner and even subtle perturbations result in a spectrum of disease phenotypes of varying severity. In the canonical TGF-β pathway, TGF-β signals are mediated by activated receptor-regulated Smads (R-Smads, Smad2/3) that form a complex with Smad4 and participate in transcriptional regulation of TGF-β-mediated genes with sequence specific DNA binding factors and context-specific co-regulators. Both Smad2/3 and Smad4 regulate signal duration and intensity differentially. This is consistent with the variability and spectrum of phenotypes observed upon their conditional deletions in mice, with Smad2/3-associated phenotypes being more severe than those associated with Smad4. However, precise mechanisms that modulate the functional and phenotypic differences attributed to Smad2/3 and Smad4 are poorly understood. Tripartite motif containing (Trim) 33 - a co-regulator of both activated Smad2/3 and Smad4, is a candidate gene for understanding fine tuning mechanisms of TGF-β signaling. Here, I have investigated the role of Trim33 in early embryogenesis. My results show that Trim33 controls visceral endoderm differentiation *in vitro* and pre-cardiac mesoderm differentiation *in vivo*. Epiblast-specific *Trim33* mutants die during the second half of gestation as a result of

ensuing cardiac failure. My findings imply that Trim33 is required for appropriate early mesendoderm differentiation soon after its induction, regulates TGF-β superfamily signaling in a biphasic manner in the pre-cardiac mesoderm, and that in more committed cell lineages Trim33 is dispensable.

CHAPTER 1

Overview of TGF-β superfamily signaling

Transforming growth factor-beta (TGF-β) ligands belong to a key class of secreted morphogens playing important cellular roles during embryogenesis and organogenesis, inflammation, homeostasis and cancer. Effects of TGF-β signaling are context dependent, pleiotropic and depend on the strength and duration of exposure to the signal (Wrana, 2013).

The TGF-β superfamily

TGF-β superfamily members are widely conserved across species and comprise a total of over 42 members that include TGF-β, Bone Morphogenic Proteins (BMPs), Activin/Nodal, Growth Differentiation Factor (GDFs) and Müllerian Inhibiting Substance (MIS). Sequence similarity sorts TGF-β Activin/Nodal together in one group while BMPs/GDFs form another group. Several cell types through early embryonic development and adult life secrete TGF-β /BMP family proteins. Others that are more restrictive in expression are Anti-Müllerian Hormone (AMH), also called MIS, a glycoprotein hormone secreted by Sertoli cells while GDF8/Myostatin is expressed in myocytes in skeletal muscle. The scope of this thesis is limited to TGF-β /Nodal/Activin family (Weiss and Attisano, 2013).

Binding proteins and extracellular activation of TGF-β ligands

There are 3 isoforms of TGF-β ligands, namely TGF-βs 1, 2 and 3 that signal through type I and type II TGF-β receptors while Nodal and Activin signal via type I and II activin receptors (Figure 1.1) (Massague, 2012). Precursor ligands are processed to cleave their pro domain(s) by convertases such that receptor-binding sites are made accessible on the ligand molecule. Prodomains are also thought to attribute trafficking characteristics TGF-β ligands to their appropriate sites before activating signaling pathways and also trafficking ligands for degradation, thus regulating the extent of activation of the signaling pathway. Once secreted in dimeric mature form with latency-associated peptide (LAP) complexes, TGF-β ligands eventually form complexes with large latent complex, the latent TGF-β binding protein (LTBP) (Munger and Sheppard, 2011; Robertson et al., 2015). LTBP and LAP regulate the latency of TGF-β ligands allowing the extra cellular microenvironment to control ligand availability to cell receptors (Constam, 2014; Shi and Massague, 2003).

There is one Nodal protein-coding gene known and characterized in the mouse, 3 in zebra fish and 5 in the xenopus whereas none have been described so far in drosophila and C. elegans. This plausibly reflects on the differences in functional requirements for Nodal as a mesendoderm inducer in different species (Pauklin and Vallier, 2015).

Receptors and signaling mediators

TGF-β signaling occurs via transmembrane serine/threonine kinase receptors. There are a total of seven Type I and five Type II receptors known across the entire TGF-β superfamily. TGF-β specifically binds TGF-β type I (TgfβRI or Alk5) and TGF-β type II (TgfβRII) receptors. Activin and Nodal, both signal via one of the Activin type I receptors, AcvRIa (Alk2), AcvRIb (Alk4) or AcvRIc (Alk7) and Activin type II receptors AcvRIIa or AcvRIIb. Cripto is a co-receptor for Nodal signaling or AcvRs and distinguishes the signaling process involving Activin and Activin receptors (Massague, 1996, 1998).

A widely expressed chondroitin and heparin sulphate protein, betaglycan, functions as a co-receptor for TGF-β ligands that bind TgfβRI and TgfβRII receptors. It is also known as the TGF-β type III receptor and binds TGF-β2, which has inherently low affinity binding for TgfβRII by itself. Betaglycan is a co-modulator of MAPK signaling as part of Smad-independent TGF-β signaling (discussed later in this chapter) (Bilandzic and Stenvers, 2011) (Table 1.1).

Activation of TGF-β Signal

TGF-β ligand dimers linked by disulfide bonds engage cell surface receptor heterotetramers consisting of two appropriate Type I and two Type II receptors. Type I receptors have a 30 amino acid, GS region upstream of the kinase domain which is absent from Type II receptors. Type II receptors are constitutively active. Once ligand-receptor binding occurs, the type II receptor(s)

trans phosphorylate type I receptors. The ligand-receptor complex is then internalized either by clathrin-coated pits or by lipid rafts into caveolae (Shi and Massague, 2003).

Category	TGF-β Pathway	Activin/Nodal Pathway	BMP Pathway
Ligands	TGF-β1, β2, β3	Activin A and B Nodal	BMP2, 4, 5,6, 7 BMP 8A, 8B, 9 , 10
Type I receptors	TgfβRI	AcvRIa, AcvRIb, AcvRIc	AcvRI1, AcvR1 Bmpr1a, Bmpr1b
Type II receptors	TgfβRII	AcvRIIa or AcvRIIb	Bmpr2, AcvRIIa, AcvRIIb
Type III receptors	TgfβRIII Cripto	TgfβRIII Cripto	
R-Smads	Smad2, 3	Smad2, 3	Smad1, 5, 8
Co-Smad	Smad4	Smad4	Smad4
I-Smad	Smad7	Smad7	Smad6, 7

Table 1.1. Summary of components comprising canonical TGF-β superfamily pathways. Adapted and modified from (Akhurst and Hata, 2012). R-Smads = Receptor Smads, Co-Smad = Co-receptor Smad, I-Smad = Inhibitory Smads.

Smad-dependent signaling

Phosphorylation of the type I receptor causes conformational changes of the receptor complex, which in turn facilitates docking and phosphorylation of C-

terminal serine residues in receptor-mediated Smad proteins (R-Smads). There are five R- Smads and the common mediator Smad4, which transduce signals downstream from the activated receptors to the nucleus. Smads1, 5 and 8 are specific to BMP while Smads2/3 are specific to the TGF-β/Nodal/Activin pathway. Smad4 is the only Co-Smad known in mammals whereas another less well-characterized isoform Smad4b exists in the xenopus (Howell et al., 1999; Schiffer et al., 2000).

Both TGF-βs and activins signal through Smad2 and Smad3 (Table 1.1) (Massague et al., 2005). Smad2 and Smad3 are homologous and both bind through an identical motif in their L3 loop to the L45 loop of the TgfβRI. Phosphorylated R-Smads are activated Smads. Phosphorylation enables R-Smads to form a complex with Smad4; the complex then accumulates in the nucleus. This R-Smad/Smad4 heteromeric complex regulates gene-expression in conjunction with promoter-specific transcription factors and cofactors. R-Smad proteins comprise MH1 and MH2 Mad-homology domains with an intervening flexible linker region. The MH1 domain confers DNA binding ability while the MH2 domain facilitates binding with protein partners aiding several functions such as receptor activation, cytoplasmic retention, nuclear accumulation of the Smad complex and binding with other transcriptional co-regulators. A summary schematic of the canonical TGF-β signaling pathway is depicted in (Figure 1.1). Smad3 binds directly to DNA via consensus GTGC motifs while Smad2 does not

bind DNA due to an insertion of 30 amino acids in its N-terminal MH1 domain (Macias et al., 2015; Massague et al., 2005).

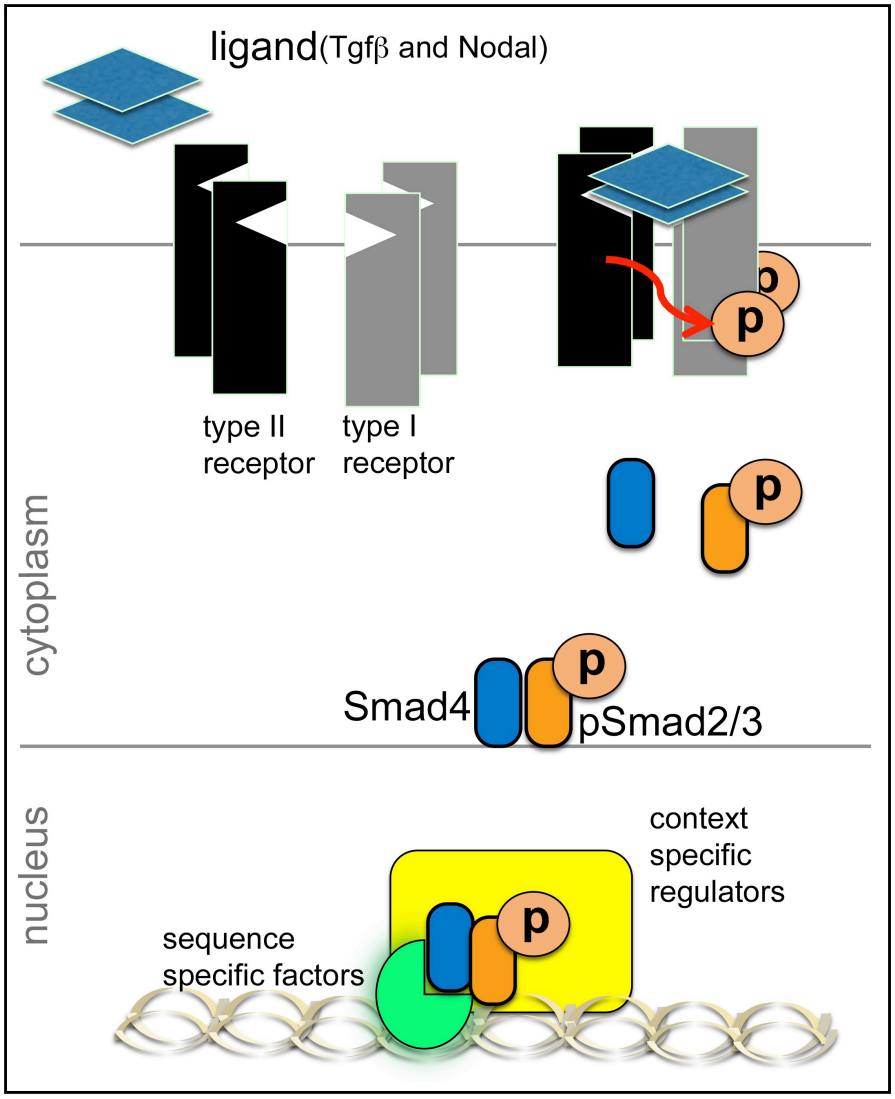

Figure 1.1. Canonical, Smad-mediated TGF-β pathway. Upon ligand binding and receptor activation, phosphorylated Smad2/3 form a complex with Smad4. This complex accumulates into the nucleus where it participates in transcriptional regulation of TGF-β-regulated genes along with sequence specific DNA binding factors and context-specific co-regulators. Adapted from (Massague and Gomis, 2006).

Smad-independent signaling

TGF-β signaling through non-Smad mediated pathways, so called non-canonical TGF-β signaling is also of relevance in many biological processes, e.g. in epithelial-to-mesenchymal transition (EMT), cell migration and metastasis. Examples include but are not limited to recruitment of Par6 by TgfβRII receptors, resulting in recruitment of RhoA GTPase via Smurf1 and MAP kinase and PI3 kinase pathway involving Traf6 and mTorc mediators (Shi and Massague, 2003). Non-canonical TGF-β signaling is outside the scope of this thesis. However, it must be emphasized that Smad-dependent and Smad-independent signaling both can converge and co-regulate transcriptional outcomes either in a sequential manner or simultaneously, depending on the context. A third variation in R-Smad- mediated signaling involves RSmads but not Smad4, such as Ikkα-pSmad2 (Brandl et al., 2010)and Trim33-pSmad2/3 (Xi et al., 2011). In addition to their role in transcriptional control of TGF-β dependent genes, Smad proteins namely, activated Smad3 and the Smad1 are crucial components of the Drosha complexes involved in microRNA biogenesis (Blahna and Hata, 2012).

Regulation of TGF-β signaling

Several factors determine the intensity and duration of TGF-β signaling. (Reviewed by (Massague et al., 2005; Miyazono, 2000; Xu et al., 2012)). Ligand availability, subtype and ligand concentration determine the extra cellular component and onset of TGF-β signaling. Smad proteins comprise a nuclear localization signal and constantly shuttle between the cytoplasm and nucleus.

However, in an unstimulated state, binding with SARA (Smad anchor for receptor activation) retains the Smads in the cytoplasm. Phosphorylation of Smad2/3 disrupts SARA-Smad association and increases their affinity for Co-Smad4 (Macias et al., 2015). R-Smad activation by phosphorylation is reversible by the activity of nuclear phosphatases that target individual or monomeric R-Smads, not R-Smad complexes (Wrighton et al., 2009). In contrast to Smad2/3, Smad4 has a nuclear export signal (Hill, 2009; Watanabe et al., 2000).

Inhibition of R-Smads

Smad 6 and Smad7 function to disrupt Smad-receptor as well as Smad-Smad interactions and are direct targets or read outs of BMP and TGF-β signaling respectively (Massague et al., 2005). Importantly, Smad6/7 recruit Smurf proteins to upstream receptor complexes and regulate their activity by facilitating endocytosis (Ebisawa et al., 2001; Kavsak et al., 2000). Other signaling pathways such as protein kinase C (phosphorylates Smad3 and interferes with its binding to DNA), MAPK (interferes with translocation of Smad2/3 to the nucleus in certain contexts) also regulate R-Smad activity (Reviewed by (Park, 2005)).

Modification of chromatin landscape and transcriptional control of TGF-β - dependent genes

At the DNA level, Smad complexes recruit context dependent co-activators and co-repressors including histone acetyl transferases (p300 and CBP) and histone

deacetylases that participate in transcriptional regulation (Janknecht et al., 1998; Pouponnot et al., 1998). In basal states, the co-repressors TGIF, Ski and SnoN (Ski –related novel gene) bind the MH2 domain of R-Smads and function as chromatin repressors (Wotton and Massague, 2001). Activated Smads reverse this repression by recruiting p300 and CBP (CREB –binidng protein). Along with co-activators, Smad complexes bind Smad binding elements (SBE) (characterized for TGF-β and Nodal activated Smad2/3) and Activin response elements (ARE), for Activin activated Smad2/3 (Dennler et al., 1998; Lau et al., 2012). The compositions of complexes assembled at the transcriptional level determine whether TGF-β signaling will induce or repress transcription of TGF-β - dependent genes. Disassembly of Smad and Smad -bound complexes at the DNA level is also a determinant of signal duration or termination. Cyclin-dependent kinases 8 and 9 (CDK8 and CDK9) dynamically phosphorylate the linker region of Smad2/3, influencing further utilization and disposal of Smad proteins (Alarcon et al., 2009). In addition, YAP1 (yes associated protein 1) - a transcriptional regulator simultaneously primes the linker for phosphorylation by GSK3 (glycogen synthase kinase 3) (Attisano and Wrana, 2013). GSK3 recruits and in addition, primes the binding of E3 ubiquitin (Ub) protein ligases SMURF1 (SMAD-specific E3 ubiquitin protein ligase 1) (Al-Salihi et al., 2012) or NEDD4L (neural precursor cell expressed developmentally downregulated protein 4-like), targeting Smad proteins for polyubiquitination and proteasomal degradation (Gao et al., 2009).

Cross talk with other signaling pathways and regulation of TGF-β signaling: Smad4 and signal convergence

Smad4 is sequentially phosphorylated in the linker region by GSK3. Smad4 is then targeted for degradation in a Wnt -dependent manner in the presence of the E3 UB ligase β -TrCP (β -transducing repeats –containing proteins) (Wan et al., 2004), thus having a negative regulatory effect on TGF-β signaling. GSK3 mediated phosphorylation of Smad4 has been shown to regulate early embryo development in the xenopus. Thus Smad4 is at the intersection of major pathways that regulate development and disease (Alarcon et al., 2009; Guo and Wang, 2009; Massague, 2012).

Post-translational modifications in Smad4 and regulation of Smad4 in non-disease states

Among the many post translational modifications regulating Smad4 activity (reviewed by (Xu, 2006)), ubiquitination is a prominent post translational modification of Smad4 that regulates its activity within the nucleus. SUMOylation (Small Ubiquitin-like Modifier) of Smad4 by SUMO1 facilitates the nuclear stability and nuclear retention of Smad4, thus enhancing TGF-β signaling (Lee et al., 2003). Jab1 and SCF E3 ubiquitin ligases signal Smad4 for proteasomal degradation, limiting its activity (Wan et al., 2004). In addition, Smad4 degradation results from Smurf activity via Smad2 or Smad6/7 (Massague et al., 2005) or by the E3 ligase CHIP (carboxy-terminus of Hsc70 interacting protein), which also uniquitinates Smad1 and 3 (Li et al., 2004). An important emerging

context in TGF-β signaling has been the discovery of monoubiquitination of Smad4, which does not signal it for degradation (Wang et al., 2008). Instead, monoubiquitination of Smad4 by Trim33 exports it into the cytoplasm where a putative deubiquitinating enzyme FAM/USP9x (Fat facets in mammals /ubiquitin specific peptidase 9, X-linked) releases the bound Ubiquitin and makes Smad4 available to oligomerize with Smad2/3, thus maintaining TGF-β signal strength (Dupont et al., 2009; Wrana, 2009).

References

Akhurst, R.J., Hata, A., 2012. Targeting the TGFbeta signalling pathway in disease. Nature reviews. Drug discovery 11, 790-811.

Al-Salihi, M.A., Herhaus, L., Sapkota, G.P., 2012. Regulation of the transforming growth factor beta pathway by reversible ubiquitylation. Open biology 2, 120082.

Alarcon, C., Zaromytidou, A.I., Xi, Q., Gao, S., Yu, J., Fujisawa, S., Barlas, A., Miller, A.N., Manova-Todorova, K., Macias, M.J., Sapkota, G., Pan, D., Massague, J., 2009. Nuclear CDKs drive Smad transcriptional activation and turnover in BMP and TGF-beta pathways. Cell 139, 757-769.

Attisano, L., Wrana, J.L., 2013. Signal integration in TGF-beta, WNT, and Hippo pathways. F1000prime reports 5, 17.

Bilandzic, M., Stenvers, K.L., 2011. Betaglycan: a multifunctional accessory. Mol. Cell. Endocrinol. 339, 180-189.

Blahna, M.T., Hata, A., 2012. Smad-mediated regulation of microRNA biosynthesis. FEBS Lett. 586, 1906-1912.

Brandl, M., Seidler, B., Haller, F., Adamski, J., Schmid, R.M., Saur, D., Schneider, G., 2010. IKK(alpha) controls canonical TGF(ss)-SMAD signaling to regulate genes expressing SNAIL and SLUG during EMT in panc1 cells. J. Cell Sci. 123, 4231-4239.

Constam, D.B., 2014. Regulation of TGFbeta and related signals by precursor processing. Semin. Cell Dev. Biol. 32, 85-97.

Dennler, S., Itoh, S., Vivien, D., ten Dijke, P., Huet, S., Gauthier, J.M., 1998. Direct binding of Smad3 and Smad4 to critical TGF beta-inducible elements in the promoter of human plasminogen activator inhibitor-type 1 gene. EMBO J. 17, 3091-3100.

Dupont, S., Mamidi, A., Cordenonsi, M., Montagner, M., Zacchigna, L., Adorno, M., Martello, G., Stinchfield, M.J., Soligo, S., Morsut, L., Inui, M., Moro, S., Modena, N., Argenton, F., Newfeld, S.J., Piccolo, S., 2009. FAM/USP9x, a deubiquitinating enzyme essential for TGFbeta signaling, controls Smad4 monoubiquitination. Cell 136, 123-135.

Ebisawa, T., Fukuchi, M., Murakami, G., Chiba, T., Tanaka, K., Imamura, T., Miyazono, K., 2001. Smurf1 interacts with transforming growth factor-beta type I receptor through Smad7 and induces receptor degradation. J. Biol. Chem. 276, 12477-12480.

Gao, S., Alarcon, C., Sapkota, G., Rahman, S., Chen, P.Y., Goerner, N., Macias, M.J., Erdjument-Bromage, H., Tempst, P., Massague, J., 2009. Ubiquitin ligase Nedd4L targets activated Smad2/3 to limit TGF-beta signaling. Mol. Cell 36, 457-468.

Guo, X., Wang, X.F., 2009. Signaling cross-talk between TGF-beta/BMP and other pathways. Cell Res. 19, 71-88.

Hill, C.S., 2009. Nucleocytoplasmic shuttling of Smad proteins. Cell Res. 19, 36-46.

Howell, M., Itoh, F., Pierreux, C.E., Valgeirsdottir, S., Itoh, S., ten Dijke, P., Hill, C.S., 1999. Xenopus Smad4beta is the co-Smad component of developmentally regulated transcription factor complexes responsible for induction of early mesodermal genes. Dev. Biol. 214, 354-369.

Janknecht, R., Wells, N.J., Hunter, T., 1998. TGF-beta-stimulated cooperation of smad proteins with the coactivators CBP/p300. Genes Dev. 12, 2114-2119.

Kavsak, P., Rasmussen, R.K., Causing, C.G., Bonni, S., Zhu, H., Thomsen, G.H., Wrana, J.L., 2000. Smad7 binds to Smurf2 to form an E3 ubiquitin ligase that targets the TGF beta receptor for degradation. Mol. Cell 6, 1365-1375.

Lau, M.T., Lin, S.W., Ge, W., 2012. Identification of Smad Response Elements in the Promoter of Goldfish FSHbeta Gene and Evidence for Their Mediation of Activin and GnRH Stimulation of FSHbeta Expression. Front. Endocrinol. (Lausanne) 3, 47.

Lee, P.S., Chang, C., Liu, D., Derynck, R., 2003. Sumoylation of Smad4, the common Smad mediator of transforming growth factor-beta family signaling. J. Biol. Chem. 278, 27853-27863.

Li, L., Xin, H., Xu, X., Huang, M., Zhang, X., Chen, Y., Zhang, S., Fu, X.Y., Chang, Z., 2004. CHIP mediates degradation of Smad proteins and potentially regulates Smad-induced transcription. Mol. Cell. Biol. 24, 856-864.

Macias, M.J., Martin-Malpartida, P., Massague, J., 2015. Structural determinants of Smad function in TGF-beta signaling. Trends Biochem. Sci. 40, 296-308.

Massague, J., 1996. TGFbeta signaling: receptors, transducers, and Mad proteins. Cell 85, 947-950.

Massague, J., 1998. TGF-beta signal transduction. Annu. Rev. Biochem. 67, 753-791.

Massague, J., 2012. TGFbeta signalling in context. Nat. Rev. Mol. Cell Biol. 13, 616-630.

Massague, J., Gomis, R.R., 2006. The logic of TGFbeta signaling. FEBS Lett. 580, 2811-2820.

Massague, J., Seoane, J., Wotton, D., 2005. Smad transcription factors. Genes Dev. 19, 2783-2810.

Miyazono, K., 2000. Positive and negative regulation of TGF-beta signaling. J. Cell Sci. 113 (Pt 7), 1101-1109.

Munger, J.S., Sheppard, D., 2011. Cross talk among TGF-beta signaling pathways, integrins, and the extracellular matrix. Cold Spring Harb. Perspect. Biol. 3, a005017.

Park, S.H., 2005. Fine tuning and cross-talking of TGF-beta signal by inhibitory Smads. J. Biochem. Mol. Biol. 38, 9-16.

Pauklin, S., Vallier, L., 2015. Activin/Nodal signalling in stem cells. Development 142, 607-619.

Pouponnot, C., Jayaraman, L., Massague, J., 1998. Physical and functional interaction of SMADs and p300/CBP. J. Biol. Chem. 273, 22865-22868.

Robertson, I.B., Horiguchi, M., Zilberberg, L., Dabovic, B., Hadjiolova, K., Rifkin, D.B., 2015. Latent TGF-beta-binding proteins. Matrix Biol. 47, 44-53.

Schiffer, M., von Gersdorff, G., Bitzer, M., Susztak, K., Bottinger, E.P., 2000. Smad proteins and transforming growth factor-beta signaling. Kidney Int. Suppl. 77, S45-52.

Shi, Y., Massague, J., 2003. Mechanisms of TGF-beta signaling from cell membrane to the nucleus. Cell 113, 685-700.

Wan, M., Tang, Y., Tytler, E.M., Lu, C., Jin, B., Vickers, S.M., Yang, L., Shi, X., Cao, X., 2004. Smad4 protein stability is regulated by ubiquitin ligase SCF beta-TrCP1. J. Biol. Chem. 279, 14484-14487.

Wang, B., Suzuki, H., Kato, M., 2008. Roles of mono-ubiquitinated Smad4 in the formation of Smad transcriptional complexes. Biochem. Biophys. Res. Commun. 376, 288-292.

Watanabe, M., Masuyama, N., Fukuda, M., Nishida, E., 2000. Regulation of intracellular dynamics of Smad4 by its leucine-rich nuclear export signal. EMBO Rep 1, 176-182.

Weiss, A., Attisano, L., 2013. The TGFbeta superfamily signaling pathway. Wiley interdisciplinary reviews. Developmental biology 2, 47-63.

Wotton, D., Massague, J., 2001. Smad transcriptional corepressors in TGF beta family signaling. Curr. Top. Microbiol. Immunol. 254, 145-164.

Wrana, J.L., 2009. The secret life of Smad4. Cell 136, 13-14.

Wrana, J.L., 2013. Signaling by the TGFbeta superfamily. Cold Spring Harb. Perspect. Biol. 5, a011197.

Wrighton, K.H., Lin, X., Feng, X.H., 2009. Phospho-control of TGF-beta superfamily signaling. Cell Res. 19, 8-20.

Xi, Q., Wang, Z., Zaromytidou, A.I., Zhang, X.H., Chow-Tsang, L.F., Liu, J.X., Kim, H., Barlas, A., Manova-Todorova, K., Kaartinen, V., Studer, L., Mark, W., Patel, D.J., Massague, J., 2011. A poised chromatin platform for TGF-beta access to master regulators. Cell 147, 1511-1524.

Xu, L., 2006. Regulation of Smad activities. Biochim. Biophys. Acta 1759, 503-513.

Xu, P., Liu, J., Derynck, R., 2012. Post-translational regulation of TGF-beta receptor and Smad signaling. FEBS Lett. 586, 1871-1884.

CHAPTER 2

Introduction to Trim33

The Trim nuclear family of proteins is the largest subset of E3 Ubiquitin ligases that contain a RING domain, which is a zinc comprising protein domain, found in proteins involved in the ubiquitination pathway. The nomenclature Trim connotes the N terminal "tripartite" motif, which is evolutionarily conserved and is a hallmark of all Trim proteins. Tripartite refers to 3 domains together: the RING domain, which is an ubiquitin (Ub) ligase, and the B1 and B2 boxes which are zinc binding (Borden, 2000; Meroni, 2012; Meroni and Diez-Roux, 2005; Petrera and Meroni, 2012; Reymond et al., 2001). Trim33, also called as transcriptional intermediary factor 1 gamma (Tif1γ), is one in the Trim family of over 70 proteins, several of which function as transcriptional co-regulators. Trim proteins play important roles in developmental processes, cell differentiation and cancer (Ikeda and Inoue, 2012; Marin, 2012; Short and Cox, 2006)

Trim33 orthologues

Trim33 was first described as *Ectodermin* (*ecto*) in the xenopus in a functional screen for ectoderm determinants, *ecto* was shown to favor neural or ectodermal differentiation while blocking the mesodermal inducing ability of TGF-β signaling (Dupont et al., 2005). Moonshine (*mon*), the Trim33 orthologue in zebra fish is required for hematopoiesis in both embryonic and adult stages (Ransom et al., 2004). Bonus (*Bon*) is the Drosophila orthologue of *Trim33* (Beckstead et al., 2005).

The mouse *Trim33* gene consists of 20 coding exons that encode an 1142-amino-acid protein with 96% sequence similarity to its human orthologue. There are two *Trim33* variants in the mouse with no specific functional differences described to date; variant 2 lacks an alternate in-frame exon in the 3' coding region compared to variant 1 and is shorter than isoform 1. http://www.ncbi.nlm.nih.gov/protein/NP_001073299.1

Apart from the Trim (RING and B1, B2 boxes) domain, which is common to all known Trim proteins, Trim33 comprises two C-terminal domains, the Plant Homeo Domain (PHD) and Bromo domain that engage histone modifications. PHD domains bind trimethylated lysines while Bromo domains bind acetylated lysines in histones (Gozani et al., 2003; Zeng and Zhou, 2002). Additionally, Trim33 proteins have a Smad binding region and a coiled- coiled domain (Yan et al., 2004). Figure 2.1 shows a schematic of Trim33 protein domains.

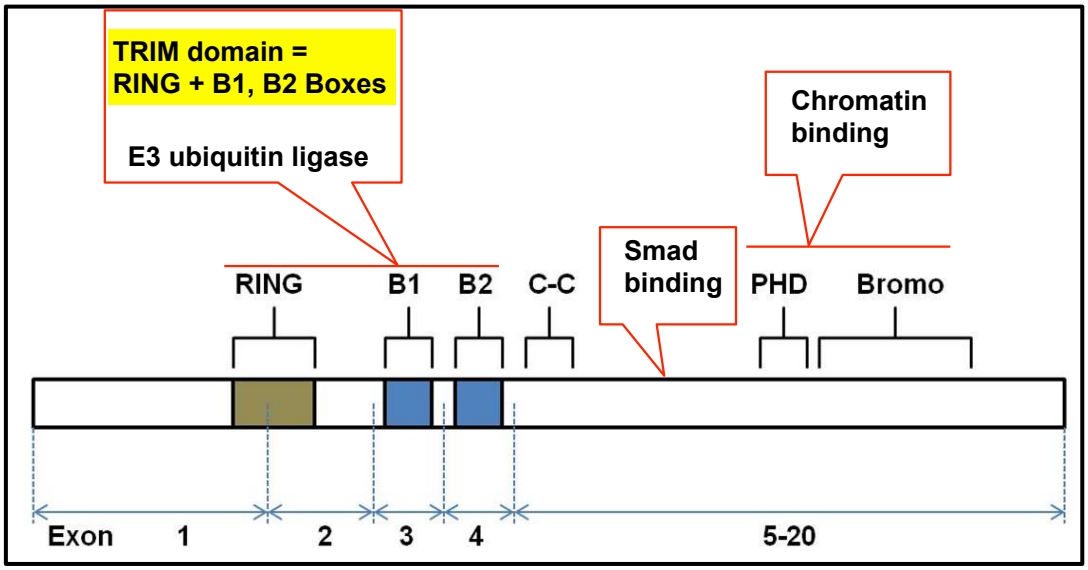

Figure 2.1. Schematic of Trim33 protein domains. The C-terminal TRIM domain itself comprises the RING, B1 and B2 boxes, which function as an E3 ubiquitin ligase, an intervening consensus Smad binding region has been described along with PHD and Bromo domains that function in chromatin binding and interactions with modified histone proteins. Exons 1- 20 are corresponding *Trim33* exons.

Trim33 and closely related proteins

Trim33 forms oligomers with Trim24 and Trim28 and the three proteins share approximately 40% sequence identity with each other (Yan et al., 2004). Both Trim24 and Trim28 have a PXVXL domain that mediates binding with heterochromatin family of proteins such as HP1 (Herquel et al., 2011). Trim33 by itself has been shown to function as a multivalent chromatin-binding module via its PHD and Bromo domains that binds specific histone H3 tails (Massague and Xi, 2012). It is noteworthy that given the similarity in sequence and protein domains, Trim33 is reportedly the only protein known Trim family member to date to bind Smad proteins, Smad2/3 and Smad4 (Agricola et al., 2011; Morikawa et al., 2013; Xi et al., 2011).

Trim33 expression in the mouse

Trim33 is ubiquitously expressed until embryonic day 10 in the mouse and comparatively highly expressed in the brain and spinal cord epithelium in later embryonic stages (Xi et al., 2011; Yan et al., 2004). Developing sensory epithelia such as the oro-nasal epithelia and developing organs such as the thymus, lung, stomach, intestine, liver, and kidney cortex show prominent expression in *in situ* hybridization assays. Northern Blot analyses at postnatal day 10 in the mouse (P10) show expression in the heart, brain, spleen, lung, liver, kidney and testis, with barely detectable expression in skeletal muscle (Yan et al., 2004).

Trim33 and TGF-β signaling in development and disease

The role of *Trim33* in development was first elucidated in the xenopus where *Trim33* was discovered in a screen of ectoderm determinants and was shown to control early germ cell specification (Dupont et al., 2005). Later in the mouse, Trim33 was shown to negatively regulate Smad4 in early patterning and *Trim33* mutants die during gastrulation or early somitogenesis (Kim and Kaartinen, 2008; Morsut et al., 2010). Thus, in different contexts, *Trim33* was consistently shown to regulate TGF-β signaling. In part, the negative regulation of TGF-β signaling by Trim33 is attributed to monoubiquitination of Smad4 by the RING domain, which in turn affects Smad4 residence time within the nucleus (Agricola et al., 2011; Dupont et al., 2012).

Several studies have indicated the role of *Trim33* in hematopoietic cells. *Trim33* is shown to be critical for hematopoietic cell fate in development as well as adult hematopoiesis and ageing of hematopoietic cells (Kusy et al., 2011; Kusy and Romeo, 2011; Ransom et al., 2004). In early cell fate determination, Trim33 regulates the differentiation response in hematopoietic progenitor cells in a Smad4 -independent manner (He et al., 2006). Aligned with its role in hematopoiesis, *Trim33* has a tumor suppressor role in chronic myelomonocytic leukemia (Aucagne et al., 2011a; Aucagne et al., 2011b).

Trim33 and Smad4 have redundant functions in regulating neural cell fates in the developing cortex (Falk et al., 2014) and share the redundancy with Transforming growth factor-β activated kinase 1 (*Tak1)*, a key transducer of Smad -independent signaling, in palatal fusion (Lane et al., 2015). In the context

of mammary epithelial cells, however, Trim33 inhibits Smad4 and is required for their terminal differentiation and lactation (Hesling et al., 2013), also effecting antagonistic responses to Smad4 mediated epithelial –to -mesenchymal transformation (EMT) (Hesling et al., 2011).

Trim33 in other contexts

Trim33 is recruited to DNA damage sites in a Poly ADP Ribose Polymerase (PARP) -dependent manner and participates in regulating the DNA damage response by limiting the activity of "Amplified in Liver Cancer" 1 (ALC1), a chromatin remodeling enzyme; cells lacking Trim33 have higher sensitivity for DNA damage (Kulkarni et al., 2013). This is consistent with the function of *Trim33* as a tumor suppressor in cancer cells (Hatakeyama, 2011), where loss of *Trim33* results in accumulation of chromosomal defects (Pommier et al., 2015) and its function as a component of APC/C-mitotic checkpoint complex (Sedgwick et al., 2013). Others have shown that the Trim33 function as a tumor suppressor is due to its role in degrading nuclear beta catenin (Xue et al., 2015). Apart from experimental data in mouse models, data from humans are consistent with the tumor suppressor role of *Trim33* (Aucagne et al., 2011a; Jain et al., 2011; Natrajan et al., 2007; Vincent et al., 2009). Additionally, autoantibodies to Trim33 have been reported in cases of dermatomyositis (Fiorentino et al., 2015; Mohassel et al., 2015; Valenzuela et al., 2014). In clinical specimens from clear cell renal cell carcinoma (ccRCC), a histological subtype of RCC, miR-629 has been shown to regulate TGF-β/Smad signaling in a *Trim33* -dependent manner.

Specifically, miR-629 directly and negatively regulates *Trim33* expression resulting in inhibition of the TGF-β pathway. Pathological grades and stages of ccRCC specimens show down regulation of *Trim33*, consistent with its postulated tumor suppressor role (Jingushi et al., 2015).

.

***Trim33* in embryonic stem cells/progenitor cell fate regulation**

In poised master regulators of differentiation in mES cells, Trim33 utilizes the dual histone mark H3K9me3K18ac as a differentiation switch. Upon Nodal stimulation, Trim33 -Smad2/3 complexes are formed simultaneous to Smad2/3 and Smad4 complexes. The association of Trim33 - Smad2/3 and H3K9me3K18ac displaces Hetero Chromatin Protein 1 gamma (HP1γ), a chromatin repressor and allows Smad2/3 - Smad4 complexes to access Nodal responsive elements, which in turn facilitates RNA Polymerase II (PolII) recruitment allowing *Gsc* and *Mixl1* transcription (Massague and Xi, 2012; Xi et al., 2011). *Trim33* functions as a cell fate regulator in erythroid precursor cells by functioning as an elongation factor and by countering PolII pausing (Bai et al., 2010). *Trim33* regulates the balance of cell fate choice of hematopoietic stem cells between lymphoid and myeloid lineages in a TGF-β signaling dependent manner (Quere et al., 2014).

Trim33 and open questions pertaining to fine tuning mechanisms of TGF-β signaling

In summary, in the context of development and stem cell/progenitor cell differentiation, Trim33 binds phosphorylated Smad2/3 (pSmad2/3) and regulates TGF-β signaling in a Smad4-dependent or Smad4 -independent manner. The question of Smad4 dependency here is not limited to the preferential binding of Trim33 with pSmad2/3 alone but also affected by regulation of residence time of Smad4 within the nucleus due to monoubiquitination by Trim33 (Agricola et al., 2011; Wrana, 2009). Whether Smad4 -dependent or not, an additional aspect pertinent to the understanding of context-dependent role of Trim33 is the function of Trim33 - pSmad2/3 complex as a chromatin reader and poised genes that regulate lineage fates (Xi et al., 2011). Thus, given its versatility of function, Trim33 is a candidate co-regulator of TGF-β signaling in contexts where Smad2/3 loss of function phenotypes cannot be reconciled with Smad4 loss of function phenotypes (Akhurst and Padgett, 2015). Moreover, it is imperative to examine the function of Trim33 in contexts where the dose of TGF-β signaling is tightly and dynamically regulated such that subtle perturbations in dosage result in abnormal outcomes of varying severity.

References

Agricola, E., Randall, R.A., Gaarenstroom, T., Dupont, S., Hill, C.S., 2011. Recruitment of TIF1gamma to chromatin via its PHD finger-bromodomain activates its ubiquitin ligase and transcriptional repressor activities. Mol. Cell 43, 85-96.

Akhurst, R.J., Padgett, R.W., 2015. Matters of context guide future research in TGFbeta superfamily signaling. Science signaling 8, re10.

Aucagne, R., Droin, N., Paggetti, J., Lagrange, B., Largeot, A., Hammann, A., Bataille, A., Martin, L., Yan, K.P., Fenaux, P., Losson, R., Solary, E., Bastie, J.N., Delva, L., 2011a. Transcription intermediary factor 1gamma is a tumor suppressor in mouse and human chronic myelomonocytic leukemia. J. Clin. Invest. 121, 2361-2370.

Aucagne, R., Droin, N., Solary, E., Bastie, J.N., Delva, L., 2011b. [TIF1gamma: a tumor suppressor gene in chronic myelomonocytic leukemia]. Med. Sci. (Paris) 27, 696-698.

Bai, X., Kim, J., Yang, Z., Jurynec, M.J., Akie, T.E., Lee, J., LeBlanc, J., Sessa, A., Jiang, H., DiBiase, A., Zhou, Y., Grunwald, D.J., Lin, S., Cantor, A.B., Orkin, S.H., Zon, L.I., 2010. TIF1gamma controls erythroid cell fate by regulating transcription elongation. Cell 142, 133-143.

Beckstead, R.B., Ner, S.S., Hales, K.G., Grigliatti, T.A., Baker, B.S., Bellen, H.J., 2005. Bonus, a Drosophila TIF1 homolog, is a chromatin-associated protein that acts as a modifier of position-effect variegation. Genetics 169, 783-794.

Borden, K.L., 2000. RING domains: master builders of molecular scaffolds? J. Mol. Biol. 295, 1103-1112.

Dupont, S., Inui, M., Newfeld, S.J., 2012. Regulation of TGF-beta signal transduction by mono- and deubiquitylation of Smads. FEBS Lett. 586, 1913-1920.

Dupont, S., Zacchigna, L., Cordenonsi, M., Soligo, S., Adorno, M., Rugge, M., Piccolo, S., 2005. Germ-layer specification and control of cell growth by Ectodermin, a Smad4 ubiquitin ligase. Cell 121, 87-99.

Falk, S., Joosten, E., Kaartinen, V., Sommer, L., 2014. Smad4 and Trim33/Tif1gamma redundantly regulate neural stem cells in the developing cortex. Cereb. Cortex 24, 2951-2963.

Fiorentino, D.F., Kuo, K., Chung, L., Zaba, L., Li, S., Casciola-Rosen, L., 2015. Distinctive cutaneous and systemic features associated with antitranscriptional intermediary factor-1gamma antibodies in adults with dermatomyositis. J. Am. Acad. Dermatol. 72, 449-455.

Gozani, O., Karuman, P., Jones, D.R., Ivanov, D., Cha, J., Lugovskoy, A.A., Baird, C.L., Zhu, H., Field, S.J., Lessnick, S.L., Villasenor, J., Mehrotra, B., Chen, J., Rao, V.R., Brugge, J.S., Ferguson, C.G., Payrastre, B., Myszka, D.G., Cantley, L.C., Wagner, G., Divecha, N., Prestwich, G.D., Yuan, J., 2003. The PHD finger of the chromatin-associated protein ING2 functions as a nuclear phosphoinositide receptor. Cell 114, 99-111.

Hatakeyama, S., 2011. TRIM proteins and cancer. Nat. Rev. Cancer 11, 792-804.

He, W., Dorn, D.C., Erdjument-Bromage, H., Tempst, P., Moore, M.A., Massague, J., 2006. Hematopoiesis controlled by distinct TIF1gamma and Smad4 branches of the TGFbeta pathway. Cell 125, 929-941.

Herquel, B., Ouararhni, K., Davidson, I., 2011. The TIF1alpha-related TRIM cofactors couple chromatin modifications to transcriptional regulation, signaling and tumor suppression. Transcription 2, 231-236.

Hesling, C., Fattet, L., Teyre, G., Jury, D., Gonzalo, P., Lopez, J., Vanbelle, C., Morel, A.P., Gillet, G., Mikaelian, I., Rimokh, R., 2011. Antagonistic regulation of EMT by TIF1gamma and Smad4 in mammary epithelial cells. EMBO Rep 12, 665-672.

Hesling, C., Lopez, J., Fattet, L., Gonzalo, P., Treilleux, I., Blanchard, D., Losson, R., Goffin, V., Pigat, N., Puisieux, A., Mikaelian, I., Gillet, G., Rimokh, R., 2013. Tif1gamma is essential for the terminal differentiation of mammary alveolar epithelial cells and for lactation through SMAD4 inhibition. Development 140, 167-175.

Ikeda, K., Inoue, S., 2012. TRIM proteins as RING finger E3 ubiquitin ligases. Adv. Exp. Med. Biol. 770, 27-37.

Jain, S., Singhal, S., Francis, F., Hajdu, C., Wang, J.H., Suriawinata, A., Wang, Y.Q., Zhang, M., Weinshel, E.H., Francois, F., Pei, Z.H., Lee, P., Xu, R.L., 2011. Association of overexpression of TIF1gamma with colorectal carcinogenesis and advanced colorectal adenocarcinoma. World J. Gastroenterol. 17, 3994-4000.

Jingushi, K., Ueda, Y., Kitae, K., Hase, H., Egawa, H., Ohshio, I., Kawakami, R., Kashiwagi, Y., Tsukada, Y., Kobayashi, T., Nakata, W., Fujita, K., Uemura, M., Nonomura, N., Tsujikawa, K., 2015. miR-629 Targets TRIM33 to Promote TGFbeta/Smad Signaling and Metastatic Phenotypes in ccRCC. Mol. Cancer Res. 13, 565-574.

Kim, J., Kaartinen, V., 2008. Generation of mice with a conditional allele for Trim33. Genesis 46, 329-333.

Kulkarni, A., Oza, J., Yao, M., Sohail, H., Ginjala, V., Tomas-Loba, A., Horejsi, Z., Tan, A.R., Boulton, S.J., Ganesan, S., 2013. Tripartite Motif-containing 33 (TRIM33) protein functions in the poly(ADP-ribose) polymerase (PARP)-dependent DNA damage response through interaction with Amplified in Liver Cancer 1 (ALC1) protein. J. Biol. Chem. 288, 32357-32369.

Kusy, S., Gault, N., Ferri, F., Lewandowski, D., Barroca, V., Jaracz-Ros, A., Losson, R., Romeo, P.H., 2011. Adult hematopoiesis is regulated by TIF1gamma, a repressor of TAL1 and PU.1 transcriptional activity. Cell stem cell 8, 412-425.

Kusy, S., Romeo, P.H., 2011. [TIF1gamma is a chief conductor of the hematopoietic system]. Med. Sci. (Paris) 27, 698-700.

Lane, J., Yumoto, K., Azhar, M., Ninomiya-Tsuji, J., Inagaki, M., Hu, Y., Deng, C.X., Kim, J., Mishina, Y., Kaartinen, V., 2015. Tak1, Smad4 and Trim33 redundantly mediate TGF-beta3 signaling during palate development. Dev. Biol. 398, 231-241.

Marin, I., 2012. Origin and diversification of TRIM ubiquitin ligases. PLoS One 7, e50030.

Massague, J., Xi, Q., 2012. TGF-beta control of stem cell differentiation genes. FEBS Lett. 586, 1953-1958.

Meroni, G., 2012. Preface. TRIM/RBCC proteins. Adv. Exp. Med. Biol. 770, vii-viii.

Meroni, G., Diez-Roux, G., 2005. TRIM/RBCC, a novel class of 'single protein RING finger' E3 ubiquitin ligases. Bioessays 27, 1147-1157.

Mohassel, P., Rosen, P., Casciola-Rosen, L., Pak, K., Mammen, A.L., 2015. Expression of the dermatomyositis autoantigen transcription intermediary factor 1gamma in regenerating muscle. Arthritis & rheumatology (Hoboken, N.J.) 67, 266-272.

Morikawa, M., Koinuma, D., Miyazono, K., Heldin, C.H., 2013. Genome-wide mechanisms of Smad binding. Oncogene 32, 1609-1615.

Morsut, L., Yan, K.P., Enzo, E., Aragona, M., Soligo, S.M., Wendling, O., Mark, M., Khetchoumian, K., Bressan, G., Chambon, P., Dupont, S., Losson, R., Piccolo, S., 2010. Negative control of Smad activity by ectodermin/Tif1gamma patterns the mammalian embryo. Development 137, 2571-2578.

Natrajan, R., Williams, R.D., Grigoriadis, A., Mackay, A., Fenwick, K., Ashworth, A., Dome, J.S., Grundy, P.E., Pritchard-Jones, K., Jones, C., 2007. Delineation of a 1Mb breakpoint region at 1p13 in Wilms tumors by fine-tiling oligonucleotide array CGH. Genes Chromosomes Cancer 46, 607-615.

Petrera, F., Meroni, G., 2012. TRIM proteins in development. Adv. Exp. Med. Biol. 770, 131-141.

Pommier, R.M., Gout, J., Vincent, D.F., Alcaraz, L.B., Chuvin, N., Arfi, V., Martel, S., Kaniewski, B., Devailly, G., Fourel, G., Bernard, P., Moyret-Lalle, C., Ansieau, S., Puisieux, A., Valcourt, U., Sentis, S., Bartholin, L., 2015. TIF1-gamma Suppresses Tumor Progression by Regulating Mitotic Checkpoints and Chromosomal Stability. Cancer Res.

Quere, R., Saint-Paul, L., Carmignac, V., Martin, R.Z., Chretien, M.L., Largeot, A., Hammann, A., Pais de Barros, J.P., Bastie, J.N., Delva, L., 2014. Tif1gamma regulates the TGF-beta1 receptor and promotes physiological aging of hematopoietic stem cells. Proc. Natl. Acad. Sci. U. S. A. 111, 10592-10597.

Ransom, D.G., Bahary, N., Niss, K., Traver, D., Burns, C., Trede, N.S., Paffett-Lugassy, N., Saganic, W.J., Lim, C.A., Hersey, C., Zhou, Y., Barut, B.A., Lin, S., Kingsley, P.D., Palis, J., Orkin, S.H., Zon, L.I., 2004. The zebrafish moonshine gene encodes transcriptional intermediary factor 1gamma, an essential regulator of hematopoiesis. PLoS Biol. 2, E237.

Reymond, A., Meroni, G., Fantozzi, A., Merla, G., Cairo, S., Luzi, L., Riganelli, D., Zanaria, E., Messali, S., Cainarca, S., Guffanti, A., Minucci, S., Pelicci, P.G., Ballabio, A., 2001. The tripartite motif family identifies cell compartments. EMBO J. 20, 2140-2151.

Sedgwick, G.G., Townsend, K., Martin, A., Shimwell, N.J., Grand, R.J., Stewart, G.S., Nilsson, J., Turnell, A.S., 2013. Transcriptional intermediary factor 1gamma binds to the anaphase-promoting complex/cyclosome and promotes mitosis. Oncogene 32, 4622-4633.

Short, K.M., Cox, T.C., 2006. Subclassification of the RBCC/TRIM superfamily reveals a novel motif necessary for microtubule binding. J. Biol. Chem. 281, 8970-8980.

Valenzuela, A., Chung, L., Casciola-Rosen, L., Fiorentino, D., 2014. Identification of clinical features and autoantibodies associated with calcinosis in dermatomyositis. JAMA dermatology 150, 724-729.

Vincent, D.F., Yan, K.P., Treilleux, I., Gay, F., Arfi, V., Kaniewski, B., Marie, J.C., Lepinasse, F., Martel, S., Goddard-Leon, S., Iovanna, J.L., Dubus, P., Garcia, S., Puisieux, A., Rimokh, R., Bardeesy, N., Scoazec, J.Y., Losson, R., Bartholin, L., 2009. Inactivation of TIF1gamma cooperates with Kras to induce cystic tumors of the pancreas. PLoS genetics 5, e1000575.

Wrana, J.L., 2009. The secret life of Smad4. Cell 136, 13-14.

Xi, Q., Wang, Z., Zaromytidou, A.I., Zhang, X.H., Chow-Tsang, L.F., Liu, J.X., Kim, H., Barlas, A., Manova-Todorova, K., Kaartinen, V., Studer, L., Mark, W.,

Patel, D.J., Massague, J., 2011. A poised chromatin platform for TGF-beta access to master regulators. Cell 147, 1511-1524.

Xue, J., Chen, Y., Wu, Y., Wang, Z., Zhou, A., Zhang, S., Lin, K., Aldape, K., Majumder, S., Lu, Z., Huang, S., 2015. Tumour suppressor TRIM33 targets nuclear beta-catenin degradation. Nature communications 6, 6156.

Yan, K.P., Dolle, P., Mark, M., Lerouge, T., Wendling, O., Chambon, P., Losson, R., 2004. Molecular cloning, genomic structure, and expression analysis of the mouse transcriptional intermediary factor 1 gamma gene. Gene 334, 3-13.

Zeng, L., Zhou, M.M., 2002. Bromodomain: an acetyl-lysine binding domain. FEBS Lett. 513, 124-128.

CHAPTER 3

Synopsis of experimental mouse mutants for TGF-β R-Smads and Smad4

As described in Chapter2, Smad2/3 and Smad4 are the main transducers of the activated, canonical TGF-β, Nodal/Activin pathway. Both Smad2/3 and Smad4 regulate signal duration and intensity differentially. However, precise mechanisms that modulate the functional and phenotypic differences attributed to Smad2/3 and Smad4 are poorly understood. With respect to this work investigating the role Trim33 - a co-regulator of both activated Smad2/3 and Smad4 in embryogenesis, it is important to review the relevant phenotypes pertaining to experimental mouse mutants for Smad2/3 and Smad4. Table 3.1 summarizes key phenotypes in experimental mouse models pertaining to *Smad* genes involved in the TGF-β pathway.

Genetic alteration	Experimental condition	Phenotype	Reference(s)
Smad $^{-/-}$	Germline deletion	Lack of mesoderm induction. Embryonic lethal between E7.5 – E8.5	(Nomura and Li, 1998; Waldrip et al., 1998; Weinstein et al., 1998)
Smad2 $^{-/+}$	Germline deletion	One fifth of the mice show gastrulation defects, craniofacial abnormalities, cyclopia	(Nomura and Li, 1998; Weinstein et al., 1998)
Smad2 $^{-/-}$	*Smad2-/-* ES	Embryonic lethal at	(Heyer et al.,

	cells in tetraploid complementation with wild type embryos	E10.5	1999)
Smad3 $^{-/-}$	Germline deletion	Colorectal carcinomas at 4-6 months and chronic infections due to lack of immune response	(Zhu et al., 1998)
Smad3 $^{-/+}$	Germline deletion	No obvious phenotype	(Zhu et al., 1998)
Smad4 $^{-/-}$	Germline deletion	Lack of distinct delineation of embryonic and extra-embryonic compartments, lack of the mesoderm, abnormal development of visceral endoderm. Embryonic lethal between E6.5 – E8.5.	(Sirard et al., 1998; Yang et al., 1998)
Smad4 $^{-/+}$	Germline deletion	Gastric and deudenal polyps > 1 year	(Takaku et al., 1999)
Smad2 $^{-/-}$ ***Smad3*** $^{-/-}$	Germline deletion	Failure to gastrulate	(Dunn et al., 2004)
Smad2 $^{-/+}$ ***Smad3*** $^{-/+}$	Germline deletion	Midline defects, defects in cardiac looping	(Liu et al., 2004)
Smad2 $^{-/-}$	Epiblast-specific deletion	Defects in precursors of the anterior definitive endoderm and prechordal plate	(Vincent et al., 2003)
Smad2 $^{dex2-/-}$	Epiblast-specific	Cardiac looping defect	(Heyer et al.,

	deletion		1999)
Smad4 $^{-/-}$	Epiblast-specific deletion	Midline defects in anterior primitive streak derivatives, looping defect of the heart	(Chu et al., 2004)

Table 3.1 Key phenotypes in experimental mouse models of *Smad* genes in the TGF-β signaling pathway.

Smad2/3 and *Smad4* loss-of-function defects share phenotypic similarities with epiblast-specific *Trim33* mutants

Comparison of germline *Smad2/3* and *Smad4* mutants show overlapping phenotypes with few differences in tissue specificity (Table 3.1). *Smad2* defects phenocopy mesendoderm defects and other phenotypes of *Nodal* and *Activin* receptor mutants; consistent with the fact that both Nodal/Activin receptors transduce signals via Smad2/3 and Smad4 (Conlon et al., 1994) and (Table 1.1). Within the *Smad2* mutants, loss of *Smad2* in a background of wild type extra embryonic tissues does not result in defects of mesendoderm induction, indicating that mesoderm induction is independent of Smad2 function in the embryo proper but a result of Smad2 function in the extra embryonic tissues.

Compared to *Smad2* and *Smad4* germline mutants, *Trim33* germline mutants survive slightly longer up to E9, i.e. past neurulation and into the early somite stage (Kim and Kaartinen, 2008).

It is critical to note that concurrent loss of *Smad2* and *Smad3* highlights redundancy as well differential regulation and dose sensitivity to TGF-β signals in

morphogenesis as demonstrated by phenotypes observed in compound *Smad2/3* mutants. The early cardiac looping defects observed in compound heterozygous *Smad2/3* mutants and epiblast-specific *Smad2*$^{dex2-/-}$ as well as epiblast-specific *Smad4*$^{-/-}$ mice implies that early cardiac morphogenesis is sensitive to TGF-β signaling dose and is consistent with cardiac defects and spatio-temporal role of *Trim33* in the embryo proper described in Chapter 5 here.

Although epiblast-specific *Trim33* mutants clearly advance beyond the cardiac looping stage, similarity with the tissue type affected in the epiblast-specific *Smad2 and Smad4* mutants implies that Trim33, Smad2/3 and Smad4 regulate identical or overlapping processes in cardiac morphogenesis.

References

Chu, G.C., Dunn, N.R., Anderson, D.C., Oxburgh, L., Robertson, E.J., 2004. Differential requirements for Smad4 in TGFbeta-dependent patterning of the early mouse embryo. Development 131, 3501-3512.

Conlon, F.L., Lyons, K.M., Takaesu, N., Barth, K.S., Kispert, A., Herrmann, B., Robertson, E.J., 1994. A primary requirement for nodal in the formation and maintenance of the primitive streak in the mouse. Development 120, 1919-1928.

Dunn, N.R., Vincent, S.D., Oxburgh, L., Robertson, E.J., Bikoff, E.K., 2004. Combinatorial activities of Smad2 and Smad3 regulate mesoderm formation and patterning in the mouse embryo. Development 131, 1717-1728.

Heyer, J., Escalante-Alcalde, D., Lia, M., Boettinger, E., Edelmann, W., Stewart, C.L., Kucherlapati, R., 1999. Postgastrulation Smad2-deficient embryos show defects in embryo turning and anterior morphogenesis. Proc. Natl. Acad. Sci. U. S. A. 96, 12595-12600.

Kim, J., Kaartinen, V., 2008. Generation of mice with a conditional allele for Trim33. Genesis 46, 329-333.

Liu, Y., Festing, M., Thompson, J.C., Hester, M., Rankin, S., El-Hodiri, H.M., Zorn, A.M., Weinstein, M., 2004. Smad2 and Smad3 coordinately regulate craniofacial and endodermal development. Dev. Biol. 270, 411-426.

Nomura, M., Li, E., 1998. Smad2 role in mesoderm formation, left-right patterning and craniofacial development. Nature 393, 786-790.

Sirard, C., de la Pompa, J.L., Elia, A., Itie, A., Mirtsos, C., Cheung, A., Hahn, S., Wakeham, A., Schwartz, L., Kern, S.E., Rossant, J., Mak, T.W., 1998. The tumor suppressor gene Smad4/Dpc4 is required for gastrulation and later for anterior development of the mouse embryo. Genes Dev. 12, 107-119.

Takaku, K., Miyoshi, H., Matsunaga, A., Oshima, M., Sasaki, N., Taketo, M.M., 1999. Gastric and duodenal polyps in Smad4 (Dpc4) knockout mice. Cancer Res. 59, 6113-6117.

Vincent, S.D., Dunn, N.R., Hayashi, S., Norris, D.P., Robertson, E.J., 2003. Cell fate decisions within the mouse organizer are governed by graded Nodal signals. Genes Dev. 17, 1646-1662.

Waldrip, W.R., Bikoff, E.K., Hoodless, P.A., Wrana, J.L., Robertson, E.J., 1998. Smad2 signaling in extraembryonic tissues determines anterior-posterior polarity of the early mouse embryo. Cell 92, 797-808.

Weinstein, M., Yang, X., Li, C., Xu, X., Gotay, J., Deng, C.X., 1998. Failure of egg cylinder elongation and mesoderm induction in mouse embryos lacking the tumor suppressor smad2. Proc. Natl. Acad. Sci. U. S. A. 95, 9378-9383.

Yang, X., Li, C., Xu, X., Deng, C., 1998. The tumor suppressor SMAD4/DPC4 is essential for epiblast proliferation and mesoderm induction in mice. Proc. Natl. Acad. Sci. U. S. A. 95, 3667-3672.

Zhu, Y., Richardson, J.A., Parada, L.F., Graff, J.M., 1998. Smad3 mutant mice develop metastatic colorectal cancer. Cell 94, 703-714.

CHAPTER 4

Trim33 function at late gastrulation is required for normal embryogenesis: implications for cardiac development

Abstract

TGF-β superfamily signaling plays important, pleiotropic roles in development as well as tissue homeostasis. TGF-β signaling is tightly regulated in a context-specific manner, and thus relatively subtle perturbations in TGF-β signaling strength result in a spectrum of birth defects and disease phenotypes of varying severity. In the canonical TGF-β pathway, receptor-regulated RSmads (Smad2/3) and Smad4 differentially mediate signal duration and intensity. However, the precise mechanisms by which Smad-dependent TGF-β signaling is regulated are still to be elucidated. Here, I show that Trim33 - a co-regulator of both activated TGF-β RSmads and Smad4 controls both visceral endoderm maturation and pre-cardiac mesoderm differentiation. Epiblast-specific *Trim33* mutants die during the second half of gestation as a result of ensuing cardiac failure. Reduction of *Smad4* gene dosage in the *Trim33*-deficient background partially rescues the cardiac phenotype, indicating that excess of Smad-dependent TGF-β signaling contributes to the phenotype. My results imply that *Trim33* is required for appropriate early mesendoderm differentiation soon after its induction, and that in more committed cell lineages *Trim33* is dispensable.

Introduction

TGF-β superfamily signaling is crucial for many important cellular functions during early embryogenesis, such as, maintenance of stem cell pluripotency and differentiation of progenitor cell populations (Wall and Hogan, 1994; Ying et al., 2003). One of the first discovered and best characterized evolutionarily conserved TGF-β functions is Nodal-induced mesendoderm formation during gastrulation (Weeks and Melton, 1987). Upon Nodal binding to Activin receptor complexes, they become activated resulting in phosphorylation of receptor-regulated RSmads, i.e. Smad2/3 (Derynck and Feng, 1997; Massague and Chen, 2000). Subsequently, phosphorylated (p) Smads2/3 form complexes with their obligate binding partner, the common Smad (CoSmad4, referred as Smad4 here) and the pSmad2/3-Smad4 complexes accumulate into the nucleus, where they induce expression of mesendoderm master regulators (*Gsc* and *Mixl1*) (Reissmann et al., 2001; Xi et al., 2011).

While Smad4, as the common Smad, was initially considered to function as a central hub coordinating all TGF-β superfamily signaling events, it soon became evident that TGF-β superfamily signaling can also occur without involvement of R- or CoSmads via the so called Smad-independent (non-canonical) mechanisms (Derynck and Zhang, 2003). Moreover, RSmad mutant phenotypes differ from, and in fact are often more severe than those of Smad4 (Sirard et al., 1998; Wisotzkey et al., 1998) suggesting that RSmads can mediate Smad4-independent signaling events (discussed in Chapter 2 and 3). Consistent with these findings, few p-RSmad binding partners that mediate Smad4-independent

TGF-β functions have been described (Descargues et al., 2008; He et al., 2006b). One of them - Trim33 (Tif1gamma, Ectodermin), was first shown to regulate TGF-β responses in erythropoiesis distinctly from Smad4, via selective binding to activated RSmads (He et al., 2006a).

Tripartite domain containing 33 (Trim33) belongs to the Tif1 subfamily of tripartite domain -containing proteins. In addition to the N-terminal tripartite domain (composed of a RING finger domain, two B-box zinc finger domains, and a coiled coil region), Trim33 contains a Smad binding region, and a tandem of PhD and Bromo domains at its C-terminal end (Venturini et al., 1999). These structural characteristics confer Trim33 both E3 ubiquitin ligase and chromatin binding abilities. Subsequent studies have shown that the effect of Trim33 on TGF-β signaling is plastic and highly context dependent. In epithelial and malignant cell lines, Trim33 is shown to repress TGF-β signaling by monoubiquitinating Smad4 via a mechanism that involves Trim33 - histone interactions (Agricola et al., 2011; Dupont et al., 2009). An opposite role for Trim33 in regulation of TGF-β signaling is shown in mesoderm induction. In this context, Trim33 promotes TGF-β signaling by functioning as a chromatin reader, which regulates access of RSmad/Smad4 transcriptional complexes to their *bona fide* response elements (Xi et al., 2011). A common theme in Trim33-regulated biological events seems to be that its function is limited to situations where differentiation of progenitor cell populations is required, and thus Trim33 has little or no relevance in homeostatic TGF-β responses. Concordantly, tissue-specific *Trim33* mutants show defects in hematopoiesis (Falk et al., 2014; Quere et al.,

2014), in malignant transformation (Aucagne et al., 2011; Pommier et al., 2015; Vincent et al., 2012) and in other physiological and/or pathological conditions where cellular plasticity in required and/or intense tissue remodeling takes place such as terminal differentiation of mammary epithelium and during lactation (Hesling et al., 2013).

While germline *Trim33* mutant mice die during or soon after gastrulation (Kim and Kaartinen, 2008; Morsut et al., 2010), the role of Trim33 in the embryo proper during post-gastrulation development remains largely unknown. Here I show that the loss of *Trim33* in differentiating ES cells immediately after mesoderm induction results in formation of viable embryoid bodies (EBs) that show enhanced ability to beat spontaneously when compared to their wild-type equivalent counterparts. *Trim33*-deficient EBs displayed reduced expression of a number of genes involved in maturation of the visceral endoderm, while only a few genes were upregulated. One of the affected genes was *Ankrd1*, a marker for cardiac distress. Consistent with elevated *Ankrd1 in vitro*, epiblast-specific *Trim33* mutant mouse embryos display atrio-ventricular septal- and myocardial defects, and die during the second half of gestation as a result of ensuing cardiac failure. My results imply that *Trim33* is required for appropriate TGF-β-controlled early mesendoderm differentiation soon after its induction, and that in more committed cell lineages *Trim33* is dispensable.

Experimental Procedures

Ethics Statement

This research was conducted in strict accordance with the recommendations in the Guide for the Care and Use of Laboratory Animals of the National Institutes of Health. Experiments described here are specifically approved by the University Committee on Use and Care of Animals (UCUCA) at the University of Michigan-Ann Arbor (Protocol Number: PRO00005004).

Establishment of embryonic stem cell lines and EB culture

Mouse embryonic stem cells (mESCs) were derived from *Trim33*^{FF}*: UbcCre*^{ERT2} blastocysts as described in (Pieters et al., 2012); mESCs were passaged in serum-containing medium (Life Technologies, Cat. No. 16141-061), dissociated with TrypLE Express (Life Technologies, Cat. No. 12605-010) and maintained in serum replacement medium (Knock Out Serum Replacement Cat No. 10828-010, Life Technologies) in a base medium of 1:1 Knock Out Dulbecco's Modified Eagle's Medium and Ham's F12. *Trim33*^{FF}*:UbcCre*^{ERT2} mESCs were maintained in feeder-free culture conditions in the presence of 2i+LIF. 2i: PD0325901 (Tocris) in final concentration of 0.4μM, CHIR99021 (Stemgent) in final concentration of 3μM and LIF: (1000X) ESGRO (Millipore ESG 1106) on 0.1% gelatin (Sigma, G1393) coated tissue culture plates. Embryoid body (EB) formation and differentiation were carried out per the ATCC protocol in 20% serum containing medium. Both media for non-differentiating and differentiating conditions were supplemented by Glutamine (GlutaMAX-I (100X), Life Technologies, Cat. No. 35050-061), β-mercaptoethanol (1000X, Life

Technologies, Cat. No. 21985-023) and Penicillin/Streptomycin (Life Technologies, Cat. No.15140-122).

4-hydroxytamoxifen (4-OHT) (Sigma Cat. No. T176) was added at intended and precise time points in a concentration of 1 µg per mL of medium. Percentage of beating EBs were counted and averaged in 3 independent sample pairs, in 6 separate areas of each culture dish, at the same time point on Days 9, 10 and 11 in a genotype-blind manner by 2 independent observers.

For relevant experiments, control and *Trim33*-deficient EBs were treated with rhTGF-β3 (R&D Systems, Cat. No. 243-B3) and rh/m/rActivin A (R&D Systems, Cat. No. A338-AC) for 40 minutes in concentrations of 10ng/mL and 100ng/mL respectively.

Mice

$Trim33^{FF}$, *Nkx2_5Cre, Mox2Cre, Sox2Cre,* TCre *and* *$UbcCre^{ERT2}$* and *$Smad4^{FF}$* have been described earlier (Kim and Kaartinen, 2008; Moses et al., 2001; Perantoni et al., 2005; Tallquist and Soriano, 2000; Yang et al., 2002). Timed matings between *$Trim33^{KoWt}$* and appropriate *Cre^{+}* males and *$Trim33^{FF}$* or *$Trim33^{FWt}$* female mice were set up to obtain *$Trim33^{FKo}$:Cre^{+}* tissue-specific mutant embryos *($Trim33^{cKo}$)*. Controls were either *$Trim33^{WtWt}$:Cre^{-}* or *$Trim33^{FWt}$:Cre^{-}* and on occasion *$Trim33^{FWt}$:Cre^{+} ($Trim33^{cHet}$)* where explicitly indicated.

Histology, immunohistochemistry

Mouse embryos were harvested in sterile DBPS and fixed overnight in commercial 10% formalin or freshly made 4% paraformaldehyde in PBS at 4^{o}C overnight (O/N). Samples for histology as well as immunohistochemistry were processed in a standard paraffin-embedding protocol. Briefly, embryonic tissues were washed, dehydrated, oriented in desired plane and embedded in fresh Blue Ribbon Tissue Embedding/Infiltration Medium (Leica Surgipath). 7µm serial sections were mounted on Superfrost plus slides (Fisher) and stored at room temperature or 4°C. Haematoxylin and eosin staining was performed using a standard protocol.

Myocardial thinning in embryonic hearts was quantified by measuring the thickness of compact myocardium in 3 independent sample pairs, in 6 separate areas per sample in serial sections. The thickness measurement was co-related with number of cell layers present by counting nuclei across the thickness of the wall; control measurements were consistent with previously described data (Sedmera et al., 2000).

Immunoflourescent detection of hypoxia levels in oro-facial tissue sections was done using the Hypoxyprobe^{TM}-1 kit per manufacturer's instructions; Hypoxyprobe detects reductive binding to 2-nitroimidazoles in hypoxic cells (Raleigh and Koch, 1990; Varghese et al., 1976).

In situ hybridization (ISH)

DIG-labeled RNA probe for *Trim33* was designed (385 bp, 1156 – 1539, refSeq NM_001079830) to span the targeting strategy for the targeted, *Trim33-floxed* allele in order to discriminate control and $Trim33^{cKo}$ embryos processed together for all experimental steps. *Trim33* ISH probes were generated using a DIG-labeled NTP mix (Roche Applied Sciences) according to manufacturer's instructions, stored at −80, or −20°C diluted in hybridization buffer.
Embryos for whole mount ISH were fixed in freshly thawed 4% paraformaldehyde in PBS O/N, washed in PBST, dehydrated and stored in 95% methanol: 5% PBST at −20°C. Samples thus prepared were Proteinase K-treated (Invitrogen, Cat. No 25530-049 in final concentration of 10µg/ml), post-fixed and pre-hybridized rotating for at least 1 hour in standard non-SDS-based hybridization buffer, pH 5, at 70°C. Probe was added in a final concentration of 0.1–1ng/µl and left rolling overnight. Embryos were subsequently washed in a roller set-up for 20 minutes each, three times in preheated hybridization buffer at 70°C, once in hybridization buffer/TBST, then in at least 6 changes of TBST at room temperature (RT) over 1 hour, blocked in 0.05% Roche block (one hour) and rocked O/N at 4°C with α-alkaline phosphatase (AP) labeled-DIG Fab fragments (Roche Applied Sciences,1:2000–5000). Samples were thoroughly washed with several changes of TBST the next day at room temperature and then O/N at 4°C. On Day 4, samples were equilibrated for 10 minutes (RT) twice in NTMT, pH 9.5 in a roller set up and stained with BM Purple AP substrate at RT in the dark for several hours. Stained embryos were washed thoroughly in PBS, fixed in 4%

paraformaldehyde and stored at 4°C. Stained embryos were imaged and processed for routine genotyping post-staining, post-fixing upon satisfactory documentation of ISH results.

Real-time PCR

Equivalent amounts/number of EBs were collected in 100-200 µl of commercially available (Qiagen) RLT buffer at intended time points. RNA was isolated using (Qiagen RNesy Mini Kit Cat. No 74104) and cDNA was synthesized using Omniscript RT(Qiagen Cat. No.205111) per standard methods. Taqman Assay reagents (Life Technoligies) were used for all targets except *Actb*, which was used to normalize expression levels. Universal Probe Library-based assays (Roche Applied Science) with gene-specific primer sequences were generated using the manufacturer's online algorithm, details are below. 30µl assays dispensed in TaqMan Universal PCR 2X master mix (Applied Biosystems) with or without universal probe were quantified using Applied Biosystems ABI7300 PCR and ViiA7 detection systems and software. All Ct values were manually checked. cDNA was diluted where necessary to avoid Cts lower than 18. At least three independent mutant samples and littermate and stage matched controls were assessed for each genotype/condition.

Taqman assay # are indicated in parenthesis: *Ankrd1* (Mm00496512_m1), *Apob* (Mm01545150_m1), *Apoc2* (Mm00437571_m1), *Gsc* (Mm00650681_g1), *Isl1* (Mm00517585_m1), *Mttp* (Mm00435015_m1), *Nestin* (Mm00450205_m1), *Pouf51* (Mm00658129_gH**),** *Tbx5* (Mm00803518_m1), *Trim33* (Mm01308695_m1).

Actb: Forward Primer (tgacaggatgcagaaggaga), Reverse Primer (cgctcaggaggagcaatg), Universal Probe #106

RNA-Sequencing

Equivalent amounts/number of EBs were collected at Day 7, comprising *Trim33*-deficient and control pairs (n=2 independent pairs), in 100-200 µl commercially available (Qiagen) RLT buffer. Total RNA was isolated using Qiagen RNesy Mini Kit Cat. No 74104. mRNA and sequencing libraries were prepared by the University of Michigan DNA Sequencing Core and reads generated on Illumina HiSeq2000. After quality assessment per sample, single-end, 52 base pair reads were aligned to mm9 (Mus musculus assembly July 2007) using STAR RNA Seq aligner (Dobin et al., 2013). On average, input reads ranged between 35 million to 42 million across all samples, out of which approximately 80 per cent reads mapped uniquely. Read counts for differential expression were obtained using HTSeq program. Differential expression analyses were performed using the DESeq program in R Statistical Package. https://bioconductor.org/packages/3.3/bioc/vignettes/DESeq/inst/doc/DESeq.pdf.

Echocardiography

At day 11.5 dpc, pregnant *Trim33*^{FF} female mice crossed with *Trim33*^{KoWt}*:Sox2Cre*$^{+}$ male mice were anesthetized in an enclosed container filled with 4% Isoflurane and the mice were then placed on a warming pad to maintain body temperature. 1–1.5% Isoflurane was supplied via a nose cone to maintain surgical plane of anesthesia. Hair was removed from the upper abdominal and thoracic area with depilatory cream. Both uteri were surgically accessed and

each embryo was monitored for ECG with non-invasive resting ECG electrodes. Two-dimensional, M-mode, Doppler and tissue Doppler echocardiographic images were recorded using a Visual Sonics' Vevo 770 high resolution *in vivo* micro-imaging system for each embryo in a genotype-blind manner. Data from each embryo recording were systematically indexed and genotyping material was collected to correlate with findings after the actual experiment. Data were recorded for following parameters: heart rate (HR) beats per minute (BPM), velocity mm per second for both dorsal aorta (DA) and umbilical artery (UA), Velocity Time Interval (VTI) in mm for DA and UA, Ejection Time (ET) in msec measured in the DA. Actual measurements obtained are summarized in table 3 below.

Western blot and Immunoprecipitation

Western blot and Immunoprecipitation studies using antibodies against Trim33 (Bethyl # A301-060A), Smad2 (D43B4) XP (Cell Signaling#5339), pSmad2/3 (Cell Signaling #8828), Smad4 (B-8) (Santa Cruz #sc7966) and Atcb (Sigma #A1978;) were carried out using standard procedures and in accordance with manufacturer's instructions. For Western blotting, EBs were lysed in Pierce IP Lysis Buffer (ThermoScientic, Prod# 87787) supplemented with sodium fluoride (NaF) and sodium ortho vanadate (Na_3VO_4) to a final concentration of 1mM. Lysates were prepared per manufacturer's instructions and used in equivalent amounts for Western blotting. Both Trim33-deficient and control samples were treated with TGFβ3 and Activin as described earlier and used as positive controls

to demonstrate alterations in Smad4 and activated (phosphorylated) Smad2/3 levels.

For immunoprecipitation, EBs were gently dissociated on Day 4, and plated onto gelatin-coated dishes. On the following day the dishes were transfected either with the superfolder-gfp (negative control (Pedelacq et al., 2006)) or *Trim33-flag* expression vectors using ViaFect transfection reagent (Promega Cat No. E4981), according to manufacturer's instructions. Two days later the cells were lysed in Pierce IP-lysis buffer (cat no. 87787). The cleared lysates were immunoprecipitated using a rabbit monoclonal anti-Flag antibody (Cell Signaling Technology #14793) and washed precipitates were analyzed using western blotting as outlined above.

Analysis of erythroid progenitors

Embryonic livers were harvested at E13 and mechanically dissociated by pushing with a syringe through a 70μm cell strainer. Cells were immunostained at 4^{o}C in PBS:0.5 % BSA in the presence of PE-conjugated anti-Ter119 (BD-Pharmingen cat#553673) and FITC-conjugated anti-CD71 (BD-Pharmingen cat#553266) antibodies. The cells were washed and analyzed on flow cytometer BD FACSAria II from BD Biosciences.

Statistical Analyses

For histological data and expression (qRT-PCR) assays, three or more samples were analyzed. Averages, standard error and probability (Student's t-test) were calculated and p values of less than or equal to 0.05 was marked as significant.

Results

4-OHT-induced deletion of *Trim33* post mesoderm induction *in vitro* reveals defects in extra-embryonic endoderm and cardiac mesoderm

Earlier studies have elucidated the role of *Trim33* in gastrulation and mesendoderm induction (Morsut et al., 2010; Xi et al., 2011). Using the mES cell-derived EB system, we examined the role of *Trim33* in stages following germ layer specification. To this end, we established embryonic stem cell lines from *Trim33*^{FF}*:UbcCre*^{ERT2} blastocysts as described by (Pieters et al., 2012) (Figure 4.1). The *UbcCre*^{ERT2} transgene (Ruzankina et al., 2007) was used to activate Cre-induced recombination by 4-hydroxytamoxifen (4-OHT) at desired time points resulting in temporally controlled deletion of the targeted, *floxed Trim33* alleles (Kim and Kaartinen, 2008). Since our objective was to investigate the role of Trim33 in normal post-gastrulation events as closely mimicking *in vivo* embryogenesis as possible (within the limits of the embryoid body technique), ES cells were allowed to undergo spontaneous differentiation in suspension culture on ultra-low attachment dishes as described in (http://diyhpl.us/~bryan/irc/protocol-online/protocol-cache/Embryoid_Body_Formation.pdf).

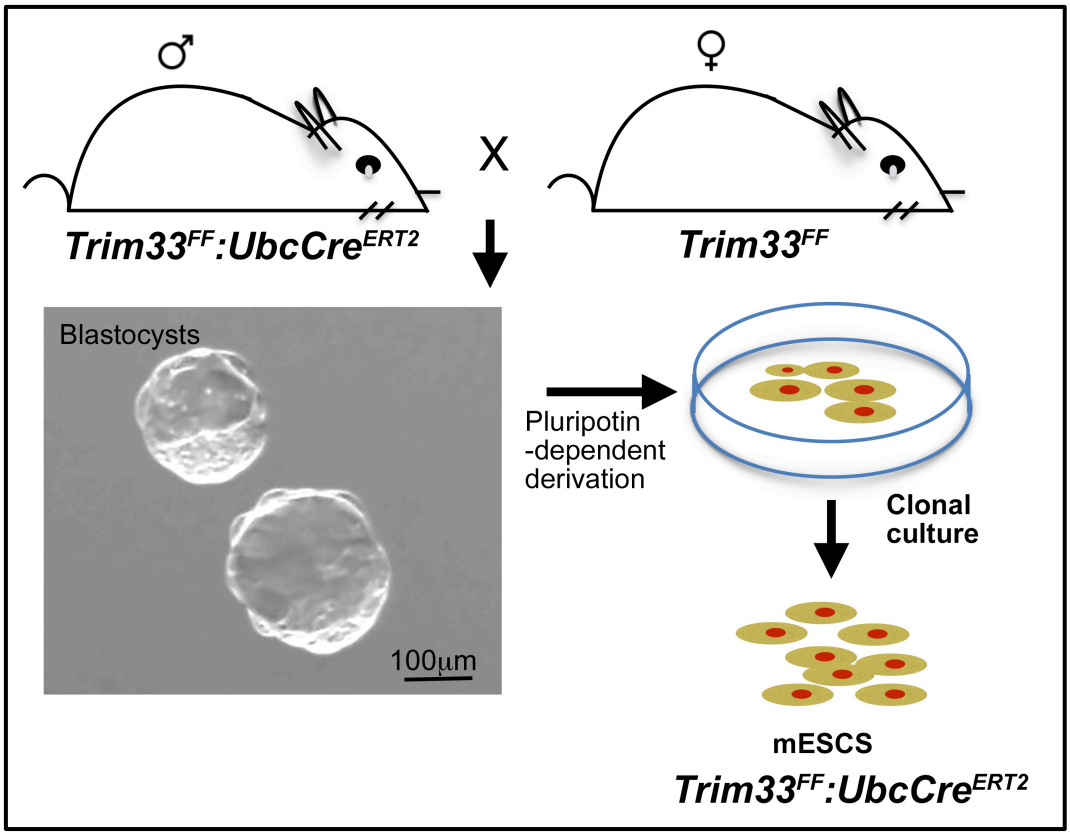

Figure 4.1. Experimental design for derivation of *Trim33^{FF}:UbcCre^{ERT2}* mouse ES cells: *Trim33^{FF}:UbcCre^{ERT2}* blastocysts were harvested from the mouse cross described and mES cells were derived using a pluripotin-based protocol described in (Pieters et al., 2012).

4-OHT was added to the culture media to induce Cre activation at day 4 after initiation of differentiation (Figure 4.2B). Expression levels of the mesodermal marker gene *Gsc* were comparable on Days 5 and 7 between 4-OHT-induced and non-induced control cultures demonstrating that this treatment regimen allowed equivalent mesoderm induction in both 4-OHT negative and positive cultures (Figure 4.2C). Although the *Trim33-floxed* allele was effectively recombined and mRNA repressed within 6 hours after 4-OHT-induction (data not shown), Trim33 protein levels remained unaltered at least for the next 24 hours (Figure 4.2A).

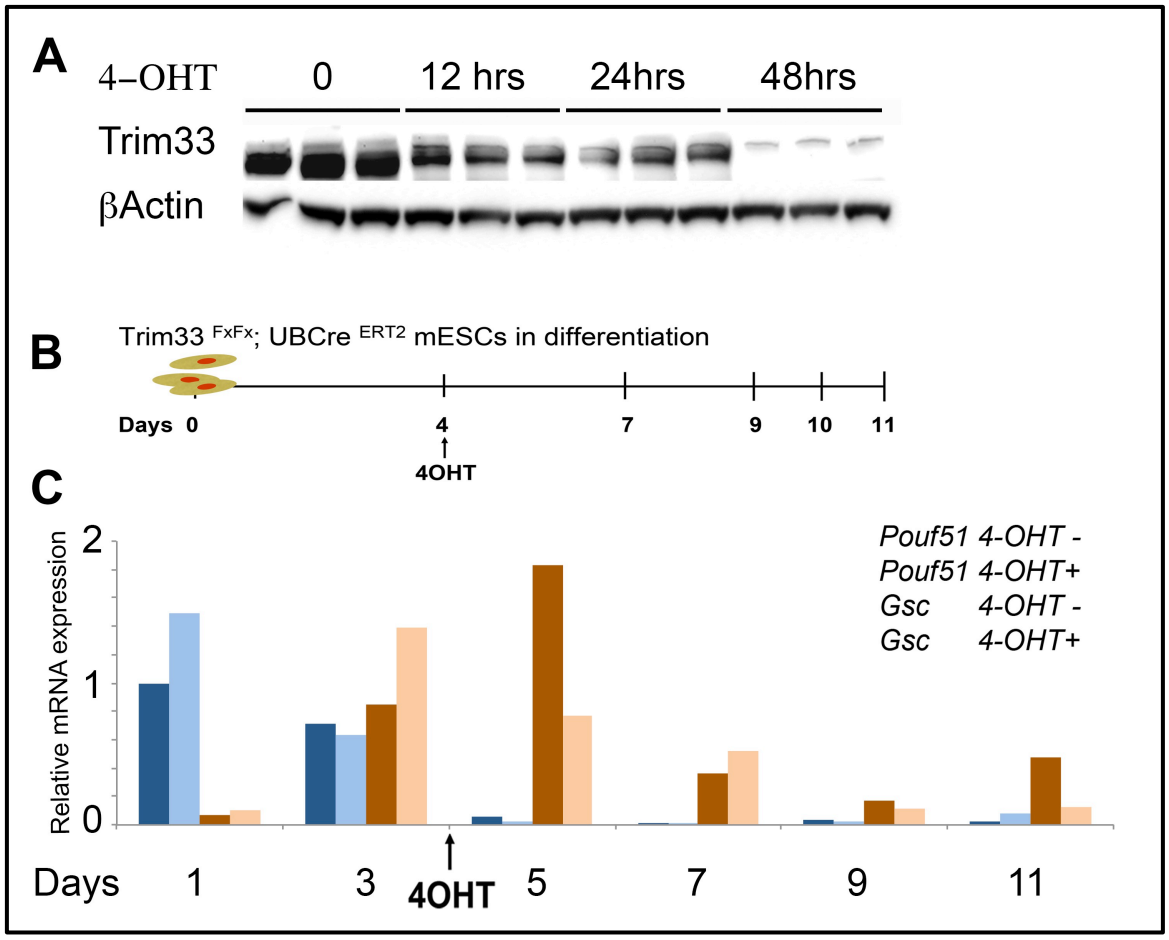

Figure 4.2. Optimization of conditions and time point of *Trim33* deletion *in vitro.*
(A) Trim33 protein is stable for at least 24 hours after 4-OHT induced Cre-recombination in *Trim33*^{FF}:*UbcCre*^{ERT2} mESCs. (B) Schematic presentation to highlight the timing of 4-OHT administration (C) Day 4 induction of *Cre* in *Trim33*^{FF}:*UbcCre*^{ERT2} EBs results in comparable initiation of differentiation assessed by *Pouf51* expression and comparable mesoderm induction assessed by *Gsc* expression. Blue bars represent *Pouf51* expression (dark blue = control, light blue = *Trim33* deficient EBs); brown bars represent *Gsc* expression (dark brown = control, tan = *Trim33* deficient EBs)

Morphological differences between *Trim33*^{FF}:*UbcCre*^{ERT2};4-OHT+ (herein *Trim33* deficient EBs) and control EBs started to become evident on day 8. *Trim33* deficient EBs were smaller and showed less expanded 'balloon-like' cystic appearance. Both mutant and control EBs displayed beating clusters between days 9 and 11; however, the number of contracting or beating EBs was higher in 4-OHT+ versus 4-OHT- cultures (Figure 4.3C).

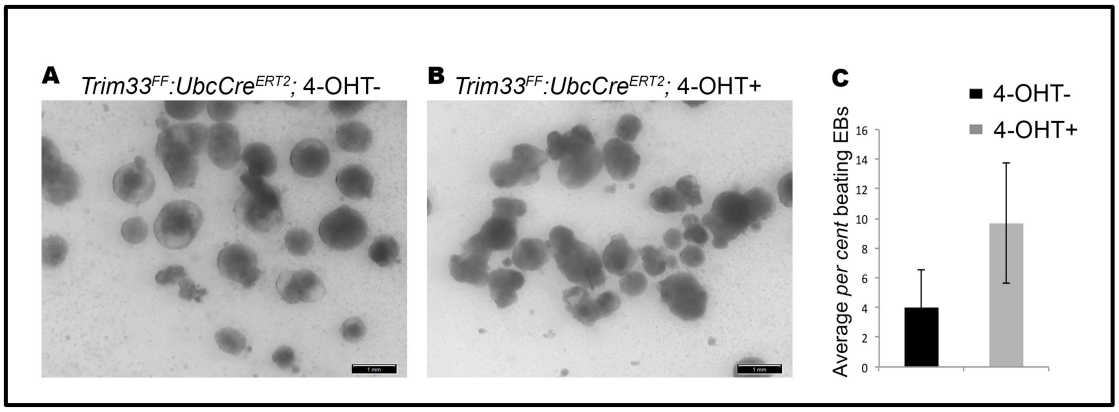

Figure 4.3. *Trim33* deficient EBs show enhanced beating clusters in differentiating culture. **(A)** Control EBs, *Trim33*^{FF}*:UbcCre*^{ERT2}*;*4-OHT- and (B)*Trim33* deficient EBs, *Trim33*^{FF}*:UbcCre*^{ERT2}*;*4-OHT+ (day4 induction) are morphologically similar at day 7, however (C) show an increased number of beating cell clusters between days 9-11. Error bars in C= +/- SEM.

I harvested both the *Trim33*-deficient and control EBs at day 7 (when the mutants and controls still showed grossly comparable appearance) and subjected them to genome-wide RNA-Seq transcriptome analysis (Figure 4.4). Of *Trim33*-dependent genes (>2-fold change; $p<0.05$), 62 were down regulated and only 10 were up regulated (Table 1 in Appendix 1). Confirmation of differential expression of selected genes by qRT-PCR provided results that were fully consistent with those obtained from the RNA-Seq screen (Figure 4.5). Moreover, none of the germ layer marker genes were differentially expressed (DE) in the screen, validating our intended model.

My data shows that a large number of differentially expressed genes (22%) are involved in various aspects of lipid metabolism. These include the gene encoding microsomal triglyceride transport protein (*Mttp*) and genes encoding several different apolipoproteins. During early embryogenesis these genes are mostly expressed in the extraembryonic endoderm, where many of them display critical non-redundant functions as demonstrated by knockout studies. Mttp

homozygous mutants die at mid gestation and half normal dose of Mttp is also not compatible with survival (Huang et al., 1995; Raabe et al., 1998). Moreover, an established extra-embryonic endoderm marker *Afp* (Krumlauf et al., 1986) was almost 30-fold down-regulated in *Trim33* deficient EBs when compared to control EBs. Eight of the differentially expressed genes have been shown to possess transporter activity and 10 of them have been implicated in maintenance of metabolic homeostasis.

Of the up-regulated genes *Shisa3* (4.4-fold up) is a putative transmembrane inhibitor of Wnt signaling (Chen et al., 2014) and *Dusp4* (2-fold up) is a regulator of the Map kinase pathway (Balko et al., 2013). *Nipal1* (11-fold up) has been implicated in pathogenesis of exencephaly and *Ankrd1* (4-fold up) is a (Bogomolovas et al., 2015) marker for cardiac distress. To conclude, morphological and expression profiling experiments in EBs suggested that abrogation of Trim33 after mesoderm induction results in changes in the extra-embryonic endoderm and cardiac mesoderm.

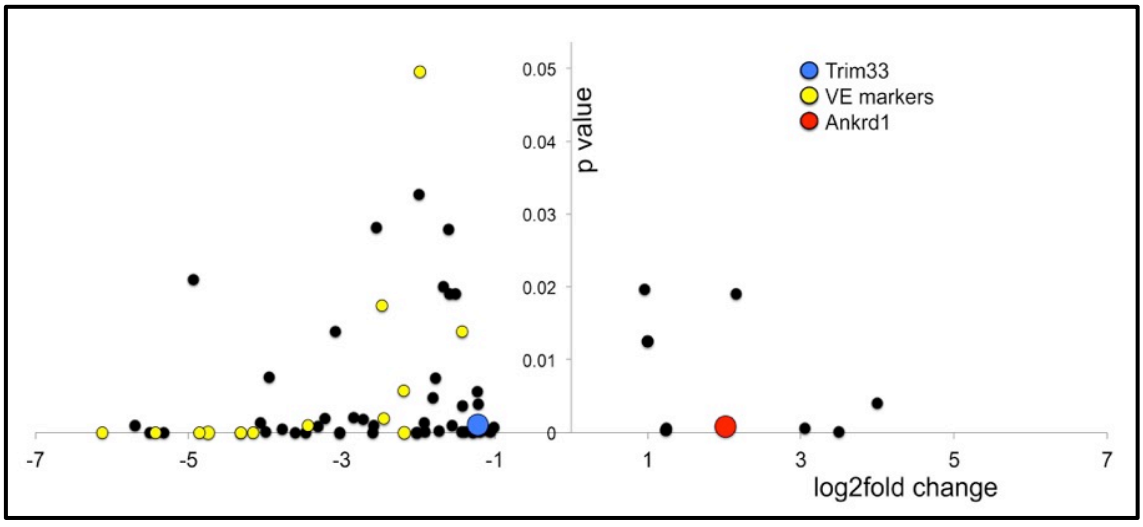

Figure 4.4. Differentially expressed genes in *Trim33*-deficient EBs at day 7 in differentiation. *Trim33*^{FF}*:UbcCre*^{ERT2} mESCs were allowed to differentiate and 4-OHT was added

to the experimental sample at Day4, inducing *Trim33* deletion after mesoderm induction. Control EBs were *Trim33^{FF}:UbcCre^{ERT2} ;* 4-OHT-. EB samples were collected at day 7 for RNA-Seq trancriptomic analyses. Statistically significant, differentially expressed genes include *Trim33* (expected positive control, highlighted in blue), Visceral Endoderm (VE) markers highlighted in yellow and *Ankrd1,* highlighted in red, n=2 independent sample pairs.

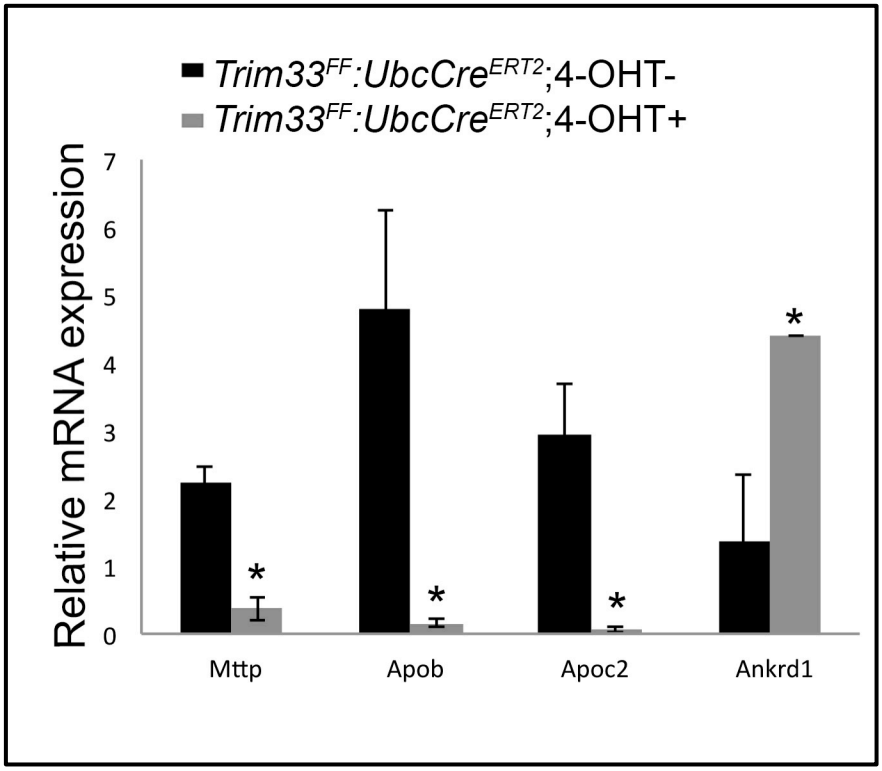

Figure 4.5. qRT-PCR validation of differentially expressed genes in RNA-Seq screen. Among the differentially expressed genes (Figure 5.4 above and Appendix 1, Table 1), *Mttp, Apob, Apoc, Ankrd expression was assayed by qRT-PCR in Trim33*-deficient and control EBs, in exactly same samples as in Figure 5.4. All 4 genes assayed show expected fold change consistent with the results from RNA-Seq data in Figure 5.4. *p < 0.05, error bars = +/- SEM, n = 3 independent sample pairs.

Trim33 interacts with activated Smad2 in differentiated ES cells and Trim33 deficiency results in sustained attenuation of canonical TGF-β signaling

To characterize the role of Trim33 in regulation of TGF-β signaling during developmental events following mesoderm induction, *Flag-tagged Trim33* was transiently expressed in day 7 EBs. Co-immunoprecipitation assay demonstrated that Flag-tagged Trim33 formed a complex with Smad2, and that this complex

formation is further strengthened by Activin induction (100ng/mL, 40 minutes). Under these conditions, complex formation between Trim33 and Smad4 was not detected (Figure 4.6).

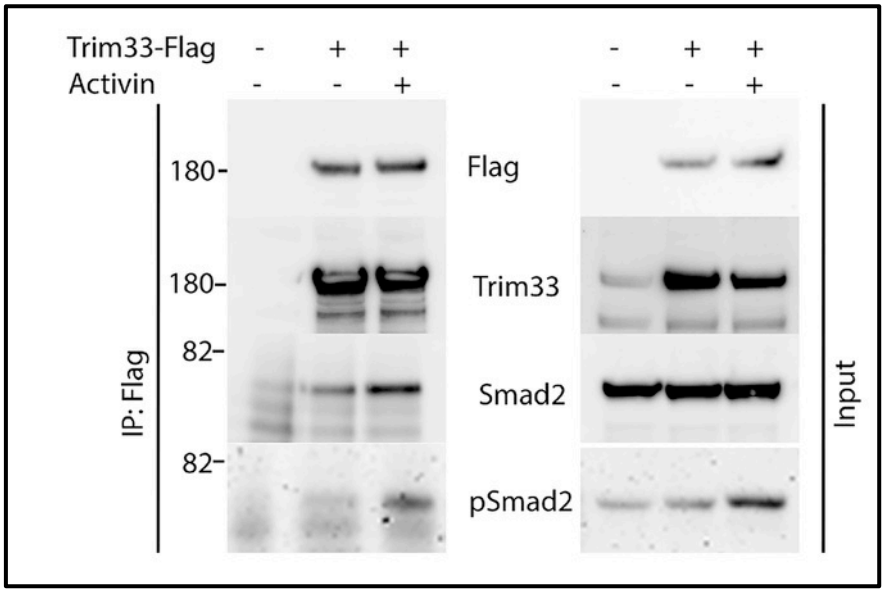

Figure 4.6. Trim33 interacts with activated Smad2 in differentiated ES cells. *Flag-tagged Trim33* was transiently expressed in day 7 EBs. Flag-tagged Trim33 formed a complex with Smad2 in the co-immunoprecipitation assay; this complex formation is further strengthened by Activin induction. Immunoprecipitates were analyzed for the presence of bound proteins using Western blotting.

To determine the effect of Trim33 on regulation of TGF-β signaling after mesoderm induction, I stimulated 4-OHT induced and non-induced EBs with Activin or TGF- β and compared C-terminal Smad2 phosphorylation levels between control and Trim33-deficient samples with or without ligand stimulation. Both control and Trim33-deficient samples responded to ligand stimulation; however, the level of C-terminal Smad2 phosphorylation was less in both unstimulated and stimulated Trim33 deficient samples (Figure 4.7).

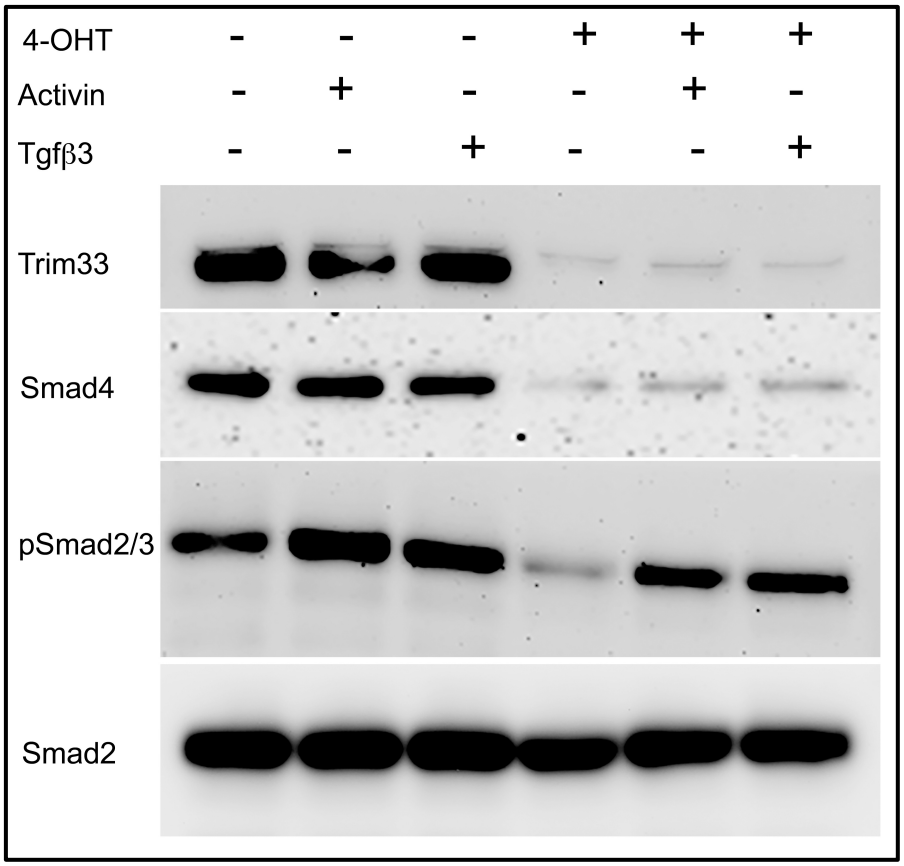

Figure 4.7. Trim33-deficient EBs show reduction in baseline Smad2 phosphorylation and decrease in Smad4 protein levels. *Trim33*^{FF}*:UbcCre*^{ERT2} mESCs in differentiation: 4-OHT was added in the experimental sample at day 4 and both Trim33 deficient and control, 4-OHT- EBs were harvested at day 7. This figure shows results from Western gel/blot analyzing protein lysates for Smad4, Smad2 phosphorylation, and Smad2 protein levels. Activin and Tgfβ stimulation was 40 minutes in appropriate samples.

These experiments show that Trim33 interacts with activated Smad2 in differentiated ES cells and that *Trim33* deficiency results in sustained down-regulation of canonical TGF-β signaling.

Deletion of *Trim33* in the mesodermal lineage *in vivo* does not result in obvious developmental phenotypes

Since *Trim33*-deficient EBs showed differences gene expression of pre-cardiac/cardiac mesoderm, I hypothesized that deletion of *Trim33* in the

mesodermal lineage using *TCre* (Perantoni et al., 2005) would result in developmental defects in mouse embryos. However, living *Trim33^{FF}:TCre* mutant embryos without overt phenotypes were obtained at the expected Mendelian frequency at all stages examined (E13-E18). Detailed histological analysis revealed a subtle delay in the formation of the inter-ventricular septum at E13 (data not shown). In addition, we used *Nkx2-5Cre* and *Tie2Cre* drivers to delete *Trim33* in pre-cardiac mesoderm and in mesoderm-derived endothelium, respectively. In both cases, mutant embryos were obtained without any detectable external or histological phenotypes (data not shown). These experiments suggest that *Trim33* is not required for development of mesodermal cell lineages after their initial specification.

Epiblast–specific *Trim33* mutants are embryonic lethal and show cardiac and craniofacial defects

Since mesoderm-specific *Trim33* mutants showed no clear developmental phenotypes, I first confirmed that *Trim33* is expressed in immediate post gastrulation stages in mouse embryos (Figure 4.8). I observed strong ubiquitous *Trim33* expression at E7-E8.5 in the embryo proper and less intense expression in extra embryonic tissues.

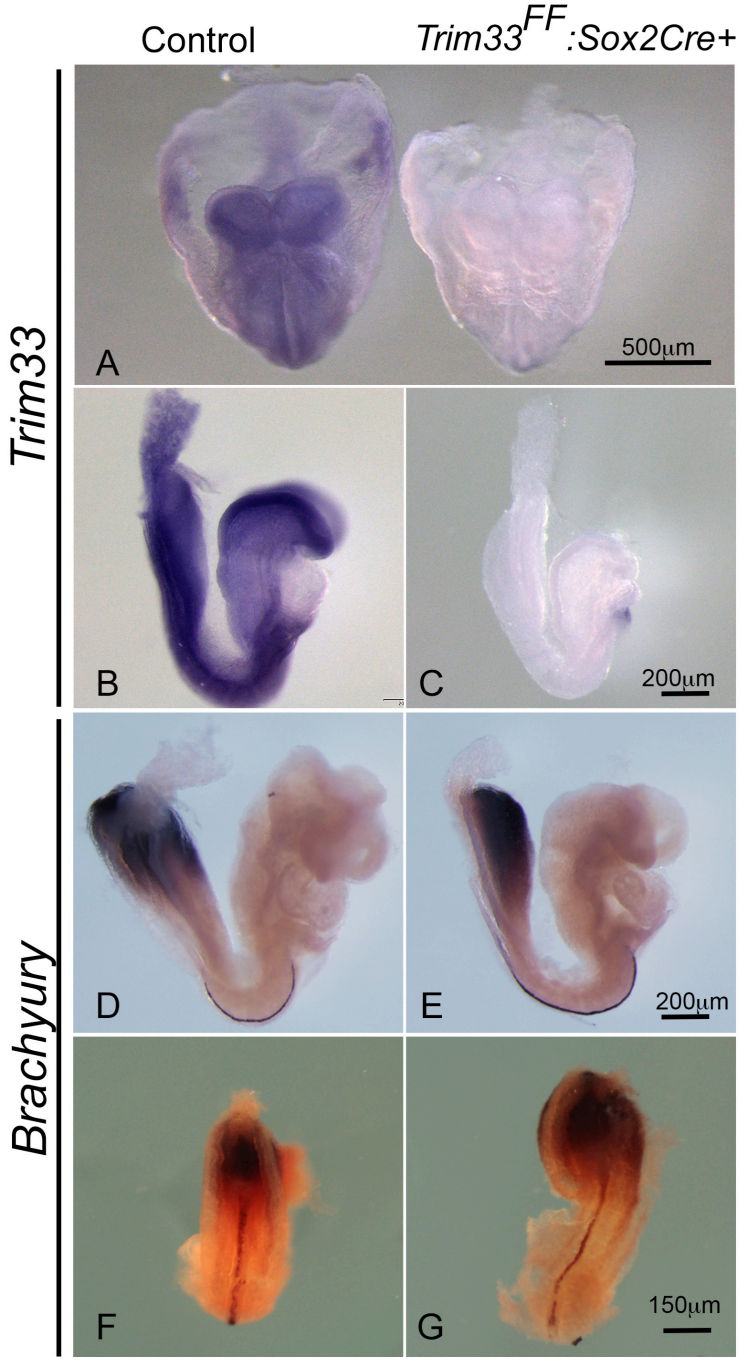

Figure 4.8. *Trim33* and *Brachyury (T)* expression in the E8.5 mouse embryo. *In situ* hybridization of control (left in A, B) and epiblast-specific *Trim33* mutants (*Trim33*^{FF}*: Sox2Cre+*), right in A, C) at E8.5 for *Trim33* and Brachyury (T) expression. *Trim33* is ubiquitously expressed in the mouse embryo at E8.5. The *Trim33* ISH probe is designed to span the sequence within the targeted, *Trim33-floxed* allele; epiblast-specific *Trim33* mutants show abrogation of *Trim33* expression as expected, confirming the putative *Trim33* expression pattern at this mouse embryonic stage. *Brachyury (T)* expression is comparable in controls (D, F) epiblast-specific *Trim33* mutants (E, G).

Next, I proceeded to delete *Trim33* conditionally over a preceding time window in embryonal tissues using the *Sox2Cre* driver, which recombines in the epiblast during gastrulation (Hayashi et al., 2002). *Trim33* mRNA expression was completely abolished in *Trim33*^{FF}:*Sox2Cre* mutants. Moreover the mesoderm marker *Brachyury(T)* is expressed on comparable level and shows a similar pattern of expression (Figure 4.8) in *Trim33*^{FF}:*Sox2Cre* mutants and controls suggesting that *Trim33* deficiency does not grossly affect mesoderm induction and gastrulation. Before E11.5, *Trim33*^{FF}:*Sox2Cre* mutant embryos did not show obvious morphological defects and they were obtained almost at the expected Mendelian frequency (60 of 278). However, at later stages starting at E13, I obtained fewer than expected mutant embryos with very few surviving through E17-18 (Figure 4.9A). No viable *Trim33*^{FF}:*Sox2Cre* embryos were obtained at birth. Among the mutant embryos collected at E13 (n>31), I frequently detected cardiac edema (Figure 5.9B) and occasionally saw embryos that displayed excencephaly (n=2, data not shown). Moreover, all the *Trim33*^{FF}*:Sox2Cre* mutants that survived beyond E15.5 showed cleft palate (Figure 4.10 A and B). Previous work from our group has demonstrated that deletion of *Trim33* alone in tissue types that contribute to palate formation such as the neural crest, palatal epithelium and palatal ectomesenchyme is not sufficient to cause cleft palate or palatal phenotypes (Lane et al., 2015). Since there was no substantial evidence of a genetic cause, we next assessed whether a systemic cause such as hypoxia, which is also known to be a causative mechanism of cleft palate was involved. Palatal shelves from epiblast-specific *Trim33* mutants showed

enhanced binding to Hypoxyprobe, which reliably detects tissue hypoxia levels (Figure 4.10 C and D). Western blot assay to detect pSmad2 and pSmad1/5/8 in control and *Trim33* mutant primary palatal ectomesenchymal cells after TGF-β stimulation shows reduction pSmad2 levels in the mutant samples, with further reduction in the baseline pSmad2 levels in non -TGF-β-stimulated mutant samples (Figure 4.10.E).

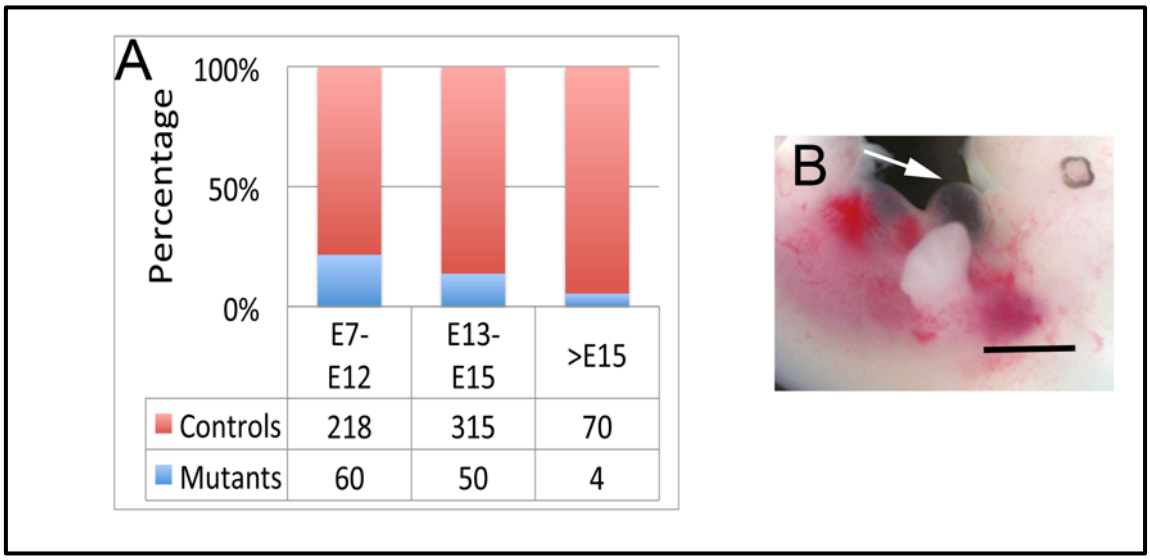

Figure 4.9. Epiblast-specific *Trim33* mutants die around E13. (A) Survival data across embryonic stages for epiblast-specific *Trim33* mutants versus controls. (B) Cardiac edema in epiblast-specific *Trim33* mutant – representative image.

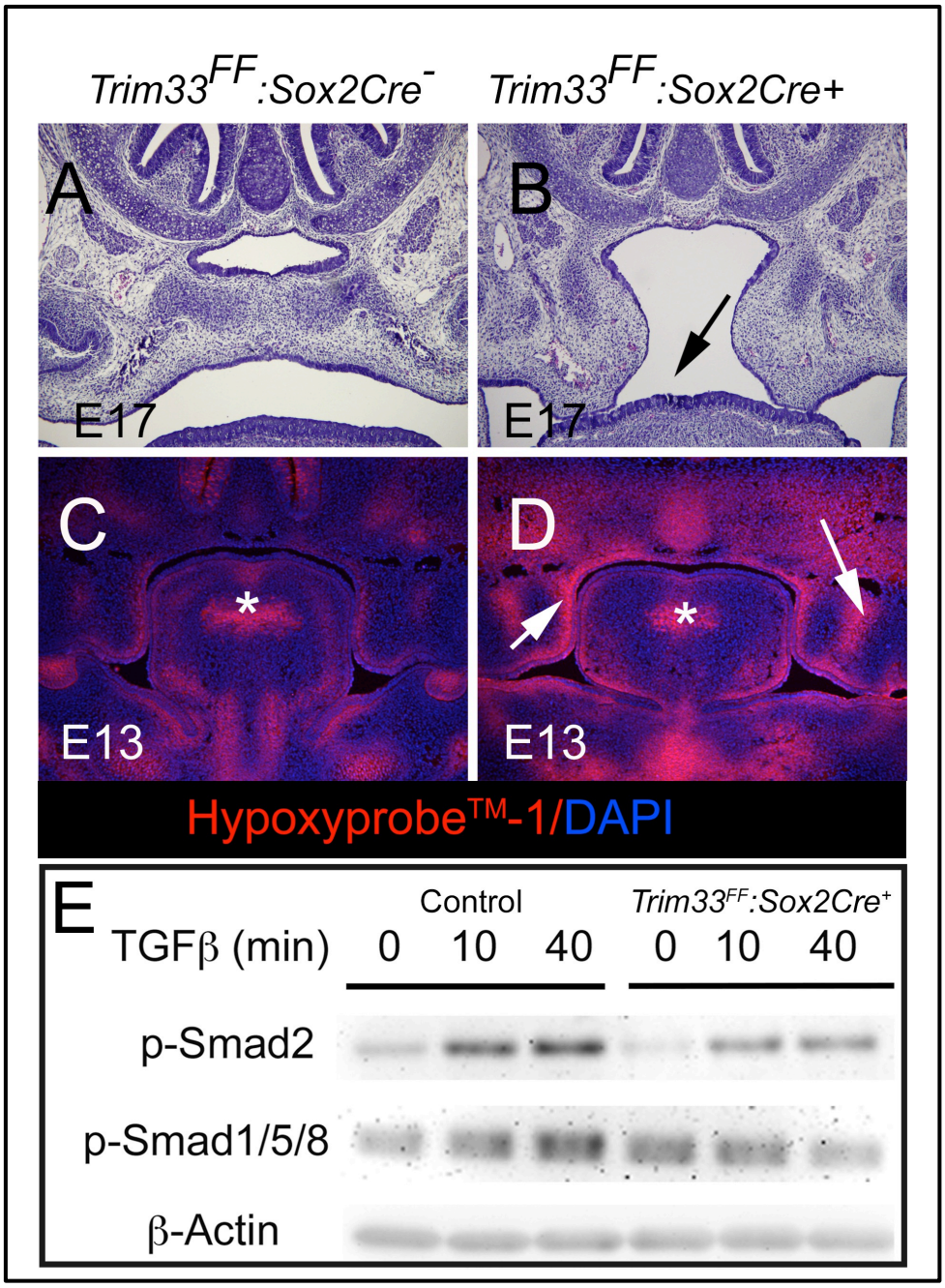

Figure 4.10. Cleft palate defect in epiblast-specific *Trim33* mutants occurs as a consequence of hypoxia. Epiblast-specific *Trim33* mutants (*Trim33^{FF}: Sox2Cre+*) that survived beyond E14 showed cleft palate with high frequency, hypoxic regions in the craniofacial tissues and reduced level of RSmad phosphorylation in primary palatal epithelial cells. Frontal sections of control (A) and mutant (B) embryos at E17, arrow in B points to the cleft between palatal shelves. Frontal sections of control (C) and mutant (D) embryos at E13 show immunostaining (red signal) to detect hypoxyprobe™ -1, counterstained with DAPI (blue). White arrows point to positively staining regions in palatal shelves in (D); asterisks in (C, D) depict similar staining in the tongue tissue. (E) Western blot assay to detect pSmad2 and pSmad1/5/8 in control and *Trim33* mutant primary palatal ectomesenchymal cells after TGF-β stimulation shows reduction in baseline (non-stimulated) pSmad2 levels in the mutant samples.

Gestational death in mouse embryos at E10-E13 has been attributed to two most likely causes: a defect in cardiac/circulatory function and/or a hematopoietic deficiency (Papaioannou and Behringer, 2012). Previous studies have shown that Trim33 can promote erythroid differentiation (He et al., 2006b) and regulate transcriptional elongation of erythroid genes (Bai et al., 2010; Bai et al., 2013). Therefore, we quantified premature and mature erythrocytes in control and *Trim33* mutant at E13.5 by using a FACS assay (Koulnis et al., 2011). While we detected a modest reduction in both $CD71^{HI}Ter119^{HI}$ and $CD71^{LO}Ter119^{HI}$ cell populations marking early and late erythroblasts, these changes alone are too subtle to result in embryonic death that we observe in epiblast-specific *Trim33* mutants (Figure 4.11).

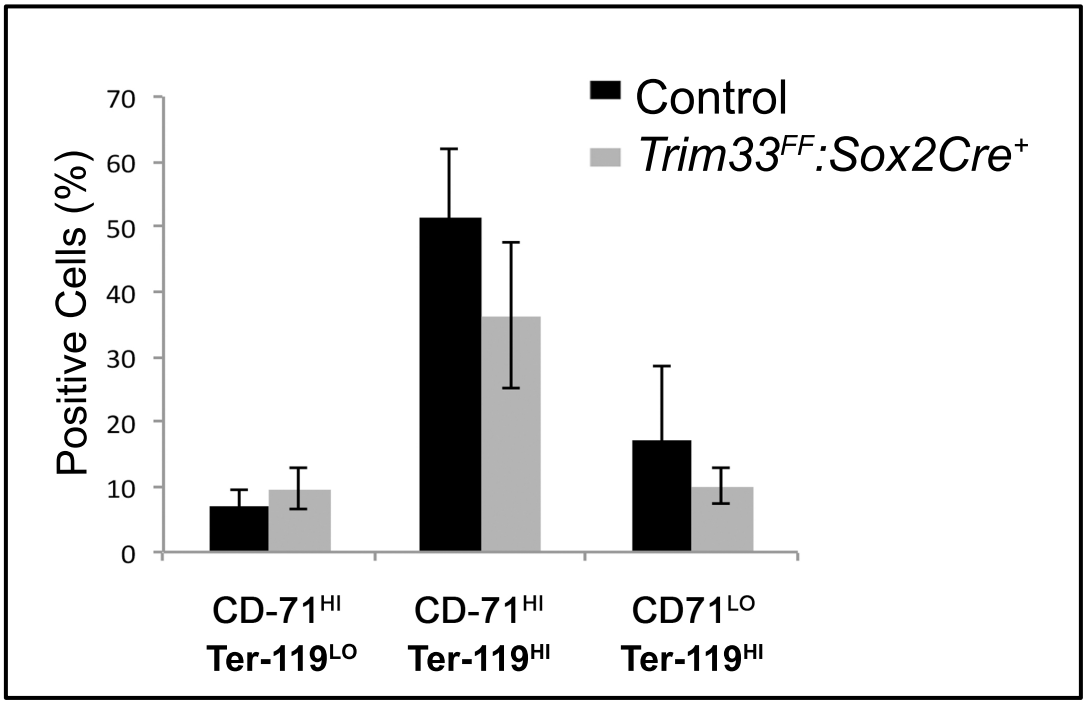

Figure 4.11. Epiblast-specific *Trim33* mutants show a modest reduction in the number of erythroblast populations. Freshly dissociated epiblast-specific *Trim33* mutant (*Trim33*^{FF}*:Sox2Cre*$^{+}$) and control livers were dissociated and labeled with FITC-conjugated antiCD-71 and PE-Conjugated antiTer-119 monoclonal antibodies to assess early and late erythroblasts. Labeled cells were analyzed using flow cytometry, dead cells were excluded from analysis. Error bars = +/- SD.

Next, we compared cardiac function between control and epiblast-specific *Trim33* mutants at E11.5 by using echocardiography. This assay identified 2 out of 4 *Trim33^{FF}:Sox2Cre* mutants with a cardiac failure (Table 4.1), which together with my finding of cardiac edema often associated with the cardiac failure (Figure 4.9B), led us to investigate the cardiac phenotype of developing *Trim33^{FF}:Sox2Cre* mutants in detail.

Control #	Heart Rate	*Trim33^{FF}:Sox2Cre^{+}* #	Heart Rate
1	71	1	77*
2	41	2	88*
3	91	3	35
4	113	4	194
Mean	**52.40**	**-**	**115**
ST DEV	**59.79**	**-**	**112**

Table 4.1. *Ex utero* echocardiography data in E11.5 control and epiblast-specific *Trim33* mutants. Echcardiography recordings detected arrhythmia (marked *) in 2 out of 4 epiblast-specific *Trim33* mutants **(***Trim33^{FF}:Sox2Cre^{+})* as compared to their littermate controls.

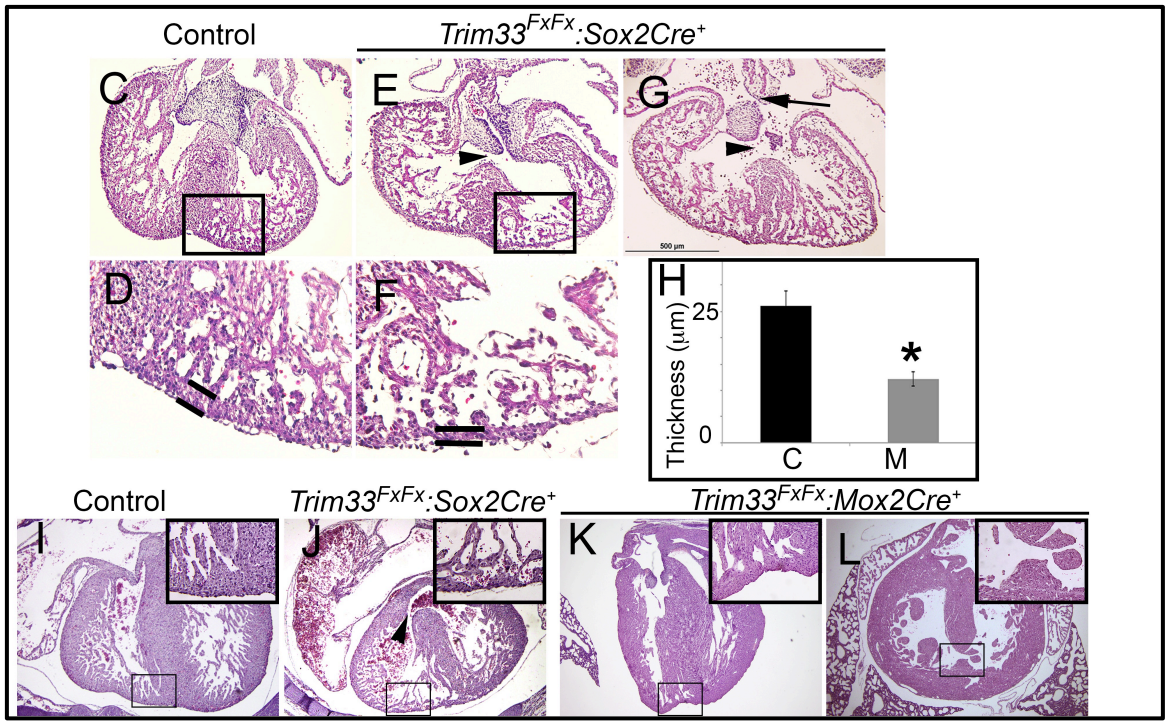

Figure 4.12. Epiblast-specific *Trim33* mutants display severe cardiac defects. (A-E) 4-chambered views of control (A, B) and *Trim33*^{FF}*:Sox2Cre*$^{+}$ mutant (C-E) hearts at E13.5. (B, D) show magnified image of inset in (A, C) showing the compact myocardial layer; area highlighted was used for quantification in (F); black arrowheads in C, E point to VSD, black arrow in E points to ASD. (F) Quantification of myocardial thickness in the compact myocardium of ventricular walls in controls (bar labeled C) and epiblast-specific *Trim33* mutant (bar labeled M). (G-J) 4-chambered view of the embryonic control (G) and surviving mutant hearts (H-J) at E17. (H, *Trim33*^{FF}*:Sox2Cre*$^{+}$ mutant. (I, J) *Trim33*^{FF}*:Mox2Cre*$^{+}$ mutants (*Mox2Cre* is a less robust epiblast-specific driver). All mutants show defects in the ventricular myocardial wall (inset in H-J. Moreover, VSDs were commonly detected (arrowhead in H and inset in J). Error bars = +/-SEM, *p<0.05.

Histological serial sections of cardiac tissues showed that all the examined mutants show either membranous or muscular ventricular defects (VSDs) and thinning of the ventricular myocardium (Figure 4.12). While differences in septum formation and myocardial thickness were not apparent in earlier stages (E9-E11), they were clearly evident at E13 (Figure 4.12 A-C). In addition, the mutants showed atrial-septal defects (ASD) with variable penetrance (Figure 4.12 E). The VSD and myocardial defects were recapitulated independently by using the *Mox2Cre* driver line, which shows a chimeric recombination pattern in the

epiblast (Tallquist and Soriano, 2000) (Figure 4.12 I, J). Consistent with my finding in EBs *in vitro*, expression levels of *Ankrd1,* a novel marker for cardiac pressure overload and failure (Bogomolovas et al., 2015), were increased in *Trim33*^{FF}*:Sox2Cre*$^{+}$ mutant hearts at E10.5 when compared to control tissues (Figure 4.13 B). Collectively, these findings suggest that the death of epiblast-specific *Trim33* mutants around E13 results from deficiency of cardiac function, likely cardiac failure.

Expression changes in epiblast-specific *Trim33* mutants

Myocardial development and heart morphogenesis are orchestrated by an array of evolutionary conserved transcription factors (McCulley and Black, 2012). Among these, *Gata4, Nkx2-5, Isl1* and *Tbx5* have been shown to be of particular importance. I therefore used a candidate approach and RNAs extracted from E8.5 embryos to analyze whether expression levels of any of these factors were altered in *Trim33*^{FF}*:Sox2Cre*$^{+}$ mutants. My results show that both *Tbx5* and *Isl1* are down regulated in epiblast-specific *Trim33* mutants as compared to littermate controls, suggesting that reduced expression of these factors may contribute to observed myocardial and ventricular septal defects (Figure 4.13 A)

Given the coinciding time points in embryonic lethality with *Trim33*^{FF}*:Sox2Cre*$^{+}$ mutants and *Mttp* homozygous mutants (Raabe et al., 1998) and my expression findings displaying reduced *Mttp* in Day7 EBs *in vitro*, I investigated whether Mttp, together with other genes associated with lipid metabolism, would show

altered expression in *Trim33-mutant* embryonic tissues at E8.5. My results show that while *Apob* and *Apoc2* were not affected by*Trim33* deficiency (data not shown), however, *Mttp* expression levels were significantly reduced at E8.5 (Figure 4.13 A).

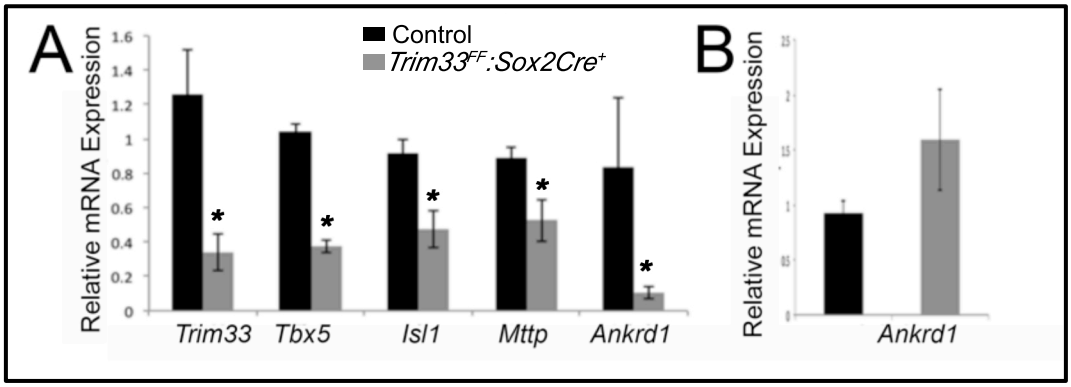

Figure 4.13. *Tbx5, Isl1, Mttp* expression is down regulated in epiblast-specific *Trim33* mutants at E8.5. Relative mRNA expression (A) in epiblast-specific *Trim33* mutant and control whole embryo samples at E8.5 and (B) in E10.5 hearts in epiblast-specific Trim33 mutants and heterozygote controls.The key cardiac transcription factors *Tbx5* and *Isl1,Mttp - a* critical regulator of lipid metabolism and *Ankrd1*, a cardiac failure marker is down-regulated in epiblast-specific *Trim33* mutant embryos. Ankrd1 is up regulated in later stages at E10.5 hearts, shown in (B). Error bars = +/- SEM, *p <0.05.

The lethal phenotype of *Trim33* embryos can be partially rescued by Smad4 haploinsufficiency

While Trim33 has been shown to regulate many cellular processes in a highly context-dependent manner (Ferri et al., 2015; Isbel et al., 2015; Wang et al., 2015; Xue et al., 2015), perhaps, the most well-documented is its role as either a negative or positive modulator of TGF-β signaling (Dupont et al., 2009; Dupont et al., 2005; He et al., 2006b; Morsut et al., 2010; Xi et al., 2011). To examine whether Smad-dependent TGF-β signaling contributes to the observed epiblast-specific*Trim33* mutant lethal phenotype, I generated epiblast-specific *Trim33* mutants, which were heterozygotes for the *Smad4* gene

(Trim33^{FF}:Smad^{FWt}:Sox2Cre^{+}), and compared their survival rate and cardiac phenotype to those of *Trim33^{FF}:Sox2Cre^{+}* mutant and Cre-negative control littermates. At E13, the survival rate of epiblast-specific *Trim33* mutants was less than 50% of the expected frequency, while the corresponding frequency of *Trim33^{FF}:Smad^{FWt}:Sox2Cre^{+}* mutants was more than 100% (Figure 4.14A).

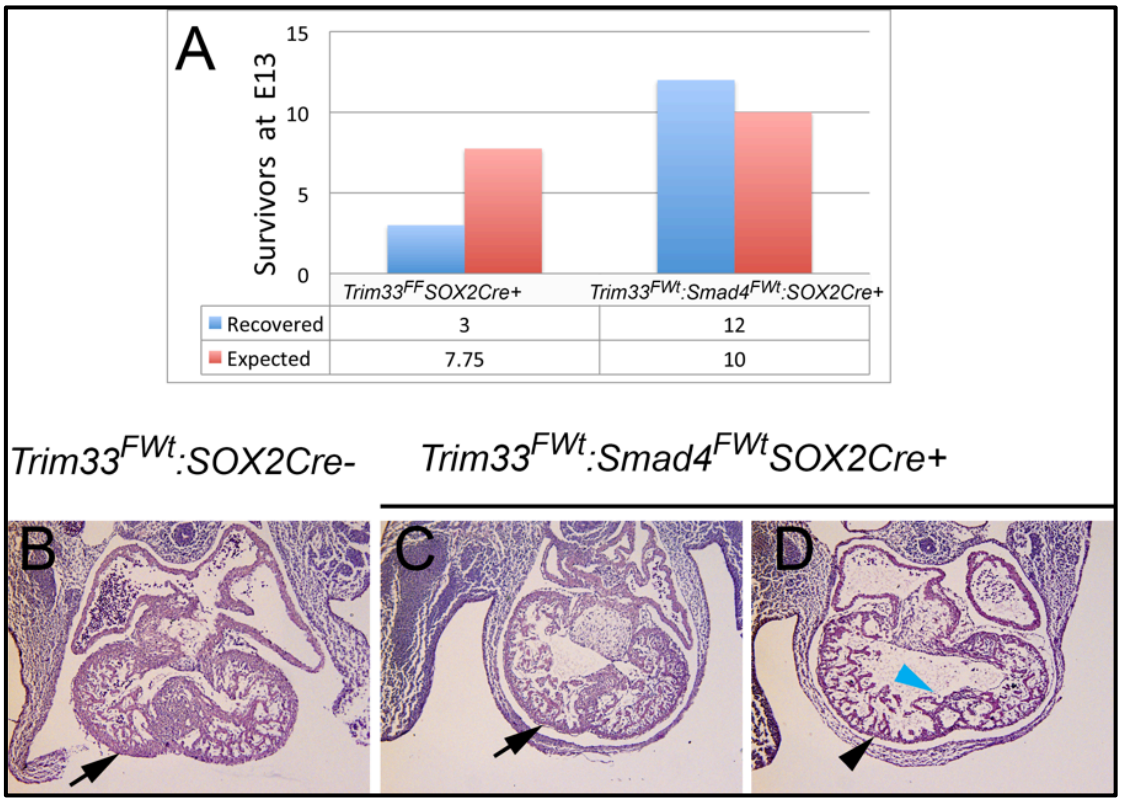

Figure 4.14. Lethal phenotype of epiblast-specific *Trim33* mutants is partially rescued by Smad4 heterozygosity. (A) Bar graph depicting surviving *Trim33^{FF}:Sox2Cre^{+}* and *Trim33^{FF}:Smad4^{FWt}:Sox2Cre^{+}* mutants at E13. (B-D) 4-chamber view of control (B) and two *Trim33^{FF}:Smad4^{FWt}:Sox2Cre^{+}* mutant (C, D) hearts. The mutant in C shows normal thickness of the compact myocardium (arrows in B and C), while another mutant littermate (D) shows characteristic thin myocardium (black arrowhead) and deficient septal growth (blue arrowhead) consistent with that observed in *Trim33^{FF}:Sox2Cre^{+}* mutants.

These data demonstrate that the lethal cardiac phenotype of the epiblast-specific *Trim33* mutants can be partially rescued by Smad4 haploinsufficiency

suggesting that Trim33 regulates Smad-dependent TGF-β superfamily signaling in mouse embryos after mesoderm induction.

Discussion

In this study, we used ES cell-based *in vitro* differentiation assays and tissue-specific knockout mouse models to investigate the role of *Trim33* in mouse development. We found that deletion of *Trim33* in embryoid bodies after mesoderm induction results in morphological, functional and molecular changes in visceral endoderm and cardiac mesoderm cells *in vitro*. Epiblast-specific *Trim33* mutants display a spectrum of cardiac defects and die after mid-gestation. The said *Trim33* phenotype is partially rescued by *Smad4* haploinsufficiency suggesting that in late-gastrulation embryos Trim33 represses canonical TGF-β signaling.

Trim33 regulates extraembryonic endoderm development *in vitro*

During normal embryogenesis, the extraembryonic endoderm (ExEn) gives rise to the parietal endoderm (PE) and visceral endoderm (VE), which provide nutrients and instructive morphogen signals for appropriate cell fate and patterning decisions (Bielinska et al., 1999). The anterior visceral endoderm (AVE) forms a distinct population of VE cells and plays a critical role in positioning of the head and heart (Madabhushi and Lacy, 2011).

Here we show that when *Trim33* is deleted in EBs after mesoderm induction, the mutant EBs are viable and form beating clusters. However, at later stages the

mutant EBs show less-expanded cystic appearance. Already before the morphological differences are obvious, many VE associated genes are dramatically down-regulated in Trim33-deficient EBs. These include VE markers *Afp,* and *Ttr (Fujikura et al., 2002) and* critical regulators of VE differentiation and lipoprotein biosynthesis *Hnf4a* and *Mttp,* respectively (Morrisey et al., 1998; Raabe et al., 1998). Moreover, the VE-specific *Amn* and *Cubn* genes, which encode multi-ligand endocytic receptors that mediate uptake of nutrients (Christensen and Birn, 2002), lipids and cholesterol in particular, and several apolipoprotein genes are expressed at much lower levels (>20-fold down-regulated) in Trim33-deficient EBs as compared to control EBs. One of the primary functions of the VE is to provide nutrition to the embryo during neurulation (Zohn and Sarkar, 2010). Therefore it is of interest that *Trim33* germline mutants die during neurulation as shown in two independent studies (Isbel et al., 2015; Kim and Kaartinen, 2008).

It is noteworthy that *Dkk1, Cer1, Lefty1* and *Hex*, established markers for the AVE, and *Gata4* and *Gata6,* the determinants of ExEn specification, were not differentially expressed between mutant and control EBs in our global transcriptomic analyses. *Gata4* expression has been shown to be sufficient for specification of cardiomyocyte fate in differentiating ES cells (Holtzinger et al., 2010). This together with the fact that the myocardial differentiation program was not blocked in EBs, in which *Trim33* was deleted after mesoderm-induction, suggests that the Nodal-Cripto signaling involved in ExEn specification is not

regulated by *Trim33* (Kruithof-de Julio et al., 2011). Instead, our *in vitro* data imply that *Trim33* deletion results in impaired VE differentiation.

Trim33 is required in the embryo proper for appropriate cardiac development

Our findings that a higher number of *Trim33*-deficient EBs show beating cell clusters and display upregulation of a cardiac failure marker *Ankrd1* suggests that Trim33 plays either a direct role in appropriate myocardial differentiation or that Trim33 contributes to the cardiac differentiation via an indirect mechanism involving VE differentiation. However, deletion of *Trim33* by using the *Sox2Cre* driver, which recombines specifically in the epiblast but not in ExEn (hence effectively does not recombine in the VE), resulted in cardiac defects, suggesting that Trim33 regulates early cardiac differentiation directly in the embryo proper. Strikingly, there were no gross cardiac phenotypes in the mesendoderm-specific *Trim33^{FF}:TCre* mutants. *Sox2Cre* has been shown to recombine at early epiblast stage prior to E5.75 (Chu et al., 2004), while strong *TCre*-induced recombination can be detected in the primitive streak and the lateral mesodermal wings at the mid-streak stage (E7.5) (Kumar et al., 2008). Our studies on EBs imply that the Trim33 protein is remarkably stable, which may contribute to the milder phenotypes we see in *Trim33^{FF}:TCre^{+}* mutants. Collectively, these results suggest that Trim33 is required at the time when the mesodermal multipotent progenitor cells commit to the cardiac lineage, and that it may play a minor or no role in more committed cell lineages.

Trim33, lipid metabolism and morphogen signaling

Trim33^{FF}*:Sox2Cre* mutants show low-penetrant defects in the neural tube closure (exencephaly) and atrial septation; the phenotypes that can be caused by deficient hedgehog (Hh) signaling (Hoffmann et al., 2009; Murdoch and Copp, 2010). Cholesterol modification of Hh ligands is required for proper Hh signaling, and consequently the mouse mutants deficient in specific apolipoproteins and lipoprotein receptors, e.g., *ApoB* and *Megalin* show phenotypes similar to those seen in Hh pathway mutants (Farese et al., 1995; Willnow et al., 1996). While VE is the main site of apolipoprotein synthesis and function in midgestation embryos, the key lipid transporter *Mttp* is also expressed in the embryo proper already at E8.5 (Figure 4.13 A). Interestingly, *Mttp* expression was downregulated in epiblast-specific *Trim33* mutants (Figure 4.13 A), which could contribute to changes in lipid metabolism resulting in exencephaly and atrial septal defects we detect with low penetrance.

Trim33 regulates TGF-β signaling during cardiac development

Although Trim33 has been implicated in many biological processes, our finding that *Smad4* haploinsufficiency partially rescues the lethal phenotype of *Trim33*^{FF}*:Sox2Cre*$^{+}$ mutants strongly suggests that in this context *Trim33* suppresses TGF-β superfamily signaling. It has been suggested that TGF-β signaling plays a bimodal stage-specific role in cardiac development in vitro (Cai et al., 2012; Kitamura et al., 2007). According to this model Smad2 would first be

activated by Nodal/Cripto to induce mesoderm formation in mES cells between days 3-5 of differentiation, then after being inhibited from days 5 to day 7, Smad2 would again be activated by TGF-β/Activin to suppress cardiomyogenesis (Kitamura et al., 2007). Paradoxically, a higher number of beating clusters in *Trim33*-deficient EBs suggests that TGF-β signaling is down-regulated in mutants during the phase in which it suppresses cardiomyogenesis. This is consistent with our biochemical data showing that Smad2 activation is less in *Trim33*-deficient EBs (Figure 4.15).

Our data imply that failure to attenuate Smad4-dependent TGF-β signaling in epiblast-specific *Trim33* mutants during the narrow but critical time window in late mesoderm induction ultimately results in sustained reduction in TGF-β superfamily signaling. Among other changes, expression levels of the key cardiac transcription factors *Tbx5* and *Isl1* were affected in the developing heart followed by elevated expression of cardiac failure marker *Ankrd1,* which can be detected both in EBs in vitro and epiblast-specific *Trim33* mutants *in vivo*. Those rare epiblast-specific *Trim33* mutants that survive beyond E15 precipitate progressive cardiac failure resulting in hypoxia in craniofacial tissues (Figure 4.10). Hypoxia during facial morphogenesis has been shown to result in cleft palate (Azarbayjani and Danielsson, 2001; Johnston and Bronsky, 1995). Previous work by our group demonstrates that abrogation of *Trim33* in any of the cell types contributing to the palate, i.e., ectoderm (*K14Cre)*, neural crest *(Wnt1Cre)* and endothelium (*Tie2Cre),* does not result in palatal phenotypes (Lane et al., 2015) and data not shown). Therefore it is likely that the palate

phenotype we see among epiblast-specific *Trim33* mutants that survive beyond E15 is secondary to the cardiac defects and associated hypoxia in craniofacial tissues.

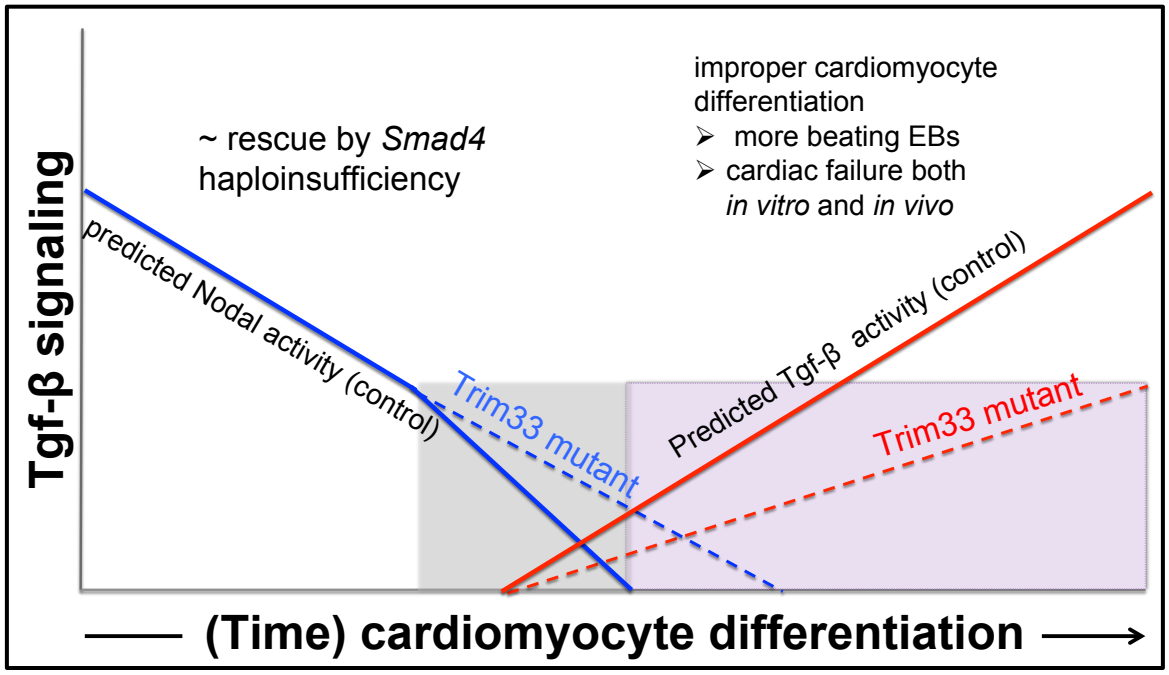

Figure 4.15. Conceptual model illustrating regulation of TGF-β superfamily signaling by Trim33 in the precardiac mesoderm.

Implications for common congenital birth defects

Our current data contribute to the bimodal stage-specific model proposed by (Cai et al., 2012; Kitamura et al., 2007). Specifically, we show that Trim33 attenuates to first wave of Tgfβ superfamily signaling. The loss of *Trim33* likely results in prolonged/abnormally high pSmad2-Smad4 -mediated signaling activity; which subsequently leads to sustained attenuation of baseline TGF-β signaling activity during early commitment of cardiac progenitors (Figure 4.15). Strikingly, mouse embryos deficient in *Trim33* suffer from VSDs and cleft palate, which belong to

the most common congenital birth defects in humans. These data generate an exciting new paradigm arguing that the common congenital birth defects can be caused by inappropriate regulation of early signaling processes preceding the organ formation, e.g. cardiogenesis or palatogenesis.

References

Agricola, E., Randall, R.A., Gaarenstroom, T., Dupont, S., Hill, C.S., 2011. Recruitment of TIF1gamma to chromatin via its PHD finger-bromodomain activates its ubiquitin ligase and transcriptional repressor activities. Mol. Cell 43, 85-96.

Aucagne, R., Droin, N., Paggetti, J., Lagrange, B., Largeot, A., Hammann, A., Bataille, A., Martin, L., Yan, K.P., Fenaux, P., Losson, R., Solary, E., Bastie, J.N., Delva, L., 2011. Transcription intermediary factor 1gamma is a tumor suppressor in mouse and human chronic myelomonocytic leukemia. J. Clin. Invest. 121, 2361-2370.

Azarbayjani, F., Danielsson, B.R., 2001. Phenytoin-induced cleft palate: evidence for embryonic cardiac bradyarrhythmia due to inhibition of delayed rectifier K+ channels resulting in hypoxia-reoxygenation damage. Teratology 63, 152-160.

Bai, X., Kim, J., Yang, Z., Jurynec, M.J., Akie, T.E., Lee, J., LeBlanc, J., Sessa, A., Jiang, H., DiBiase, A., Zhou, Y., Grunwald, D.J., Lin, S., Cantor, A.B., Orkin, S.H., Zon, L.I., 2010. TIF1gamma controls erythroid cell fate by regulating transcription elongation. Cell 142, 133-143.

Bai, X., Trowbridge, J.J., Riley, E., Lee, J.A., DiBiase, A., Kaartinen, V.M., Orkin, S.H., Zon, L.I., 2013. TiF1-gamma plays an essential role in murine hematopoiesis and regulates transcriptional elongation of erythroid genes. Dev. Biol. 373, 422-430.

Balko, J.M., Schwarz, L.J., Bhola, N.E., Kurupi, R., Owens, P., Miller, T.W., Gomez, H., Cook, R.S., Arteaga, C.L., 2013. Activation of MAPK pathways due to DUSP4 loss promotes cancer stem cell-like phenotypes in basal-like breast cancer. Cancer Res 73, 6346-6358.

Bielinska, M., Narita, N., Wilson, D.B., 1999. Distinct roles for visceral endoderm during embryonic mouse development. Int J Dev Biol 43, 183-205.

Bogomolovas, J., Brohm, K., Celutkiene, J., Balciunaite, G., Bironaite, D., Bukelskiene, V., Daunoravicus, D., Witt, C.C., Fielitz, J., Grabauskiene, V.,

Labeit, S., 2015. Induction of Ankrd1 in Dilated Cardiomyopathy Correlates with the Heart Failure Progression. Biomed Res Int 2015, 273936.
Cai, W., Guzzo, R.M., Wei, K., Willems, E., Davidovics, H., Mercola, M., 2012. A Nodal-to-TGFbeta cascade exerts biphasic control over cardiopoiesis. Circ. Res. 111, 876-881.

Chen, C.C., Chen, H.Y., Su, K.Y., Hong, Q.S., Yan, B.S., Chen, C.H., Pan, S.H., Chang, Y.L., Wang, C.J., Hung, P.F., Yuan, S., Chang, G.C., Chen, J.J., Yang, P.C., Yang, Y.C., Yu, S.L., 2014. Shisa3 is associated with prolonged survival through promoting beta-catenin degradation in lung cancer. Am J Respir Crit Care Med 190, 433-444.

Christensen, E.I., Birn, H., 2002. Megalin and cubilin: multifunctional endocytic receptors. Nat Rev Mol Cell Biol 3, 256-266.

Chu, G.C., Dunn, N.R., Anderson, D.C., Oxburgh, L., Robertson, E.J., 2004. Differential requirements for Smad4 in TGFbeta-dependent patterning of the early mouse embryo. Development 131, 3501-3512.

Derynck, R., Feng, X.H., 1997. TGF-beta receptor signaling. Biochim Biophys Acta 1333, F105-150.

Derynck, R., Zhang, Y.E., 2003. Smad-dependent and Smad-independent pathways in TGF-beta family signalling. Nature 425, 577-584.

Descargues, P., Sil, A.K., Sano, Y., Korchynskyi, O., Han, G., Owens, P., Wang, X.J., Karin, M., 2008. IKKalpha is a critical coregulator of a Smad4-independent TGFbeta-Smad2/3 signaling pathway that controls keratinocyte differentiation. Proc Natl Acad Sci U S A 105, 2487-2492.

Dobin, A., Davis, C.A., Schlesinger, F., Drenkow, J., Zaleski, C., Jha, S., Batut, P., Chaisson, M., Gingeras, T.R., 2013. STAR: ultrafast universal RNA-seq aligner. Bioinformatics 29, 15-21.

Dupont, S., Mamidi, A., Cordenonsi, M., Montagner, M., Zacchigna, L., Adorno, M., Martello, G., Stinchfield, M.J., Soligo, S., Morsut, L., Inui, M., Moro, S., Modena, N., Argenton, F., Newfeld, S.J., Piccolo, S., 2009. FAM/USP9x, a deubiquitinating enzyme essential for TGFbeta signaling, controls Smad4 monoubiquitination. Cell 136, 123-135.

Dupont, S., Zacchigna, L., Cordenonsi, M., Soligo, S., Adorno, M., Rugge, M., Piccolo, S., 2005. Germ-layer specification and control of cell growth by Ectodermin, a Smad4 ubiquitin ligase. Cell. 121, 87-99.

Falk, S., Joosten, E., Kaartinen, V., Sommer, L., 2014. Smad4 and Trim33/Tif1gamma redundantly regulate neural stem cells in the developing cortex. Cereb. Cortex 24, 2951-2963.

Farese, R.V., Jr., Ruland, S.L., Flynn, L.M., Stokowski, R.P., Young, S.G., 1995. Knockout of the mouse apolipoprotein B gene results in embryonic lethality in homozygotes and protection against diet-induced hypercholesterolemia in heterozygotes. Proc Natl Acad Sci U S A 92, 1774-1778.

Ferri, F., Parcelier, A., Petit, V., Gallouet, A.S., Lewandowski, D., Dalloz, M., van den Heuvel, A., Kolovos, P., Soler, E., Squadrito, M.L., De Palma, M., Davidson, I., Rousselet, G., Romeo, P.H., 2015. TRIM33 switches off Ifnb1 gene transcription during the late phase of macrophage activation. Nat Commun 6, 8900.

Fujikura, J., Yamato, E., Yonemura, S., Hosoda, K., Masui, S., Nakao, K., Miyazaki Ji, J., Niwa, H., 2002. Differentiation of embryonic stem cells is induced by GATA factors. Genes Dev 16, 784-789.

Hayashi, S., Lewis, P., Pevny, L., McMahon, A.P., 2002. Efficient gene modulation in mouse epiblast using a Sox2Cre transgenic mouse strain. Mech. Dev. 119 Suppl 1, S97-s101.

He, W., Dorn, D.C., Erdjument-Bromage, H., Tempst, P., Moore, M.A., Massague, J., 2006a. Hematopoiesis controlled by distinct TIF1gamma and Smad4 branches of the TGFbeta pathway. Cell 125, 929-941.

He, W., Dorn, D.C., Erdjument-Bromage, H., Tempst, P., Moore, M.A., Massague, J., 2006b. Hematopoiesis controlled by distinct TIF1gamma and Smad4 branches of the TGFbeta pathway. Cell. 125, 929-941.

Hesling, C., Lopez, J., Fattet, L., Gonzalo, P., Treilleux, I., Blanchard, D., Losson, R., Goffin, V., Pigat, N., Puisieux, A., Mikaelian, I., Gillet, G., Rimokh, R., 2013. Tif1gamma is essential for the terminal differentiation of mammary alveolar epithelial cells and for lactation through SMAD4 inhibition. Development 140, 167-175.

Hoffmann, A.D., Peterson, M.A., Friedland-Little, J.M., Anderson, S.A., Moskowitz, I.P., 2009. sonic hedgehog is required in pulmonary endoderm for atrial septation. Development 136, 1761-1770.

Holtzinger, A., Rosenfeld, G.E., Evans, T., 2010. Gata4 directs development of cardiac-inducing endoderm from ES cells. Dev. Biol. 337, 63-73.

Huang, L.S., Voyiaziakis, E., Markenson, D.F., Sokol, K.A., Hayek, T., Breslow, J.L., 1995. apo B gene knockout in mice results in embryonic lethality in

homozygotes and neural tube defects, male infertility, and reduced HDL cholesterol ester and apo A-I transport rates in heterozygotes. J Clin Invest 96, 2152-2161.

Isbel, L., Srivastava, R., Oey, H., Spurling, A., Daxinger, L., Puthalakath, H., Whitelaw, E., 2015. Trim33 Binds and Silences a Class of Young Endogenous Retroviruses in the Mouse Testis; a Novel Component of the Arms Race between Retrotransposons and the Host Genome. PLoS Genet 11, e1005693.

Johnston, M.C., Bronsky, P.T., 1995. Prenatal craniofacial development: new insights on normal and abnormal mechanisms. Crit Rev Oral Biol Med 6, 368-422.

Kim, J., Kaartinen, V., 2008. Generation of mice with a conditional allele for Trim33. Genesis 46, 329-333.

Kitamura, R., Takahashi, T., Nakajima, N., Isodono, K., Asada, S., Ueno, H., Ueyama, T., Yoshikawa, T., Matsubara, H., Oh, H., 2007. Stage-specific role of endogenous Smad2 activation in cardiomyogenesis of embryonic stem cells. Circ Res 101, 78-87.

Koulnis, M., Pop, R., Porpiglia, E., Shearstone, J.R., Hidalgo, D., Socolovsky, M., 2011. Identification and analysis of mouse erythroid progenitors using the CD71/TER119 flow-cytometric assay. J Vis Exp.

Kruithof-de Julio, M., Alvarez, M.J., Galli, A., Chu, J., Price, S.M., Califano, A., Shen, M.M., 2011. Regulation of extra-embryonic endoderm stem cell differentiation by Nodal and Cripto signaling. Development 138, 3885-3895.

Krumlauf, R., Chapman, V.M., Hammer, R.E., Brinster, R., Tilghman, S.M., 1986. Differential expression of alpha-fetoprotein genes on the inactive X chromosome in extraembryonic and somatic tissues of a transgenic mouse line. Nature 319, 224-226.

Kumar, A., Lualdi, M., Lewandoski, M., Kuehn, M.R., 2008. Broad mesodermal and endodermal deletion of Nodal at postgastrulation stages results solely in left/right axial defects. Dev Dyn 237, 3591-3601.

Lane, J., Yumoto, K., Azhar, M., Ninomiya-Tsuji, J., Inagaki, M., Hu, Y., Deng, C.X., Kim, J., Mishina, Y., Kaartinen, V., 2015. Tak1, Smad4 and Trim33 redundantly mediate TGF-beta3 signaling during palate development. Dev. Biol. 398, 231-241.

Madabhushi, M., Lacy, E., 2011. Anterior visceral endoderm directs ventral morphogenesis and placement of head and heart via BMP2 expression. Dev Cell 21, 907-919.

Massague, J., Chen, Y.G., 2000. Controlling TGF-beta signaling. Genes Dev. 14, 627-644.

McCulley, D.J., Black, B.L., 2012. Transcription factor pathways and congenital heart disease. Curr Top Dev Biol 100, 253-277.

Morrisey, E.E., Tang, Z., Sigrist, K., Lu, M.M., Jiang, F., Ip, H.S., Parmacek, M.S., 1998. GATA6 regulates HNF4 and is required for differentiation of visceral endoderm in the mouse embryo. Genes Dev 12, 3579-3590.

Morsut, L., Yan, K.P., Enzo, E., Aragona, M., Soligo, S.M., Wendling, O., Mark, M., Khetchoumian, K., Bressan, G., Chambon, P., Dupont, S., Losson, R., Piccolo, S., 2010. Negative control of Smad activity by ectodermin/Tif1gamma patterns the mammalian embryo. Development 137, 2571-2578.

Moses, K.A., DeMayo, F., Braun, R.M., Reecy, J.L., Schwartz, R.J., 2001. Embryonic expression of an Nkx2-5/Cre gene using ROSA26 reporter mice. Genesis 31, 176-180.

Murdoch, J.N., Copp, A.J., 2010. The relationship between sonic Hedgehog signaling, cilia, and neural tube defects. Birth Defects Res A Clin Mol Teratol 88, 633-652.

Papaioannou, V.E., Behringer, R.R., 2012. Early embryonic lethality in genetically engineered mice: diagnosis and phenotypic analysis. Vet. Pathol. 49, 64-70.

Pedelacq, J.D., Cabantous, S., Tran, T., Terwilliger, T.C., Waldo, G.S., 2006. Engineering and characterization of a superfolder green fluorescent protein. Nat Biotechnol 24, 79-88.

Perantoni, A.O., Timofeeva, O., Naillat, F., Richman, C., Pajni-Underwood, S., Wilson, C., Vainio, S., Dove, L.F., Lewandoski, M., 2005. Inactivation of FGF8 in early mesoderm reveals an essential role in kidney development. Development 132, 3859-3871.

Pieters, T., Haenebalcke, L., Hochepied, T., D'Hont, J., Haigh, J.J., van Roy, F., van Hengel, J., 2012. Efficient and user-friendly pluripotin-based derivation of mouse embryonic stem cells. Stem cell reviews 8, 768-778.

Pommier, R.M., Gout, J., Vincent, D.F., Alcaraz, L.B., Chuvin, N., Arfi, V., Martel, S., Kaniewski, B., Devailly, G., Fourel, G., Bernard, P., Moyret-Lalle, C., Ansieau, S., Puisieux, A., Valcourt, U., Sentis, S., Bartholin, L., 2015. TIF1gamma Suppresses Tumor Progression by Regulating Mitotic Checkpoints and Chromosomal Stability. Cancer Res 75, 4335-4350.

Quere, R., Saint-Paul, L., Carmignac, V., Martin, R.Z., Chretien, M.L., Largeot, A., Hammann, A., Pais de Barros, J.P., Bastie, J.N., Delva, L., 2014. Tif1gamma regulates the TGF-beta1 receptor and promotes physiological aging of hematopoietic stem cells. Proc. Natl. Acad. Sci. U. S. A. 111, 10592-10597.

Raabe, M., Flynn, L.M., Zlot, C.H., Wong, J.S., Veniant, M.M., Hamilton, R.L., Young, S.G., 1998. Knockout of the abetalipoproteinemia gene in mice: reduced lipoprotein secretion in heterozygotes and embryonic lethality in homozygotes. Proc. Natl. Acad. Sci. U. S. A. 95, 8686-8691.

Raleigh, J.A., Koch, C.J., 1990. Importance of thiols in the reductive binding of 2-nitroimidazoles to macromolecules. Biochem. Pharmacol. 40, 2457-2464.

Reissmann, E., Jornvall, H., Blokzijl, A., Andersson, O., Chang, C., Minchiotti, G., Persico, M.G., Ibanez, C.F., Brivanlou, A.H., 2001. The orphan receptor ALK7 and the Activin receptor ALK4 mediate signaling by Nodal proteins during vertebrate development. Genes Dev. 15, 2010-2022.

Ruzankina, Y., Pinzon-Guzman, C., Asare, A., Ong, T., Pontano, L., Cotsarelis, G., Zediak, V.P., Velez, M., Bhandoola, A., Brown, E.J., 2007. Deletion of the developmentally essential gene ATR in adult mice leads to age-related phenotypes and stem cell loss. Cell stem cell 1, 113-126.

Sedmera, D., Pexieder, T., Vuillemin, M., Thompson, R.P., Anderson, R.H., 2000. Developmental patterning of the myocardium. Anat. Rec. 258, 319-337.

Sirard, C., de la Pompa, J.L., Elia, A., Itie, A., Mirtsos, C., Cheung, A., Hahn, S., Wakeham, A., Schwartz, L., Kern, S.E., Rossant, J., Mak, T.W., 1998. The tumor suppressor gene Smad4/Dpc4 is required for gastrulation and later for anterior development of the mouse embryo. Genes Dev. 12, 107-119.

Tallquist, M.D., Soriano, P., 2000. Epiblast-restricted Cre expression in MORE mice: a tool to distinguish embryonic vs. extra-embryonic gene function. Genesis 26, 113-115.

Varghese, A.J., Gulyas, S., Mohindra, J.K., 1976. Hypoxia-dependent reduction of 1-(2-nitro-1-imidazolyl)-3-methoxy-2-propanol by Chinese hamster ovary cells and KHT tumor cells in vitro and in vivo. Cancer Res. 36, 3761-3765.

Venturini, L., You, J., Stadler, M., Galien, R., Lallemand, V., Koken, M.H., Mattei, M.G., Ganser, A., Chambon, P., Losson, R., de, T.H., 1999. TIF1gamma, a novel member of the transcriptional intermediary factor 1 family. Oncogene. 18, 1209-1217.

Vincent, D.F., Gout, J., Chuvin, N., Arfi, V., Pommier, R.M., Bertolino, P., Jonckheere, N., Ripoche, D., Kaniewski, B., Martel, S., Langlois, J.B., Goddard-Leon, S., Colombe, A., Janier, M., Van Seuningen, I., Losson, R., Valcourt, U., Treilleux, I., Dubus, P., Bardeesy, N., Bartholin, L., 2012. Tif1gamma suppresses murine pancreatic tumoral transformation by a Smad4-independent pathway. Am. J. Pathol. 180, 2214-2221.

Wall, N.A., Hogan, B.L., 1994. TGF-beta related genes in development. Curr Opin Genet Dev 4, 517-522.

Wang, E., Kawaoka, S., Roe, J.S., Shi, J., Hohmann, A.F., Xu, Y., Bhagwat, A.S., Suzuki, Y., Kinney, J.B., Vakoc, C.R., 2015. The transcriptional cofactor TRIM33 prevents apoptosis in B lymphoblastic leukemia by deactivating a single enhancer. eLife 4, e06377.

Weeks, D.L., Melton, D.A., 1987. A maternal mRNA localized to the vegetal hemisphere in Xenopus eggs codes for a growth factor related to TGF-beta. Cell 51, 861-867.

Willnow, T.E., Hilpert, J., Armstrong, S.A., Rohlmann, A., Hammer, R.E., Burns, D.K., Herz, J., 1996. Defective forebrain development in mice lacking gp330/megalin. Proc Natl Acad Sci U S A 93, 8460-8464.

Wisotzkey, R.G., Mehra, A., Sutherland, D.J., Dobens, L.L., Liu, X., Dohrmann, C., Attisano, L., Raftery, L.A., 1998. Medea is a Drosophila Smad4 homolog that is differentially required to potentiate DPP responses. Development 125, 1433-1445.

Xi, Q., Wang, Z., Zaromytidou, A.I., Zhang, X.H., Chow-Tsang, L.F., Liu, J.X., Kim, H., Barlas, A., Manova-Todorova, K., Kaartinen, V., Studer, L., Mark, W., Patel, D.J., Massague, J., 2011. A poised chromatin platform for TGF-beta access to master regulators. Cell 147, 1511-1524.

Xue, J., Chen, Y., Wu, Y., Wang, Z., Zhou, A., Zhang, S., Lin, K., Aldape, K., Majumder, S., Lu, Z., Huang, S., 2015. Tumour suppressor TRIM33 targets nuclear beta-catenin degradation. Nature communications 6, 6156.

Yang, X., Li, C., Herrera, P.L., Deng, C.X., 2002. Generation of Smad4/Dpc4 conditional knockout mice. Genesis 32, 80-81.

Ying, Q.L., Nichols, J., Chambers, I., Smith, A., 2003. BMP induction of Id proteins suppresses differentiation and sustains embryonic stem cell self-renewal in collaboration with STAT3. Cell 115, 281-292.

Zohn, I.E., Sarkar, A.A., 2010. The visceral yolk sac endoderm provides for absorption of nutrients to the embryo during neurulation. Birth Defects Res A Clin Mol Teratol 88, 593-600.

CHAPTER 5

Trim33 regulates the naïve pluripotency network in mouse embryonic stem cells

Abstract

Embryonic stem cells (ESCs) are an established model for investigating developmental processes, disease conditions, tissue regeneration as well as therapeutic targets. While biochemical mechanisms that maintain the non-differentiated, naïve state of pluripotency in both mouse (m) ESCs and human (h) ESCs are well understood, transcriptional networks that prime ESCs to exit from pluripotency and initiate the first events of differentiation, and mechanisms that dismantle ground state pluripotency are poorly known. Here I report that mESCs deficient in *Trim33* are indistinguishable from control cells when cultured under non-differentiating conditions. However, when induced to differentiate, they show pronounced morphological changes and display sustained up-regulation of key pluripotency factors e.g., *Esrrb*, *Tfcp2l1, Klf5.* My results suggest that Trim33 regulates equilibrium between naïve pluripotency and reversible/transitional phases prior to achieving primed pluripotency and earliest lineage segregation events in differentiating mESCs.

Introduction

Embryonic stem cells (ESCs) have been used to investigate developmental processes, disease conditions, tissue regeneration as well as therapeutic targets *in vitro* (Evans, 2011). Transcriptional networks underlying ground state pluripotency have been a subject of intense study in both mouse as well as human embryonic stem cells and used effectively for derivation of induced pluripotent cells (Gafni et al., 2013; Hanna et al., 2010; Posfai et al., 2014; Robinton and Daley, 2012). During the last 3 decades several key findings have contributed to the development of protocols that allow culture of non-differentiated, naïve state mESCs and hESCs *in vitro*. Mouse ESCs are dependent on Leukemia Inhibitory Factor (LIF) and BMP signaling while hESCs require Fgf and Nodal/Activin signaling for successful propagation in culture in their pluripotent state (Besser, 2004; James et al., 2005; Martello and Smith, 2014; Williams et al., 1988; Ying et al., 2003; Ying et al., 2008). Mouse ESCs can also be effectively maintained in undifferentiated state with specific small molecule inhibitors of ERK and the GSK3β kinase signaling (2i conditions) without LIF (Ying et al., 2008). The fact that ESCs require special, defined conditions for propagation in culture in ground state pluripotency and respond to external changes by rapidly defaulting to a differentiated fate suggests that naïve pluripotency is wired to collapse (Martello and Smith, 2014). However, transcriptional networks that prime ES cells to exit from pluripotency and mechanisms by which the ground state pluripotency is dismantled are currently poorly known (Martello and Smith, 2014). Here we demonstrate that *Trim33*, a

tumor suppressor and transcriptional regulator, is required for normal early mESC differentiation. Specifically, differentiating mESCs deficient in *Trim33* fail to form morphologically normal appearing embryoid bodies (EBs) during the early phases of differentiation, and display sustained up-regulation of core pluripotency factors. Our results imply that *Trim33* regulates the balance between the naïve pluripotency and transitional/primed phases in early differentiating mESCs.

Results and Discussion

mESC lines were established from mouse blastocysts that were homozygous for the floxed *Trim33* allele and additionally carried the $UbcCre^{ERT2}$ transgene ($Trim33^{FF}$:$UbcCre^{ERT2}$ ESCs). When these cells were exposed to 4-hydroxytamoxifen (4-OHT), sequences encoded by exons 2-4 were excised, and ESCs lacking the functional *Trim33* gene ($Trim33^{KO}$) were generated (Figure 5.1). $Trim33^{KO}$ ESCs were indistinguishable from control cells when cultured under non-differentiating conditions in the presence of LIF+2i (Figure 5.1. A-D). They expressed the stem cell markers SSEA-1 (Figure 5.1. E-F), the key pluripotency factor Pou5f1 and showed characteristic ESC colony morphology identical to that of control mESCs. $Trim33^{KO}$ ESCs were propagated in culture over 20 days, corresponding to 6 passages without detectable morphological changes (Figure 5.1).

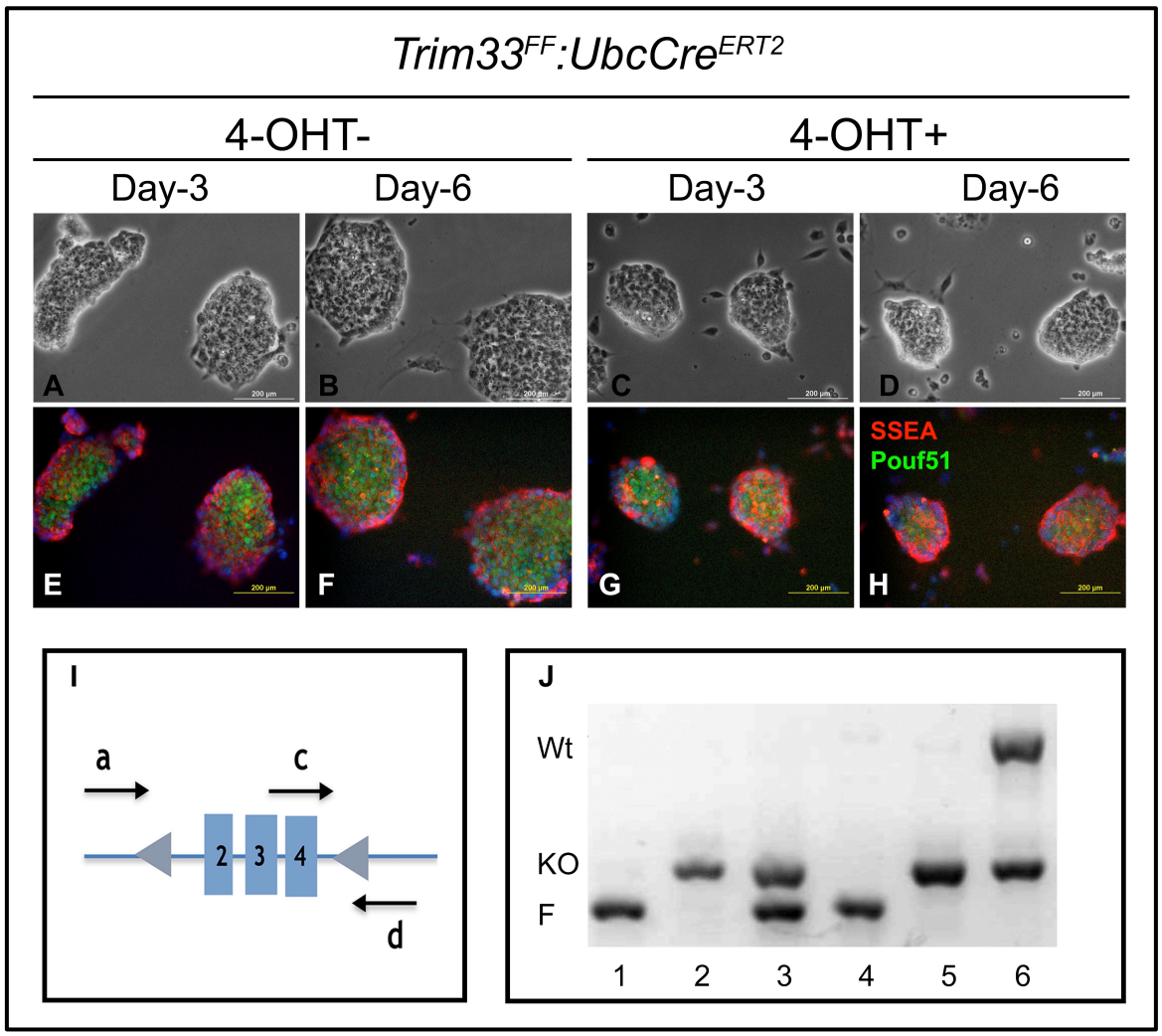

Figure 5.1. *Trim33*^{KO} ESCs are indistinguishable from control ESCs under non-differentiating culture conditions. (A-H) shows mESCs cultured with LIF+2i (A-D): Bright field images of control (A, B, 4-OHT-) and *Trim33*^{KO} (C, D, 4-OHT+) *Trim33*^{FF}*:UbcCre*^{ERT2} ES cells showing characteristic ESC colony morphology. (E-H): Immunohistochemistry images for control (E, F) and *Trim33*^{KO} cells (G, H), both expressing the SSEA and Pouf51 antigen. Scale bar (A-H) 200µm. (I) shows schematic presentation of the targeted *Trim33* locus. Arrows a, b, and c depict the primers used in the genotyping assay (F). F: #1 is *Trim33*^{FF}*:UbcCre*^{ERT2}, 4-OHT- and #2 is *Trim33*^{FF}*:UbcCre*^{ERT2}, 4-OHT+, other lanes are known controls.

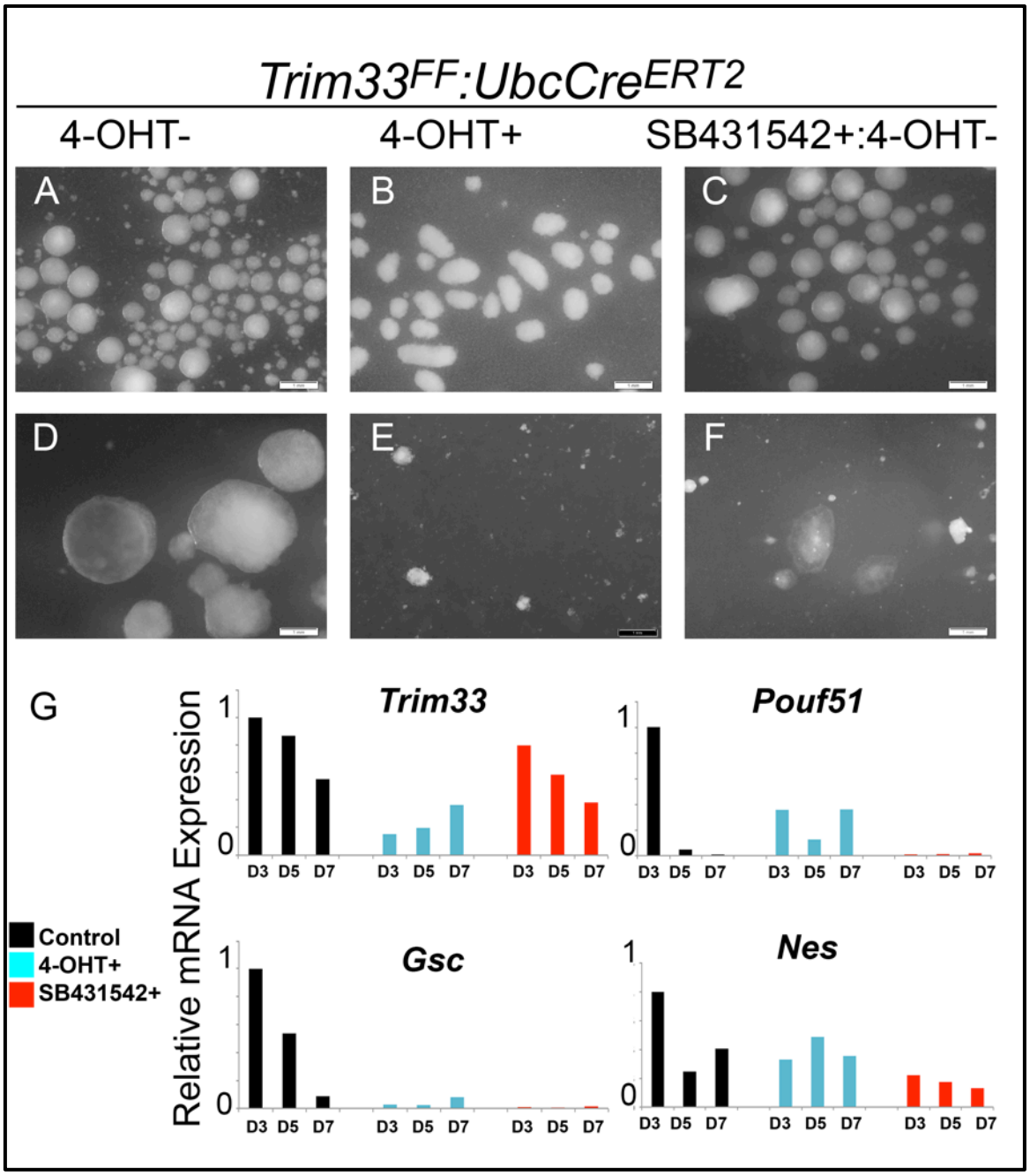

Figure 5.2. *Trim33*^{KO} EBs show distinct morphology and expression profile as compared to control and SB431542-treated EBs. (A-F) Representative images of EBs at day 5 (A-C) and day 9 (D-F) in differentiation. EBs were treated with 4-OHT (B, E) and SB431542 (C, F) at 24 hours into differentiation culture. EBs in (B) have a flattened appearance and are shedding cells on periphery. Scale bars=1mm (G) mRNA expression by qRT-PCR for *Trim33*, pluripotency marker *Pouf51*, mesoderm marker *Gsc* and ectoderm marker *Nes* in corresponding EB samples as in A-F.

The critical role of TGF-β/Nodal signaling in mesendoderm induction is well-established (Conlon et al., 1994). Moreover, previous studies have shown that the function of Trim33 as a chromatin reader is required for Nodal-triggered mesendoderm induction (Xi et al., 2011). To complement and expand these findings, we tested whether deletion of *Trim33* and inactivation of TGF-β/Nodal type I receptors (by a chemical inhibitor SB431542 (Inman et al., 2002)) would result in identical outcomes. To this end, ESCs were cultured without LIF and 2i in the presence of Fetal Calf Serum (FCS), i.e., conditions that are permissive for ESCs to form EBs and differentiate. Under these culture conditions, control ESCs (4-OHT-) formed well-defined, cystic EBs (Figure 5. 2 A and D). In contrast, *Trim33*^{FF}*UbcCre*^{ERT2} ESCs treated with 4-OHT failed to form discernable EBs and showed a large amount of shedding cells on the surface of the EB (Figure 5.2 B); there were an insignificant number of clusters beyond day 5 (Figure 5. 2 E). SB431542-treated cultures appeared to form differentiating EBs comparable to control cultures in earlier stages, however, beyond day 5 they lost the EB-like structure and assumed a flattened, amoeboid-like morphology. Clusters that survived remained attached to the low attachment dish used for the EB culture (Figure 5.2 F).

Since the control EBs and those cultured in the presence of 4-OHT or SB431542 appeared all morphologically distinct, I analyzed expression levels of well-established germ layer and pluripotency markers by using qRT-PCR. As expected, both SB431542-treated and 4-OHT-treated EBs failed to express mesendoderm markers *Gsc* and *Foxa2* (Figure 5.2 G and data not shown), while

the ectoderm marker *Nestin* was normally expressed (Figure 5.2 G). However, the key pluripotency marker *Pou5f1* was barely detectable in SB431542-treated cultures, while the 4-OHT+ *Trim33*^{KO} cultures showed high levels of *Pou5f1* expression both 5 and 7 days after induction of differentiation (Figure 5.2.G). These data suggest that cells lacking *Trim33* favor more primitive, closer-to-ground state pluripotency, and thus the role of *Trim33* during these first days of differentiation is not simply to regulate Nodal-induced mesendoderm formation.

Characterization of *Trim33*^{KO} EBs showed an increased number of apoptotic cells at day 3.5 when assayed for cleaved caspase-3 (Figure 5.3). However, the positively staining cells did not co-localize with peripherally shedding cells on the surface of the *Trim33*^{KO} EBs. A recent study showed that *Trim33* deficiency correlates with enhanced sensitivity to DNA damage (Kulkarni et al., 2013). To examine whether DNA damage would contribute to the *Trim33*^{KO} EB phenotype, we stained both control and *Trim33*^{KO} EBs for the DNA damage marker γH2AX (Figure 5.4). This assay revealed that in differentiating EBs there are no detectable differences in γH2AX staining between controls and *Trim33* mutants suggesting that in this context *Trim33* is not involved in a DNA damage response.

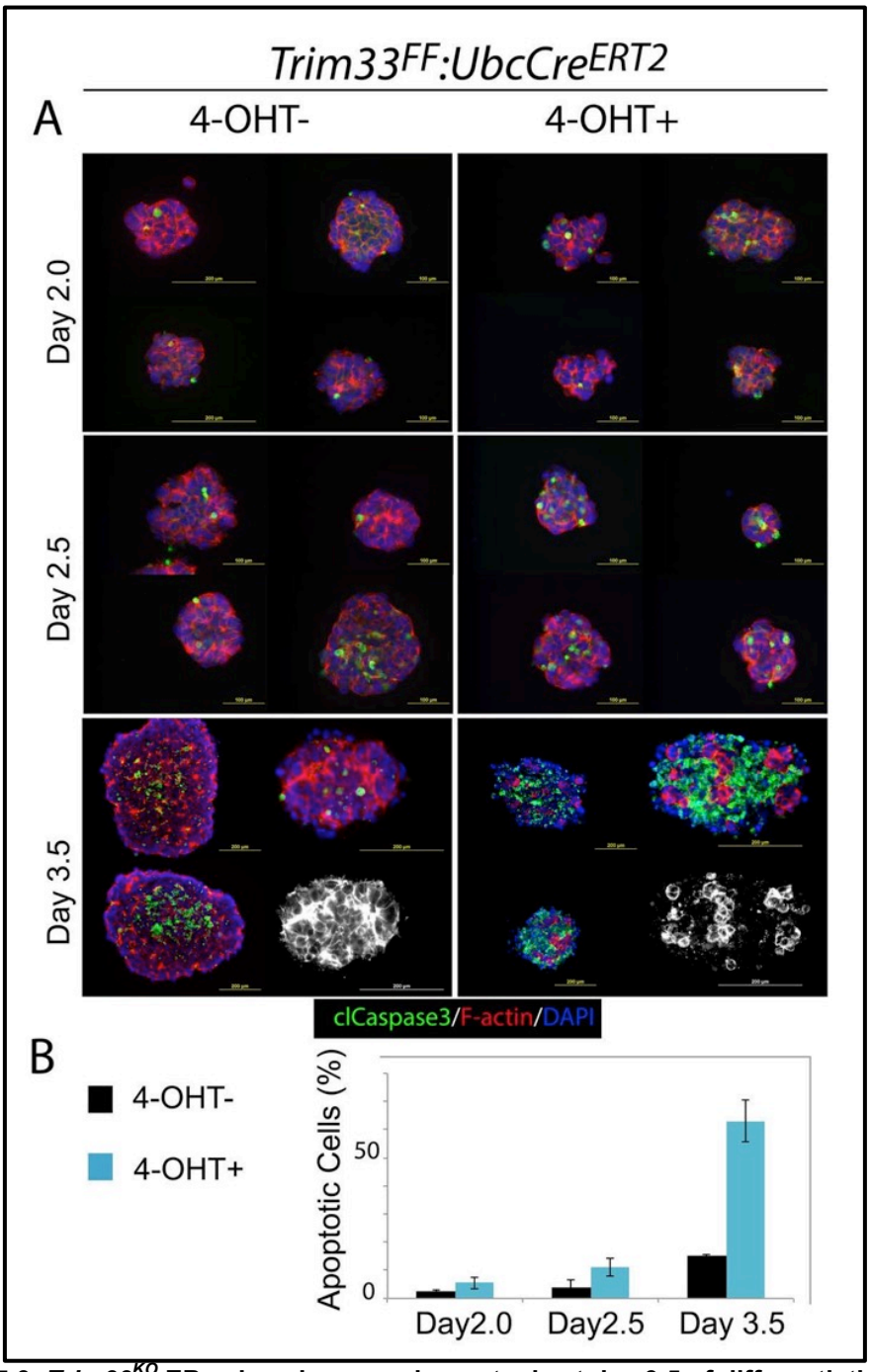

Figure 5.3. *Trim33*^{KO} EBs show increased apoptosis at day 3.5 of differentiation. Cre induction at day 0 of differentiation. (A) Representative images of control and *Trim33*^{KO} EBs at days 2, 2.5 and 3.5 in differentiation showing immunostaining for cleaved caspase3 (clcaspase3, green). To identify cell boundaries, the EBs were stained for F-actin (red, also highlighted in single channel black and white day 3.5 images; lower right pictures). Nuclear staining with DAPI, blue. Scale bars, Day 2.0 and 2.5, 100μm; Day 3.5, 200μm (B) Quantification of *per cent* apoptotic cells. Error bars = +/- SEM.

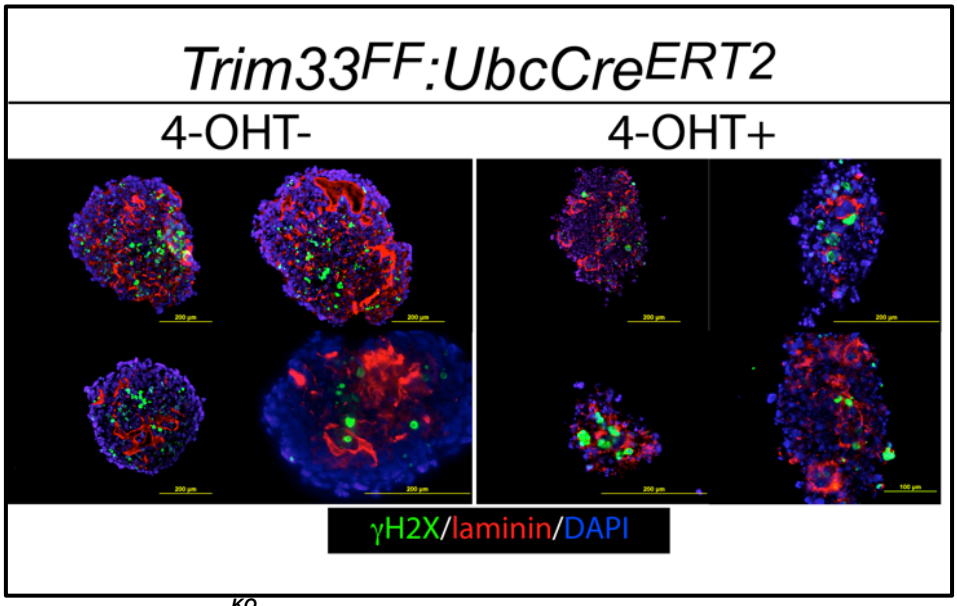

Figure 5.4. *Trim33*^{KO} EBs do not accumulate DNA double strand breaks. Representative images of control and *Trim33*^{KO} EBs at days 2.5 showing immunostaining for γH2AX (green); the basement membrane was stained for laminin (red) Scale bars, 200μm. Nuclear staining with DAPI, blue).

To better understand the role of Trim33 in initial phases of ESC differentiation, we performed genome-wide transcriptomic analyses using RNASeq on RNAs harvested from control 4-OHT- and 4-OHT+ differentiating mESCs (*Trim33*^{FF}*:UbcCre*^{ERT2}*)* at day-2 and day-2.5 of differentiation (4-OHT induction at the initiation of differentiation). These assays returned several differentially expressed genes involved in ESC self-renewal, while only a few genes involved in ESC differentiation were differentially expressed (Figure 5.5). None of the differentially expressed genes were directly involved in apoptotic responses suggesting that the increased apoptosis detected in mutant EBs during the 4th day of differentiation is secondary to the earlier changes in cell differentiation. In addition to *Trim33,* only a few genes were down regulated (Figure 5.5). One of them was *Rac1* (2-fold down at day 2), which has been implicated in EB survival

(He et al., 2010). Notably, within 48 hours of *Trim33* transcriptional deletion, *Stat3*, *Socs3, Klf* factors, *Tfcp2l1* and *Esrrb* were up regulated. The aforementioned *Klf* factors and *Tfcp2l1,* both of which are downstream targets of Stat3 (in effect downstream of LIF), have been validated as mediators of pluripotency (Gafni et al., 2013; Matsuda et al., 1999; Niwa et al., 1998; Qiu et al., 2015; Ware et al., 2014; Ye et al., 2013). While *Stat3* activation downstream of LIF signaling plays a critical and well-characterized role in mESC renewal (Matsuda et al., 1999; Niwa et al., 1998), recent reports suggest that it could carry a similar function in naïve human stem cells as well (Gafni et al., 2013; Ware et al., 2014). Moreover, high *Stat3* expression has been shown to be able to prime mouse epiblast stem cells towards a more naïve pluripotent state (van Oosten et al., 2012; Yang et al., 2010). *Socs3,* a well-known target of LIF-Stat3 signaling, has been suggested to play an important regulatory role in ESC survival (Duval et al., 2000), while Tfcp2l1 is a common downstream mediator of both Stat3 and Wnt signaling pathways (Qiu et al., 2015; Ye et al., 2013). Esrrb, which has been known to be able to activate *Pou5f1* and sustain ES cells in pluripotent state in the absence of LIF (Zhang et al., 2008), is concomitantly highly up regulated in *Trim3*^{KO} EBs. Esrrb itself functions downstream of Gsk3 inhibition (Martello et al., 2012). Its up regulation in *Trim3*^{KO} cultures would therefore create a parallel circuitry maintaining pluripotency independent of the LIF-Stat3 pathway. Taken together, these data suggest that Trim33 actively regulates equilibrium between naïve pluripotency and reversibility/transitional phases before the earliest lineage segregation events in differentiating mESCs.

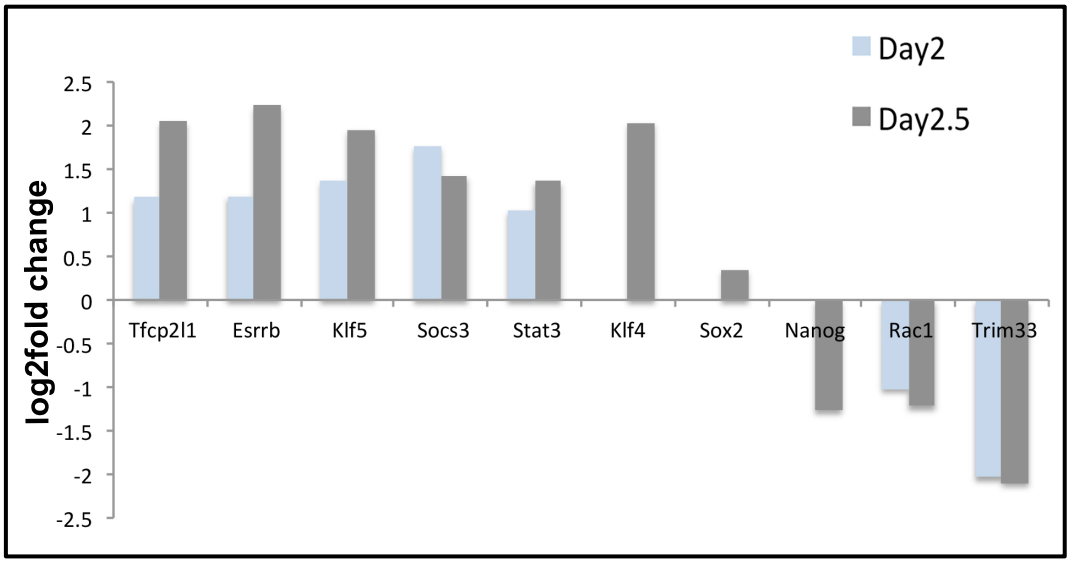

Figure 5.5. Several core pluripotency genes are upregulated in *Trim33*^{KO} EBs.Log2fold change of selected targets from differentially expressed genes from RNA-Seq data at days 2 and 2.5 in differentiation. N = 3 independent sample pairs of control and *Trim33*^{KO} EBs.

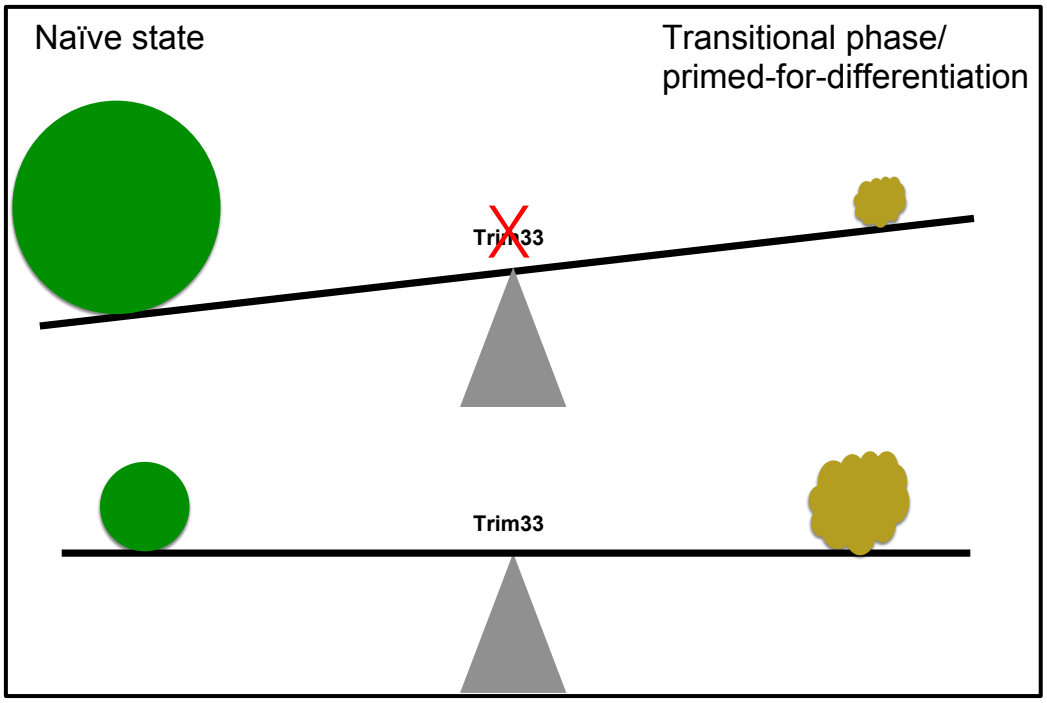

Figure 5.6. A conceptual model of regulation of pluripotency network and exit from pluripotency by *Trim33*. *Trim33* regulates meta-states of pluripotency *in vitro*, in particular exit from pluripotency to the transitional or primed-for-differentiation phase. In the absence of *Trim33*, the equilibrium shifts toward predominance of a core transcriptional program that sensitizes progenitor cells towards inappropriately differentiated cell fates.

Implications for developmental processes and cancer

Trim33 has been shown to redundantly regulate differentiation of neural stem cells (Falk et al., 2014) and terminal differentiation of mammary epithelial cells (Hesling et al., 2013). In both contexts, Trim33 appears to control differentiation fates early on. In concordance, Trim33 has been shown to function as a tumor suppressor in different malignancies, such as chronic myelomonocytic leukemia, hepatocellular carcinoma and pancreatic ductal adenocarcinoma (Aucagne et al., 2011; Herquel et al., 2011; Vincent et al., 2009). One of the salient features of malignant cancerous lesions is poor differentiation and amplification of transformed cell populations. Our current results suggest that *Trim33*-deficiency keeps stem cells in a naïve pluripotent state (or sensitizes progenitor cells

towards undifferentiated cell fates), which could also explain why cells that have defects in Trim33-regulated processes are insensitive to differentiation signals during pathological conditions, such as cancer. Our results suggest that Trim33 controls the balance between stem/progenitor cell self-renewal and their ability to commit definitively to appropriate differentiation fates in a context dependent manner by actively regulating disassembly of the naïve pluripotency network (Figure 5.6).

Experimental Procedures

Ethics Statement

This research was conducted in strict accordance with the recommendations in the Guide for the Care and Use of Laboratory Animals of the National Institutes of Health. Experiments described are specifically approved by the University Committee on Use and Care of Animals at the University of Michigan-Ann Arbor (Protocol Number: PRO00005004).

Establishment of embryonic stem cell lines and EB culture

Mouse ES cells were derived from *Trim33*^{FF}*: UbcCre*^{ERT2} blastocysts as described in (Pieters et al., 2012); ESCs were passaged in serum-containing medium (Life Technologies, Cat. No. 16141-061), dissociating with TrypLE Express (Life Technologies, Cat. No. 12605-010) and maintained in serum replacement medium (Knock Out Serum Replacement Cat No. 10828-010, Life Technologies) in a base medium of 1:1 Knock Out Dulbecco's Modified Eagle's Medium and Ham's F12. *Trim33*^{FF}*: UbcCre*^{ERT2} ESCs were maintained in feeder-

free culture conditions in the presence of 2i+LIF (2i: PD0325901 (Stemgent) in final concentration of 0.4μM and CHIR99021 (Stemgent) in final concentration of 3μM, LIF: (1000X) ESGRO (Millipore) ESG 1106) on 0.1% gelatin (Sigma, G1393) coated tissues culture plates. EB formation and differentiation were carried out per the ATCC protocol in 20% serum containing medium. Both the media for non-differentiating and differentiating conditions were supplemented by Glutamine (GlutaMAX-I (100X), Life Technologies, Cat. No. 35050-061), β-mercaptoethanol (1000X, Life Technologies, Cat. No. 21985-023) and Penicillin/Streptomycin (Life Technologies, Cat. No.15140-122).

4-hydroxytamoxifen (4-OHT) (Sigma Cat. No. T176) was added at intended and precise time points in a concentration of 1 μg per mL of medium. EB cultures were treated with SB431542 (Sigma) at concentration of 10μM, in parallel with 4-OHT treatments for equivalent duration of time.

Real-time PCR

Equivalent amounts/number of EBs were collected in 100-200 μL of commercially available (Qiagen) RLT buffer at intended time points. RNA was isolated using (Qiagen RNesy Mini Kit Cat. No 74104) and cDNA was synthesized using Omniscript RT(Qiagen Cat. No.205111) with standard methods. Taqman Assay reagents (Life Technoligies) were used for all targets except *Actb*, which was used to normalize expression levels. Universal Probe Library-based assays for *Actb* (Roche Applied Science) with gene-specific primer sequences generated by the manufacturer's online algorithm and Taqman assay details are below. 30μl assays dispensed in TaqMan Universal PCR 2X master mix (Applied

Biosystems) with or without universal probe were quantified using Applied Biosystems ABI7300 PCR and ViiA7 detection systems and software. All Ct values were manually checked. cDNA was diluted where necessary to avoid Cts lower than 18.

Taqman Assays # are provided in parenthesis*: Gsc* (Mm00650681_g1)*, Nes* (Mm00450205_m1)*, Pouf51* (Mm00658129_gH)*, Trim33 (*Mm01308695_m1)

Actb: Forward Primer (tgacaggatgcagaaggaga), Reverse Primer (cgctcaggaggagcaatg), Universal Probe #106.

RNA-Seq

Equivalent amounts/number of EBs were collected at Day 7 in triplicate mutant-control pairs, in 100-200 µL commercially available (Qiagen) RLT buffer. Total RNA was isolated using (Qiagen RNeasy Mini Kit Cat. No. 74104). mRNA and sequencing libraries were prepared by the University of Michigan DNA Sequencing Core and reads generated on Illumina HiSeq2000. After quality assessment per sample, single-end, 52 base pair reads were aligned to mm9 (Mus musculus assembly July 2007) using STAR RNA Seq aligner (Dobin et al., 2013). On average, input reads ranged between 35 million to 42 million across all samples, out of which approximately 80 per cent reads mapped uniquely. Read counts for differential expression were obtained using HTSeq program. Differential expression analyses were performed using the DESeq program in R Statistical Package.

https://bioconductor.org/packages/3.3/bioc/vignettes/DESeq/inst/doc/DESeq.pdf.

Immunohistochemistry

EBs were collected in sterile DBPS and fixed for 15 minutes in fresh 4% paraformaldehyde in PBS at RT. Briefly, for cryo sections, EBs were washed in PBS, processed through sterile 10% sucrose in PBS, 7% gelatin (Sigma G6650, 75 bloom) and 15% sucrose in PBS. EBs were embedded in fresh 7% gelatin: 15% sucrose in PBS on ice, held on dry ice to store at −20 or −80 °C. 10μm cryo sections were cut and stored at −20 or −80°C. Antigen retrieval was not needed. Primary antibodies to SSEA (Developmental Studies Hybridoma Bank Cat.No. MC480), Pouf51 (C30A3) (Cell Signaling Cat. No. 2840), cleaved caspase3 (Asp 175) (Cell Signaling Cat.No.9661), γH2AX (EMD Millipore Cat. No. DR1016) and laminin (Sigma Cat.No. L9393) were used according to manufacturer's instructions.

References

Aucagne, R., Droin, N., Paggetti, J., Lagrange, B., Largeot, A., Hammann, A., Bataille, A., Martin, L., Yan, K.P., Fenaux, P., Losson, R., Solary, E., Bastie, J.N., Delva, L., 2011. Transcription intermediary factor 1gamma is a tumor suppressor in mouse and human chronic myelomonocytic leukemia. J. Clin. Invest. 121, 2361-2370.

Besser, D., 2004. Expression of nodal, lefty-a, and lefty-B in undifferentiated human embryonic stem cells requires activation of Smad2/3. J. Biol. Chem. 279, 45076-45084.

Conlon, F.L., Lyons, K.M., Takaesu, N., Barth, K.S., Kispert, A., Herrmann, B., Robertson, E.J., 1994. A primary requirement for nodal in the formation and maintenance of the primitive streak in the mouse. Development 120, 1919-1928.

Dobin, A., Davis, C.A., Schlesinger, F., Drenkow, J., Zaleski, C., Jha, S., Batut, P., Chaisson, M., Gingeras, T.R., 2013. STAR: ultrafast universal RNA-seq aligner. Bioinformatics 29, 15-21.

Duval, D., Reinhardt, B., Kedinger, C., Boeuf, H., 2000. Role of suppressors of cytokine signaling (Socs) in leukemia inhibitory factor (LIF) -dependent embryonic stem cell survival. FASEB J 14, 1577-1584.

Evans, M., 2011. Discovering pluripotency: 30 years of mouse embryonic stem cells. Nat. Rev. Mol. Cell Biol. 12, 680-686.

Falk, S., Joosten, E., Kaartinen, V., Sommer, L., 2014. Smad4 and Trim33/Tif1gamma redundantly regulate neural stem cells in the developing cortex. Cereb. Cortex 24, 2951-2963.

Gafni, O., Weinberger, L., Mansour, A.A., Manor, Y.S., Chomsky, E., Ben-Yosef, D., Kalma, Y., Viukov, S., Maza, I., Zviran, A., Rais, Y., Shipony, Z., Mukamel, Z., Krupalnik, V., Zerbib, M., Geula, S., Caspi, I., Schneir, D., Shwartz, T., Gilad, S., Amann-Zalcenstein, D., Benjamin, S., Amit, I., Tanay, A., Massarwa, R., Novershtern, N., Hanna, J.H., 2013. Derivation of novel human ground state naive pluripotent stem cells. Nature 504, 282-286.

Hanna, J., Cheng, A.W., Saha, K., Kim, J., Lengner, C.J., Soldner, F., Cassady, J.P., Muffat, J., Carey, B.W., Jaenisch, R., 2010. Human embryonic stem cells with biological and epigenetic characteristics similar to those of mouse ESCs. Proc. Natl. Acad. Sci. U. S. A. 107, 9222-9227.

He, X., Liu, J., Qi, Y., Brakebusch, C., Chrostek-Grashoff, A., Edgar, D., Yurchenco, P.D., Corbett, S.A., Lowry, S.F., Graham, A.M., Han, Y., Li, S., 2010. Rac1 is essential for basement membrane-dependent epiblast survival. Mol Cell Biol 30, 3569-3581.

Herquel, B., Ouararhni, K., Khetchoumian, K., Ignat, M., Teletin, M., Mark, M., Bechade, G., Van Dorsselaer, A., Sanglier-Cianferani, S., Hamiche, A., Cammas, F., Davidson, I., Losson, R., 2011. Transcription cofactors TRIM24, TRIM28, and TRIM33 associate to form regulatory complexes that suppress murine hepatocellular carcinoma. Proc. Natl. Acad. Sci. U. S. A. 108, 8212-8217.

Hesling, C., Lopez, J., Fattet, L., Gonzalo, P., Treilleux, I., Blanchard, D., Losson, R., Goffin, V., Pigat, N., Puisieux, A., Mikaelian, I., Gillet, G., Rimokh, R., 2013. Tif1gamma is essential for the terminal differentiation of mammary alveolar epithelial cells and for lactation through SMAD4 inhibition. Development 140, 167-175.

Inman, G.J., Nicolas, F.J., Callahan, J.F., Harling, J.D., Gaster, L.M., Reith, A.D., Laping, N.J., Hill, C.S., 2002. SB-431542 is a potent and specific inhibitor of transforming growth factor-beta superfamily type I activin receptor-like kinase (ALK) receptors ALK4, ALK5, and ALK7. Mol. Pharmacol. 62, 65-74.

James, D., Levine, A.J., Besser, D., Hemmati-Brivanlou, A., 2005. TGFbeta/activin/nodal signaling is necessary for the maintenance of pluripotency in human embryonic stem cells. Development 132, 1273-1282.

Kulkarni, A., Oza, J., Yao, M., Sohail, H., Ginjala, V., Tomas-Loba, A., Horejsi, Z., Tan, A.R., Boulton, S.J., Ganesan, S., 2013. Tripartite Motif-containing 33 (TRIM33) protein functions in the poly(ADP-ribose) polymerase (PARP)-dependent DNA damage response through interaction with Amplified in Liver Cancer 1 (ALC1) protein. J. Biol. Chem. 288, 32357-32369.

Martello, G., Smith, A., 2014. The nature of embryonic stem cells. Annu. Rev. Cell Dev. Biol. 30, 647-675.

Martello, G., Sugimoto, T., Diamanti, E., Joshi, A., Hannah, R., Ohtsuka, S., Gottgens, B., Niwa, H., Smith, A., 2012. Esrrb is a pivotal target of the Gsk3/Tcf3 axis regulating embryonic stem cell self-renewal. Cell stem cell 11, 491-504.

Matsuda, T., Nakamura, T., Nakao, K., Arai, T., Katsuki, M., Heike, T., Yokota, T., 1999. STAT3 activation is sufficient to maintain an undifferentiated state of mouse embryonic stem cells. EMBO J. 18, 4261-4269.

Niwa, H., Burdon, T., Chambers, I., Smith, A., 1998. Self-renewal of pluripotent embryonic stem cells is mediated via activation of STAT3. Genes Dev. 12, 2048-2060.

Pieters, T., Haenebalcke, L., Hochepied, T., D'Hont, J., Haigh, J.J., van Roy, F., van Hengel, J., 2012. Efficient and user-friendly pluripotin-based derivation of mouse embryonic stem cells. Stem cell reviews 8, 768-778.

Posfai, E., Tam, O.H., Rossant, J., 2014. Mechanisms of pluripotency in vivo and in vitro. Curr. Top. Dev. Biol. 107, 1-37.

Qiu, D., Ye, S., Ruiz, B., Zhou, X., Liu, D., Zhang, Q., Ying, Q.L., 2015. Klf2 and Tfcp2l1, Two Wnt/beta-Catenin Targets, Act Synergistically to Induce and Maintain Naive Pluripotency. Stem cell reports 5, 314-322.

Robinton, D.A., Daley, G.Q., 2012. The promise of induced pluripotent stem cells in research and therapy. Nature 481, 295-305.

van Oosten, A.L., Costa, Y., Smith, A., Silva, J.C., 2012. JAK/STAT3 signalling is sufficient and dominant over antagonistic cues for the establishment of naive pluripotency. Nature communications 3, 817.

Vincent, D.F., Yan, K.P., Treilleux, I., Gay, F., Arfi, V., Kaniewski, B., Marie, J.C., Lepinasse, F., Martel, S., Goddard-Leon, S., Iovanna, J.L., Dubus, P., Garcia, S., Puisieux, A., Rimokh, R., Bardeesy, N., Scoazec, J.Y., Losson, R., Bartholin, L.,

2009. Inactivation of TIF1gamma cooperates with Kras to induce cystic tumors of the pancreas. PLoS genetics 5, e1000575.

Ware, C.B., Nelson, A.M., Mecham, B., Hesson, J., Zhou, W., Jonlin, E.C., Jimenez-Caliani, A.J., Deng, X., Cavanaugh, C., Cook, S., Tesar, P.J., Okada, J., Margaretha, L., Sperber, H., Choi, M., Blau, C.A., Treuting, P.M., Hawkins, R.D., Cirulli, V., Ruohola-Baker, H., 2014. Derivation of naive human embryonic stem cells. Proc. Natl. Acad. Sci. U. S. A. 111, 4484-4489.

Williams, R.L., Hilton, D.J., Pease, S., Willson, T.A., Stewart, C.L., Gearing, D.P., Wagner, E.F., Metcalf, D., Nicola, N.A., Gough, N.M., 1988. Myeloid leukaemia inhibitory factor maintains the developmental potential of embryonic stem cells. Nature 336, 684-687.

Xi, Q., Wang, Z., Zaromytidou, A.I., Zhang, X.H., Chow-Tsang, L.F., Liu, J.X., Kim, H., Barlas, A., Manova-Todorova, K., Kaartinen, V., Studer, L., Mark, W., Patel, D.J., Massague, J., 2011. A poised chromatin platform for TGF-beta access to master regulators. Cell 147, 1511-1524.

Yang, J., van Oosten, A.L., Theunissen, T.W., Guo, G., Silva, J.C., Smith, A., 2010. Stat3 activation is limiting for reprogramming to ground state pluripotency. Cell stem cell 7, 319-328.

Ye, S., Li, P., Tong, C., Ying, Q.L., 2013. Embryonic stem cell self-renewal pathways converge on the transcription factor Tfcp2l1. EMBO J. 32, 2548-2560.

Ying, Q.L., Nichols, J., Chambers, I., Smith, A., 2003. BMP induction of Id proteins suppresses differentiation and sustains embryonic stem cell self-renewal in collaboration with STAT3. Cell 115, 281-292.

Ying, Q.L., Wray, J., Nichols, J., Batlle-Morera, L., Doble, B., Woodgett, J., Cohen, P., Smith, A., 2008. The ground state of embryonic stem cell self-renewal. Nature 453, 519-523.

Zhang, X., Zhang, J., Wang, T., Esteban, M.A., Pei, D., 2008. Esrrb activates Oct4 transcription and sustains self-renewal and pluripotency in embryonic stem cells. J. Biol. Chem. 283, 35825-35833.

CHAPTER 6

Summary, conclusions and prospects

Trim33 in cardiac differentiation

Both mouse genetics and embryonic stem cell (ESC) differentiation systems have been widely used to dissect molecular mechanisms of disease. ESCs as well induced pluripotent stem cells (iPSCs) have also been used extensively to model regenerative mechanisms and to develop therapeutic targets *in vitro.*

In this study, I used ES cell-based *in vitro* differentiation assays and tissue-specific knockout mouse models to investigate the role of *Trim33* in mouse development.

I found that deletion of *Trim33* in embryoid bodies after mesoderm induction results in morphological, functional and molecular changes in visceral endoderm and cardiac mesoderm *in vitro*. Visceral endoderm (VE) provides nutrients and instructive morphogen signals for appropriate cell fate and patterning decisions (Bielinska et al., 1999). The anterior visceral endoderm (AVE) constitutes a distinct population of ExEn cells and plays critical role in positioning of the head and heart (Madabhushi and Lacy, 2011). In my experimental conditions (Chapter 4), *Trim33*-deficient EBs are viable and form beating clusters. However, at later stages the mutant EBs show less-expanded cystic appearance and several VE associated genes are dramatically down regulated in *Trim33*-deficient EBs even before the morphological differences are obvious (Chapter 4).

My findings that a higher number of *Trim33*-deficient EBs show beating cell clusters and display up regulation of a cardiac failure marker *Ankrd1* suggests that *Trim33* plays either a direct role in appropriate myocardial differentiation or that *Trim33* contributes to the cardiac differentiation via an indirect mechanism involving VE differentiation. *Trim33* deletion in the embryo proper (i.e. epiblast) using the *Sox2Cre* driver results in embryonic lethality around embryonic day (E) 13 in mice, VSD and cardiac failure as a primary phenotype. However, the *Sox2Cre* driver specifically recombines and deletes *Trim33* in the epiblast but not in the VE, suggesting that Trim33 regulates early cardiac differentiation directly in the embryo proper. Mesendoderm-specific deletion of *Trim33* using the *TCre* driver did not result in gross cardiac phenotypes. *Sox2Cre* has been shown to recombine at early epiblast stage prior to E5.75 (Chu et al., 2004), while strong *TCre*-induced recombination can be detected in the primitive streak and the lateral mesodermal wings at the mid-streak stage (E7.5) (Kumar et al., 2008). Collectively, these results suggest that *Trim33* is required at the time when the mesodermal multipotent progenitor cells commit to the cardiac lineage. *In vivo*, posterior epiblast cells comprise mesoderm precursors that also include cardiac progenitors. These presumptive cardiac progenitors assume cardiac identity in part during their ingression from the primitive streak and simultaneously retain lineage potency of the epiblast i.e. cell fates are plastic (Tam et al., 1997). In addition, cardiac-specific deletion of *Trim33* using the *Nkx2_5Cre* driver did not result in any abnormalities in the heart, *Trim33FF:Nkx2_5Cre+* mutants are viable, fertile and live normal life spans. Taken together, *Trim33* plays a non-

redundant role between the onset of gastrulation and cardiac specification. Whether the phenotypic outcomes *in vivo* are cell autonomous or not remains to be shown. As discussed earlier, the AVE plays important roles in positioning of the head and heart. In addition, the definitive endoderm, which is arises in concert with mesoderm as cells ingress through the streak (Lewis and Tam, 2006) also influences cardiac patterning (Sugi and Lough, 1994; Uosaki et al., 2012; Van Vliet et al., 2012). Although the endoderm-derived molecules that specifically signal to induce normal cardiac patterning are not fully understood, TGF-β signaling components among other signaling pathways are strong candidates implicated in such a role (Lough and Sugi, 2000; Sugi and Lough, 1995; Van Vliet et al., 2012). Concordantly, *Trim33* as a regulator of TGF-β signaling would be a logical candidate and my data provide circumstantial evidence coinciding with the timing of the aforementioned inductive effects by definitive endoderm and cardiac differentiation *in vivo*. The strongest evidence that *Trim33* regulates TGF-β signaling in cardiac morphogenesis is provided by the partial rescue of the epiblast-specific *Trim33* lethal phenotype by *Smad4* haploinsufficiency.

A biphasic stage-specific role of Smad2 activity downstream of Activin/Nodal and TGF-β signaling in cardiac development has been demonstrated *in vitro.* In this model, Activin/Nodal signals are positive regulators for the early differentiation of mESCs in the initial phase while TGF-β signals play inhibitory roles in cardiac differentiation in the latter phase. (Cai et al., 2012; Kitamura et al., 2007). The higher number of beating clusters in *Trim33*-deficient EBs

suggests that TGF-β signaling is down regulated in mutants during the phase in which it suppresses cardiomyogenesis and consistent with this observation, day 7 *Trim33*-deficient EBs show reduction in Smad4 and pSmad2 protein levels *in vitro*.

Apart from the cardiac phenotype, all epiblast-specific *Trim33* mutants that were occasionally retrieved in stages E17-18 showed cleft palate defect, evidently a secondary hypoxic phenotype from ensuing cardiac failure.

Other less penetrant phenotypes observed in epiblast-specific *Trim33* mutants, in particular those associated with down regulation of *Mttp* and lipoprotein-associated mechanisms are intriguing given the similarity in timing of embryonic lethality.

Trim33 in early mES cell differentiation

Results from *Trim33*^{KO} ES cells in differentiation (Chapter 5) highlights the role of Trim33 in maintaining the equilibrium between meta-states of pluripotency. Specifically, on a continuum of pluripotency to the earliest differentiation event, *Trim33*^{KO} ES cells favor a more primitive fate; up regulating several core pluripotency factors including some that are critical in maintaining mESCs in culture (Chapter 5). Whether the mES cell on the periphery of pluripotency reciprocally interprets *Trim33* deficiency as an instruction to pause impending differentiation cannot be concluded from transcriptional analyses alone. It does generate the next hypothesis and the *Trim33*^{KO} ES cell differentiation data are therefore valuable from a stem cell biology aspect.

Conclusions

Collectively, *Trim33* regulates extra embryonic endoderm development *in vitro and Trim33* is required in the embryo proper for normal cardiac development. Trim33 regulates TGF-β signaling in cardiac differentiation. In addition, *Trim33* is required for exit of mES cells from pluripotent phase towards a primed-for-differentiation phase. Thus, from two independent contexts, the emerging paradigm is that *Trim33* plays a non-redundant role in regulating progenitor cell fate within the window of plasticity and that in more committed lineages, *Trim33* is dispensable.

Observations from the scope of *in vitro* and *in vivo* experimental methods

Within my EB experimental set up, mES cells were allowed to undergo native differentiation in suspension culture and *Trim33* was deleted post mesendoderm induction at day 4 and EBs were harvested at day 7. As expected, none of the mesendoderm genes were differentially expressed. However, *Trim33*-deficient EBs clearly showed functional aberrancy in cardiomyocyte differentiation reflected by elevation of *Ankrd1,* which was recapitulated *in vivo* in epiblast-specific *Trim33* mutants along with prominent structural defects of VSD and thin compact myocardium and functionally, cardiac failure. The EBs thus successfully recapitulate early development of the embryo proper. It should be noted that the complexity of cell-cell interactions and timing of events in embryogenesis do not overlap perfectly with those in the EB *in vitro* although it is a practical and close

approximation. For instance, the described *Trim33*-deficient EBs do not have the equivalent of an epiblast-specific *Trim33* deletion. Native differentiation of EBs captures in part processes implicit to the epiblast or embryo proper while simultaneously capturing processes that are counterparts of extra embryonic tissues; the VE-related findings in *Trim33* deficient EBs meet the latter criteria. The *in vivo* data from relevant *Trim33* conditional mutants described here are consistent and align with the extrapolations made from *Trim33* deficient EBs. Taken together, both the *in vitro* and *in vivo* experimental models elucidate the complexity of the *Trim33* mutant phenotype in what is a differentiation as well as patterning defect.

Prospects

Several independent aspects can be further investigated for the comprehensive understanding of the role of *Trim33* in early embryogenesis. It will be interesting to further detail the role of Trim33 as a chromatin reader regulating the interactions between Smad2/3 and modified histones in the context of cardiomyocyte differentiation using techniques such as Chromatin Immunoprecitation with parallel sequencing (ChIP-Seq) (Morikawa et al., 2013; Postma et al., 2016; Robertson et al., 2007).*Trim33*-deficient EBs described here show down regulation of several VE-associated genes, which plausibly suggests a mechanism underlying the phenotype and early lethality observed in germline *Trim33* mutants (Kim and Kaartinen, 2008). If the said hypothesis is true, deletion of *Trim33* in a VE-specific manner using an appropriate Cre driver such as the

TtrCre (Kwon and Hadjantonakis, 2009) should phenocopy the *Trim33* germline mutant phenotype. Given the similarity of timing of embryonic lethality in epiblast-specific *Trim33* mutants and *Mttp* mutants (Raabe et al., 1998) and down regulation of *Mttp* in epiblast-specific *Trim33* mutants, it will be interesting to generate an allelic series of *Trim33* and *Mttp* mutants and observe their phenotypes. Finally, with respect to precisely mapping cell types that contribute to the cardiac phenotype in epiblast-specific *Trim33* mutants, a combination of genetic tools and advanced live imaging techniques (Chen et al., 2014; Liu and Keller, 2016) will be valuable in further detailing the role of *Trim33* in cardiac morphogenesis.

Significance

The incidence of Congenital Heart Disease (CHD) is 1-2% of all live births and covers the entire spectrum of congenital heart defects (Hoffman and Kaplan, 2002; van der Linde et al., 2011). Ventricular Septal Defects (VSDs) are the most common among all CHDs and the primary cause remains genetic ranging from chromosomal abnormalities, single gene mutations, epigenetic as well as environmental effects although sporadic VSDs are also known (Edwards and Gelb, 2016; Richards and Garg, 2010; Wolf and Basson, 2010; Yuan et al., 2013). Most CHDs including VSD are multifactorial in etiology and occur either as isolated defects or as part of syndromes, often with craniofacial anomalies (Blue et al., 2012).

From the paradigm of the conclusions of this research, it is critical to understand fine-tuning and precise timing of mechanisms underlying congenital defects, in particular the importance of not excluding causes distant to the observed phenotype(s). This includes discriminating between global effects of genetic loss of function such as down regulation of *Mttp* observed in epiblast-specific *Trim33* mutants versus identifying lineage restricted phenotypes such as the VSD as well as the secondary hypoxic phenotype of cleft palate observed in the same mouse model. In the context of Trim33 as a regulator of TGF-β signaling, this work contributes and furthers the known repertoire of CHD resulting from disruption of TGF-β signaling dosage (Arthur and Bamforth, 2011). Decoding intertwining global and tissue/organ specific phenotypes will allow for better approaches in screening and identification of therapeutic targets for precise causative mechanisms underlying common human congenital defects.

References

Arthur, H.M., Bamforth, S.D., 2011. TGFbeta signaling and congenital heart disease: Insights from mouse studies. Birth Defects Res. A Clin. Mol. Teratol. 91, 423-434.

Bielinska, M., Narita, N., Wilson, D.B., 1999. Distinct roles for visceral endoderm during embryonic mouse development. Int J Dev Biol 43, 183-205.

Blue, G.M., Kirk, E.P., Sholler, G.F., Harvey, R.P., Winlaw, D.S., 2012. Congenital heart disease: current knowledge about causes and inheritance. Med. J. Aust. 197, 155-159.

Cai, W., Guzzo, R.M., Wei, K., Willems, E., Davidovics, H., Mercola, M., 2012. A Nodal-to-TGFbeta cascade exerts biphasic control over cardiopoiesis. Circ. Res. 111, 876-881.

Chen, B.C., Legant, W.R., Wang, K., Shao, L., Milkie, D.E., Davidson, M.W., Janetopoulos, C., Wu, X.S., Hammer, J.A., 3rd, Liu, Z., English, B.P., Mimori-Kiyosue, Y., Romero, D.P., Ritter, A.T., Lippincott-Schwartz, J., Fritz-Laylin, L., Mullins, R.D., Mitchell, D.M., Bembenek, J.N., Reymann, A.C., Bohme, R., Grill, S.W., Wang, J.T., Seydoux, G., Tulu, U.S., Kiehart, D.P., Betzig, E., 2014. Lattice light-sheet microscopy: imaging molecules to embryos at high spatiotemporal resolution. Science 346, 1257998.

Chu, G.C., Dunn, N.R., Anderson, D.C., Oxburgh, L., Robertson, E.J., 2004. Differential requirements for Smad4 in TGFbeta-dependent patterning of the early mouse embryo. Development 131, 3501-3512.

Edwards, J.J., Gelb, B.D., 2016. Genetics of congenital heart disease. Curr. Opin. Cardiol.

Hoffman, J.I., Kaplan, S., 2002. The incidence of congenital heart disease. J. Am. Coll. Cardiol. 39, 1890-1900.

Kim, J., Kaartinen, V., 2008. Generation of mice with a conditional allele for Trim33. Genesis 46, 329-333.

Kitamura, R., Takahashi, T., Nakajima, N., Isodono, K., Asada, S., Ueno, H., Ueyama, T., Yoshikawa, T., Matsubara, H., Oh, H., 2007. Stage-specific role of endogenous Smad2 activation in cardiomyogenesis of embryonic stem cells. Circ Res 101, 78-87.

Kumar, A., Lualdi, M., Lewandoski, M., Kuehn, M.R., 2008. Broad mesodermal and endodermal deletion of Nodal at postgastrulation stages results solely in left/right axial defects. Dev Dyn 237, 3591-3601.

Kwon, G.S., Hadjantonakis, A.K., 2009. Transthyretin mouse transgenes direct RFP expression or Cre-mediated recombination throughout the visceral endoderm. Genesis 47, 447-455.

Lewis, S.L., Tam, P.P., 2006. Definitive endoderm of the mouse embryo: formation, cell fates, and morphogenetic function. Dev. Dyn. 235, 2315-2329.

Liu, Z., Keller, P.J., 2016. Emerging Imaging and Genomic Tools for Developmental Systems Biology. Dev. Cell 36, 597-610.

Lough, J., Sugi, Y., 2000. Endoderm and heart development. Dev. Dyn. 217, 327-342.

Madabhushi, M., Lacy, E., 2011. Anterior visceral endoderm directs ventral morphogenesis and placement of head and heart via BMP2 expression. Dev Cell 21, 907-919.

Morikawa, M., Koinuma, D., Miyazono, K., Heldin, C.H., 2013. Genome-wide mechanisms of Smad binding. Oncogene 32, 1609-1615.

Postma, A.V., Bezzina, C.R., Christoffels, V.M., 2016. Genetics of congenital heart disease: the contribution of the noncoding regulatory genome. J. Hum. Genet. 61, 13-19.

Raabe, M., Flynn, L.M., Zlot, C.H., Wong, J.S., Veniant, M.M., Hamilton, R.L., Young, S.G., 1998. Knockout of the abetalipoproteinemia gene in mice: reduced lipoprotein secretion in heterozygotes and embryonic lethality in homozygotes. Proc. Natl. Acad. Sci. U. S. A. 95, 8686-8691.

Richards, A.A., Garg, V., 2010. Genetics of congenital heart disease. Curr. Cardiol. Rev. 6, 91-97.

Robertson, G., Hirst, M., Bainbridge, M., Bilenky, M., Zhao, Y., Zeng, T., Euskirchen, G., Bernier, B., Varhol, R., Delaney, A., Thiessen, N., Griffith, O.L., He, A., Marra, M., Snyder, M., Jones, S., 2007. Genome-wide profiles of STAT1 DNA association using chromatin immunoprecipitation and massively parallel sequencing. Nature methods 4, 651-657.

Sugi, Y., Lough, J., 1994. Anterior endoderm is a specific effector of terminal cardiac myocyte differentiation of cells from the embryonic heart forming region. Dev. Dyn. 200, 155-162.

Sugi, Y., Lough, J., 1995. Activin-A and FGF-2 mimic the inductive effects of anterior endoderm on terminal cardiac myogenesis in vitro. Dev. Biol. 168, 567-574.

Tam, P.P., Parameswaran, M., Kinder, S.J., Weinberger, R.P., 1997. The allocation of epiblast cells to the embryonic heart and other mesodermal lineages: the role of ingression and tissue movement during gastrulation. Development 124, 1631-1642.

Uosaki, H., Andersen, P., Shenje, L.T., Fernandez, L., Christiansen, S.L., Kwon, C., 2012. Direct contact with endoderm-like cells efficiently induces cardiac progenitors from mouse and human pluripotent stem cells. PLoS One 7, e46413.

van der Linde, D., Konings, E.E., Slager, M.A., Witsenburg, M., Helbing, W.A., Takkenberg, J.J., Roos-Hesselink, J.W., 2011. Birth prevalence of congenital heart disease worldwide: a systematic review and meta-analysis. J. Am. Coll. Cardiol. 58, 2241-2247.

Van Vliet, P., Wu, S.M., Zaffran, S., Puceat, M., 2012. Early cardiac development: a view from stem cells to embryos. Cardiovasc. Res. 96, 352-362.

Wolf, M., Basson, C.T., 2010. The molecular genetics of congenital heart disease: a review of recent developments. Curr. Opin. Cardiol. 25, 192-197.

Yuan, S., Zaidi, S., Brueckner, M., 2013. Congenital heart disease: emerging themes linking genetics and development. Curr. Opin. Genet. Dev. 23, 352-359.

APPENDIX 1

Output list of differentially expressed genes in RNA-Sequencing data

Column names as indicated. (padj = adjusted p value)

Table A.1. Differentially expressed genes at day 7 in control and *Trim33^{FF}:UBCre^{ERT2}* (4-OHT+) embryoid bodies. Cre was induced at day 4 in differentiation culture. N= 2 independent sample pairs (Chapter 4).

Gene Id	log2FoldChange	padj
Cdhr2	-Inf	0.002133191
Krt79	3.994900516	0.004073151
Nipal1	3.4968914	0.0000443
Prl3b1	3.047026522	0.000625295
Shisa3	2.15091521	0.019047286
Ankrd1	2.014463001	0.00084171
Nfxl1	1.243005403	0.000625295
Cd44	1.235540874	0.000342188
Scd1	0.99666188	0.012472549
Dusp4	0.953691444	0.019703088
Scd2	0.931683852	0.000841271
Cyp51	0.892550394	0.005913254
Il6st	0.85269803	0.029935889
Sqle	0.84279181	0.022036397
Ldlr	0.808181619	0.034221117
Tpi1	-0.747736027	0.033110325
Slc2a1	-0.752625189	0.0236023
Galk1	-0.773304278	0.049597367
Aldoa	-0.851215013	0.004073151
Gpi1	-0.86714941	0.00660598
Ddit4	-0.868007681	0.014142097
Ldha	-0.877594523	0.003202994
Egln1	-0.929101674	0.006339872
Pgk1	-0.995003146	0.0236023
Slc16a3	-1.007216709	0.000647973
Pfkl	-1.061333572	0.000139558
Lgmn	-1.109833043	0.000277474
Pdk1	-1.19881452	0.00006
Egln3	-1.219590481	0.003850968
Trim33	-1.221779639	0.001085018
Tmprss2	-1.224883891	0.005584933

Slc2a3	-1.28941248	0.000000222
Ak4	-1.385472863	0.0000443
Cited1	-1.422925645	0.003672725
Pappa	-1.42614138	0.013824788
Bnip3	-1.435735016	0.0000919
Gstm1	-1.507158753	0.019047286
Ctsc	-1.554228405	0.000989765
Ano1	-1.597088494	0.019047286
Pdzk1	-1.602985985	0.027840759
Clic6	-1.672027398	0.020051197
Reep6	-1.723923757	0.000187476
Camkv	-1.775138836	0.007446037
B4galnt2	-1.813206138	0.004727369
Sepp1	-1.91541629	0.0000935
Hkdc1	-1.922288786	0.001369785
Fgfr4	-1.977882434	0.049597367
Habp2	-1.986214932	0.032661808
Ctsh	-2.008981963	4.94E-10
Gli1	-2.025765329	8.85E-08
Mttp	-2.17955073	0.00000156
Dpp4	-2.190025705	0.005762538
Ttr	-2.449391718	0.001906598
Hnf4a	-2.472472179	0.017445548
2610528J11Rik	-2.528230892	0.002171964
Klb	-2.553091813	0.028146909
Fgb	-2.579024037	0.000978705
Npl	-2.59657454	0.00000117
Lgals2	-2.714073368	0.001836455
Abcc2	-2.840831294	0.002066163
2810459M11Rik	-2.900913359	0.012472549
Slc13a4	-3.020413127	1.8E-10
S100g	-3.026267738	9.6E-09
Slc39a5	-3.083548834	0.013824788
Pla2g12b	-3.223048157	0.001906598
Soat2	-3.310471541	0.000813961
Apoa2	-3.437208856	0.000978705
Cldn2	-3.471504863	0.000000177
Trf	-3.608709594	1.01E-15
F2	-3.773771206	0.000424684
Muc13	-3.943504297	0.007605514
Serpinf2	-3.997991214	0.0000499
Creb3l3	-4.061423165	0.001296533

Apoa1	-4.154425087	0.00000342
Amn	-4.313600839	1E-24
Apob	-4.323436687	0.0000067
Cubn	-4.749035918	3.19E-46
Afp	-4.857191998	1.83E-10
Fga	-4.934903394	0.02099508
Spp2	-5.322511087	0.000005
Apoa4	-5.429069677	0.00000096
Aldob	-5.507023145	5.94E-11
Slc2a2	-5.703781631	0.000978705
Apoc2	-6.12733823	4.29E-41

Table A. 2. Differentially expressed genes at day 2 in control and *Trim33^{FF}:UBCre^{ERT2}* (4-OHT+) embryoid bodies. Cre was induced at day 0 in differentiation culture. N= 3 independent sample pairs. A threshold of 0.5 in the log2FoldChange was used to include differentially expressed genes in this table.

Gene Id	log2FoldChange	Padj
Mir377	2.258006014	0.031442616
Creb5	2.020352456	0.028342324
Fgfbp1	1.999159881	1.24E-15
Slitrk3	1.838329547	0.016942864
Kctd19	1.812067287	0.004125777
Socs3	1.765805929	0.01593901
Cacna1e	1.736254001	0.045494784
Dusp8	1.732085895	7.90E-05
Ahnak	1.662613764	0.01299176
Ctrb1	1.65588798	0.039090641
Ctgf	1.583495846	6.08E-09
Irak3	1.546580951	0.010055033
Thsd7a	1.528926352	1.51E-05
1700061G19Rik	1.526764205	0.000523912
Rsph6a	1.492009043	0.044342729
Pdzrn4	1.403049848	1.13E-05
Mme	1.392074373	4.17E-08
Klhdc7a	1.385200645	0.015461789
Klf5	1.370987078	0.013050111
E330020D12Rik	1.363978676	0.013050111
Tfap2c	1.361777532	0.003953708
P2rx7	1.356557819	0.000925968
Bcl3	1.346259717	0.00750789
Rasgrf2	1.344678207	0.038004671
Ccdc141	1.331394119	0.006601896
Ccdc85a	1.289748522	1.84E-11
Sstr5	1.267906908	0.000285193
Cyb5r2	1.244766224	0.019362732
Tgfbr2	1.241732396	0.04393892
Cyr61	1.241690732	1.02E-11
Map3k8	1.226611648	0.022273279
Abca8b	1.221413193	0.008958065

Esrrb	1.195277986	0.00012266
Arid5b	1.194030156	0.020356107
Lats2	1.18813035	0.000107015
Tfcp2l1	1.172393244	0.00113212
Trim61	1.170559911	0.035556167
Prex2	1.16797677	0.000164204
Shank1	1.12375529	0.015277611
Sox8	1.117741527	0.013653199
S100a11	1.105622465	0.011556456
Lamc2	1.092276751	0.020811885
Fmn2	1.08742535	7.32E-06
Egfr	1.083207935	0.000856005
Fam83h	1.06810464	0.00244242
Chst1	1.064329372	1.84E-15
Scrn1	1.037812358	6.84E-06
Pdgfa	1.034372738	0.041122826
Stat3	1.032348343	3.08E-10
Ano3	1.0209393	0.020900836
Nrip3	1.016738677	0.004540785
Diap2	1.006366602	8.24E-07
Apela	1.003420318	2.47E-15
Pclo	0.997807035	0.000815197
Neb	0.992190282	0.00093445
Csdc2	0.988961203	0.016188924
Tdh	0.979167438	0.000573214
Jun	0.951661986	5.97E-05
Bmp7	0.949778066	0.016188924
Perp	0.944117969	0.000140176
Ddx58	0.943958876	7.82E-06
Plk2	0.941499904	0.002032867
Sned1	0.940864578	0.001801624
Tbx3	0.936950672	0.020811885
Adrb3	0.934752906	0.000595851
Inpp5d	0.927105162	0.001302245
Lpar6	0.926063366	8.29E-11
Neat1	0.922352734	0.010229192
1700030C10Rik	0.918427609	0.009395207
Loxl1	0.916617042	0.040827362
Vwf	0.91196589	0.023176252
Slc12a8	0.90837773	0.028935728
Chrd	0.906951436	0.00076802
Rreb1	0.897584182	2.67E-07
Ppfibp2	0.894636931	2.41E-05

Plxnc1	0.890644851	0.043207506
Fam129a	0.882260361	2.43E-05
Chrnb1	0.87430884	0.047245655
Shisa6	0.866336213	9.98E-05
Icam1	0.857818993	0.027337927
Pdk4	0.856728271	0.002545057
Vwa5a	0.849979956	1.07E-08
Dll1	0.848537189	5.22E-09
Zhx1	0.841376303	0.01502115
Acox3	0.83864258	0.001302245
Aldh1l1	0.834303664	0.036056074
C330046G13Rik	0.828502097	0.025034798
Dscaml1	0.823691677	0.040656833
Tpd52l1	0.822514569	2.88E-08
Clvs2	0.820553081	0.008593968
Sh3tc1	0.813874023	0.012301207
Ap3b2	0.811474907	6.21E-08
Gna15	0.809224875	0.001302245
Mmrn2	0.80709085	0.014264504
Apobec1	0.805703491	0.023251994
Slco4a1	0.805413939	0.002694
Frem2	0.799679431	0.00266818
Serping1	0.796585481	0.004437604
Rusc2	0.792568967	0.012344075
Nab2	0.791135505	0.005621243
Cyp51	0.772716957	1.28E-18
Pwwp2b	0.769847561	0.001013909
Dusp10	0.769163865	0.034890405
Msmo1	0.755164648	1.19E-16
Renbp	0.752250328	1.20E-09
Zmat4	0.750583624	0.015397528
E030030I06Rik	0.749630243	0.023422419
Slc4a11	0.748007142	0.002260379
Sat1	0.742525431	9.92E-05
Cd55	0.737000103	0.04128065
Artn	0.734588924	0.026222107
Ldlr	0.734317278	2.00E-16
Tspan2	0.726202494	0.002545057
Cdkn1a	0.726022089	3.54E-06
Patl2	0.723801985	0.047022566
Cdh2	0.721801708	0.002130789
Slc17a9	0.719799717	0.013922037
Star	0.717603995	0.023422419

Etnk1	0.710049184	0.000250712
Cpeb2	0.7081141	0.002004899
Sh2d3c	0.70329578	0.004328251
Scn1b	0.701846674	0.018657452
Plce1	0.701826442	0.012744548
Fbxo15	0.701648918	0.002590633
Srcrb4d	0.700664133	0.022344077
Fry	0.699713961	0.029492716
Tex19.1	0.696767197	0.005128945
Frmd4b	0.696331683	0.016185377
Btg2	0.694692248	3.08E-10
Olig1	0.693549145	0.00094358
Trim56	0.687163347	0.013141869
Bambi	0.687018657	0.000367737
Mpv17l	0.675352307	4.21E-05
Plagl1	0.673588354	0.009395207
Rap2b	0.671720363	0.000922718
Plekhm1	0.670884639	0.000117367
Sdc4	0.668858822	1.01E-11
Fah	0.663811252	0.028342324
Mcam	0.663048799	0.000228003
Efr3b	0.662621704	2.01E-06
Klf6	0.661770757	6.63E-11
Trp53inp1	0.65720006	2.69E-09
Tlr2	0.650966281	0.012626124
Fam212b	0.647322364	0.041122826
Dsg2	0.64376608	2.14E-06
Tek	0.643145689	0.0130686
Il3ra	0.640067792	0.046429425
Fbxl16	0.638544807	0.041122826
Tmem47	0.6375625	1.64E-07
Bach2	0.63420271	0.017188405
Lama3	0.633470938	0.001608618
Hmgcr	0.631299514	1.26E-13
Cflar	0.628773352	0.035556167
Aacs	0.628371261	7.26E-07
Relb	0.627032898	0.020811885
Colec12	0.623850568	0.000432108
Ptpn14	0.623689642	0.000369308
Nr4a1	0.623216881	0.000359023
S100a10	0.622168686	0.001409935
Eng	0.620849685	1.18E-06
Sqle	0.620786569	3.17E-12
Slc27a2	0.620725522	0.005684583

Thbs2	0.612970748	0.04341116
Mdm2	0.606862221	0.00015132
Gpr153	0.600585102	0.022428415
Ppm1k	0.59831043	0.043911349
Lamb2	0.59511478	0.000628038
Slc4a2	0.592592021	0.000107015
Insig1	0.589580639	0.001424673
Rfx2	0.58910845	0.048941643
Slc23a1	0.588733839	0.00230334
Fut9	0.586878846	0.000190657
Ryr3	0.584907461	0.008677159
Trap1a	0.58390147	0.000716408
4930483K19Rik	0.583325587	0.012176364
Idh1	0.583056884	6.55E-09
Unc13a	0.581971029	0.023017874
Hivep2	0.58040254	0.018370838
Cers4	0.577861497	0.005943364
Large	0.573944004	0.001144302
Dsp	0.572640824	0.00626634
Pmm1	0.571259759	5.84E-06
Commd3	0.566486342	0.000741653
Gucy1a2	0.555587362	0.020356107
Triml1	0.555394424	0.041635419
Cpt1a	0.546996395	0.002694
Slc38a2	0.546110257	0.038842999
D630023F18Rik	0.545761804	0.020811885
Rbm20	0.544061124	0.020811885
Igdcc4	0.543182838	0.006856887
Habp4	0.542605694	0.029492716
Zfp36l1	0.540958644	0.012311663
Prkx	0.540193289	0.023901764
Sh3pxd2a	0.534216589	0.032416068
Gli1	0.532829693	0.002891529
Parp4	0.530225219	0.027946367
Dcxr	0.530195977	0.003181556
Agrn	0.524331966	4.44E-08
Syt9	0.52345954	0.000317847
Cdc42ep5	0.522194126	0.003659795
Zbtb10	0.521852093	0.007838324
Map3k9	0.521190824	0.001388762
Trim11	0.520175609	0.001719853
C77080	0.519805205	0.010216508

Il6st	0.519383432	0.000140176
Lefty1	0.51859976	3.70E-06
Ajuba	0.518012355	0.000270476
Kcnh3	0.51725818	0.020811885
Gcnt2	0.515752802	0.000943776
Arid3a	0.515703396	0.022428415
Lnpep	0.515052179	0.016942864
Gprc5c	0.513889608	0.012344393
Mbnl2	0.512894041	4.77E-05
Amotl2	0.511565657	4.71E-07
Zcchc24	0.511098337	0.003518386
Atp1a3	-0.506504182	0.002500133
Srl	-0.514290872	0.000250712
2810417H13Rik	-0.524526124	3.42E-05
Tnnt1	-0.531282851	0.0170436
Arl4d	-0.53847818	0.001409935
Ccnd1	-0.545020762	0.007083928
Ccne2	-0.545681111	0.005004541
Sgk1	-0.547934447	5.16E-09
Aif1l	-0.555707515	0.002611517
Prickle1	-0.570869614	0.020787015
Crym	-0.571741039	0.021402848
Mns1	-0.57653028	0.000750046
Pde2a	-0.592405029	0.000628038
Trim46	-0.593476491	0.02215252
Ccdc40	-0.595706035	0.002260379
LOC100503496	-0.598703172	0.032967957
Lmo2	-0.605559076	0.049150132
Tdrd1	-0.623006087	0.02172162
Tpt1	-0.645103025	0.000815197
Slc16a6	-0.654921884	0.000100324
Ntrk2	-0.665315464	0.00191656
Stox2	-0.671249703	7.43E-05
Plac8	-0.711020652	0.001645116
Fgf15	-0.715201062	5.97E-05
Prr19	-0.71979047	0.001753224
Pla2g1b	-0.721261475	6.06E-06
Enpp2	-0.733409016	0.000544805
Myl9	-0.773280859	0.000943776
Psors1c2	-0.787829456	0.020307352
Nrcam	-0.81891483	0.010147349
Nlgn3	-0.879340594	0.009820923
Hlf	-0.894493928	0.025718165

Rac1	-1.018275145	1.16E-28
Gdpd1	-1.046965159	0.012902938
Trim33	-2.037457292	6.50E-119

Table A. 3. Differentially expressed genes at day 2.5 in control and *Trim33^{FF}:UBCre^{ERT2}* (4-OHT+) embryoid bodies. Cre was induced at day 0 in differentiation culture. N= 3 independent sample pairs. A threshold of 2 in the log2FoldChange was used to include differentially expressed genes in this table.

Id	log2FoldChange	Padj
Msln	Inf	6.63E-07
Smok4a	3.806525662	9.14E-09
Cacna1e	3.711899487	3.19E-05
Sh3rf2	3.51937051	3.10E-09
E330020D12Rik	3.353313111	1.30E-10
Lgals3	3.309490055	5.16E-39
Sim2	3.146621736	0.000810748
P2rx7	3.140584496	2.47E-14
Ms4a10	3.125133569	1.64E-08
Ahnak	3.113684398	2.13E-16
Aox3	3.111070825	0.000361309
Sox8	3.084415001	4.74E-16
Fgfbp1	3.05458284	7.14E-84
A730082K24Rik	3.0068022	7.06E-06
1700061G19Rik	2.991691796	1.54E-18
Tlr5	2.975935494	0.000373971
Ebf2	2.941305605	0.000678282
Gm17019	2.815398046	0.000957665
Rapgef4	2.791762118	0.001396859
Sstr5	2.782287102	1.96E-40
Gm10863	2.687164148	0.001010824
Itga8	2.676234632	5.78E-12
Anxa8	2.575615552	1.77E-30
Pcdhgb8	2.565688682	0.000439818
Clec10a	2.560928364	0.000308382
Anxa1	2.550036936	3.17E-06
2700054A10Rik	2.53920818	3.48E-25
C130021I20Rik	2.532292581	1.05E-06
Slc9a9	2.523065091	0.000784979
Slfn2	2.507651258	0.000667761
A730036I17Rik	2.501488952	0.000199983
Ctrb1	2.498473459	7.06E-08
Tspan32	2.497249474	7.94E-07
Slfn3	2.488455617	0.008975749
Mgst2	2.485411302	0.00026834

Ccdc141	2.479711522	4.33E-09
Irak3	2.474308505	4.46E-22
Scg2	2.451860136	0.009218866
3830417A13Rik	2.451408867	0.004102275
Erv3	2.441121901	1.11E-07
Th	2.43828259	0.00843696
Efhb	2.406921821	4.48E-06
Dll1	2.381565436	2.86E-10
Mir8091	2.380410031	0.007049365
Creb5	2.376043841	1.36E-06
Jam2	2.354175718	5.75E-36
Spata31d1b	2.339751153	0.000205062
Rasgrf2	2.326602927	8.39E-09
Inpp5d	2.325755919	5.06E-61
5830418P13Rik	2.307600423	1.86E-07
Cml2	2.307274096	1.46E-28
Diras2	2.296614329	4.81E-08
Ltb4r1	2.295954709	6.31E-10
Plxna4	2.291587121	0.001908596
Slc25a45	2.284222179	0.000112082
Olfml1	2.277021117	5.77E-06
2410021H03Rik	2.271917171	2.44E-06
Foxd1	2.25236321	0.000101835
C86695	2.226168874	9.60E-05
Esrrb	2.225846674	2.90E-19
Pdgfa	2.22420142	4.32E-41
Cd80	2.207447658	9.65E-14
Neb	2.202727601	3.34E-24
Klhl6	2.188473914	3.37E-05
Mmrn2	2.182942899	9.98E-12
Gm10696	2.182396623	6.82E-06
Ttn	2.182200808	3.88E-12
Upk3b	2.177271117	0.010041369
Mylpf	2.161639012	4.62E-50
Pou3f3	2.161325668	3.99E-06
Tchh	2.15292874	3.62E-15
Mir292b	2.138296005	0.016204244
Neat1	2.133785513	1.09E-15
Abca8b	2.129601389	1.24E-13
Ak7	2.124054162	6.62E-06
9130227L01Rik	2.109717762	0.015842782
Arid5b	2.109110749	2.29E-66
C130026I21Rik	2.108896147	0.018957603

Sva	2.102609365	0.01100749
Tfap2c	2.096585037	2.35E-35
Hoxc13	2.09511869	7.29E-07
Synpo2l	2.089942864	2.96E-05
Tpo	2.081591074	0.000138276
Olfr815	2.080304341	2.46E-05
Gm4858	2.07629699	1.16E-17
BC064078	2.073850861	0.000165856
4930525G20Rik	2.071789846	0.008185063
Scn3b	2.063165234	9.75E-14
Vmn2r1	2.062746123	0.004050919
Tfcp2l1	2.047943092	1.02E-21
Tlx3	2.045706989	0.001429538
Nkx2-9	2.041335174	1.23E-11
Pik3ap1	2.039072413	1.09E-05
Klf4	2.038754173	1.67E-11
Prdm14	2.035229667	5.39E-05
Megf11	2.034920771	9.39E-12
Ctsw	2.029207275	0.000253257
Gm5039	2.028008081	1.60E-39
Mapt	2.02670327	6.01E-14
Calcoco2	2.024959598	7.75E-17
Itln1	2.024529979	0.00032023
Phf11a	2.023413218	1.16E-05
Igsf23	2.020146167	4.30E-08
Dusp27	2.017825458	1.04E-25
Zbtb7c	2.013278725	0.000755916
Iqcf1	2.010747316	0.015531641
Plaur	2.007498925	3.20E-31
AU015836	2.006988281	2.75E-22
Pdzd2	2.005244071	1.12E-17
Txlnb	2.004376675	3.45E-06
1700096K18Rik	2.003765664	0.01564669
Fbxo15	2.001792999	1.60E-39
Tex19.1	2.001465877	6.89E-59
Gm9926	-2.034847034	0.013477627
Ldb2	-2.077879052	2.42E-09
Trim33	-2.098173819	1.70E-143
Megf10	-2.128969248	0.016184187
Fhl2	-2.14284755	0.000949023
Camk1g	-2.214747808	0.000314614